2013

Preferred Sensor Selection for Damage Estimation in Civil Structures

Matthew Styckiewicz
University of Massachusetts Amherst, mstyckiewicz@gmail.com

PREFERRED SENSOR SELECTION FOR DAMAGE ESTIMATION IN CIVIL STRUCTURES

A Thesis Presented

by

MATTHEW M. STYCKIEWICZ

Submitted to the Graduate School of the

University of Massachusetts Amherst in fulfillment

of the requirements for the degree of

MASTERS OF SCIENCE IN CIVIL ENGINEERING

February 2013

Department of Civil Engineering

PREFERRED SENSOR SELECTION FOR DAMAGE ESTIMATION IN CIVIL STRUCTURES

A Thesis Presented

by

MATTHEW M. STYCKIEWICZ

Approved as to style and content by:

_____

Scott A. Civjan, Chair

_____

Kourosh Danai, Member

_____

Sanjay R. Arwade, Department Head

Department of Civil and Environmental Engineering

ABSTRACT

PREFERRED SENSOR SELECTION FOR DAMAGE ESTIMATION IN CIVIL STRUCTURES

FEBRUARY 2013

B.S.C.E., UNIVERSITY OF MASSACHUSETTS AMHERST

M.S.C.E., UNIVERSITY OF MASSACHUSETTS AMHERST

Directed by: Scott Civjan

Detecting structural damage in civil structures through non-destructive means is a growing field in civil engineering. There are many viable methods, but they can often be time consuming and costly; requiring large amounts of data to be collected. By determining which data are the most optimal at detecting damage and which are not the methods can be better optimized. The objective of this thesis was to adapt an existing method of data optimization, used for damage detection in mechanical engineering applications, for use with civil structures. The existing method creates Parameter Signatures based on characteristics from the system being analyzed, from which preferred locations for recording data are determined. For civil structures this method could potentially be used to locate the preferred locations to place accelerometers such that the minimum number of accelerometers is needed to properly detect the location and severity of damage in the structure. This method was first tested on fully analytical computer model structures under perfect conditions to determine its mathematical feasibility with civil structures. It was then tested on data recorded from physical test structures under "real-world" conditions to determine its feasibility as an actual damage detection optimization procedure. Results from the analytical testing show that this is in fact a

viable method for determining the preferred sensor positions in civil structures. Furthermore, these results were verified for a variety of excitation types. Physical testing was inconclusive, leading to great insight about what obstacles are impeding this method and should looked at in future research.

TABLE OF CONTENTS

LIST OF TABLES

LIST OF FIGURES

CHAPTER I

INTRODUCTION

Current methods for diagnosing damage in buildings and other structures that are used by practitioners include visual inspection, acoustics, ultrasound, magnetic field, radiography, thermal field and strain gauges. These can effectively be used to determine if damage has occurred in a structure but are not always feasible. For instance, these methods may not be able to be used on some of the harder to reach members in a structure. They also have the disadvantage of not always being able to quantify the severity of damage (Farrar and Jauregui, 1997). Most importantly, they are effective when the location of damage is known, but are sometimes difficult to implement when damage can occur throughout a structure.

In order to better and more efficiently estimate damage, the current methods can be supplemented with a study of the changes to the physical properties of the structure due to damage. There have been a number of methods developed recently which examine the natural frequencies, mode shapes and damping ratios of a structure in order to determine the likelihood of damage and in some cases the location of damage within the structure. These methods are based on the idea that damage in a structure would effectively change the dynamic properties of the structure, allowing an engineer to isolate and quantify the damage according to these changes (Friswell, 2007). To implement these methods, the dynamic properties of the structure must first be observed for the undamaged structure and then again after an event that may have caused damage. The most common ways of determining the dynamic properties of a structure are from its

dynamic response, recorded as either acceleration or force measurements taken at various locations throughout the structure. The dynamic responses can be generated from ambient motion caused by wind or seismic activity as well as forced motion caused by a controlled vibration generator, vehicles, or other methods (Farrar and Jauregui, 1997).

There are currently many types of damage detection methods that use the fundamental principle that damage causes the dynamic characteristics of a structure to change (Friswell, 2007). Two of the most common are the direct and inverse methods of damage detection. The direct methods of damage isolation is dependent on measuring the changes that have occurred in the structure, recognizing patterns in those changes and linking those patterns to specific damage configurations that could have occurred throughout the structure (Danai et al., 2011). The inverse methods of damage estimation use a system of iteratively updating a structural model until the dynamic characteristics of the model match the actual structure (Friswell, 2007). Once a response is found to match the actual structure the corresponding damage introduced in a model is expected to correspond to the actual conditions. Both methods have been proven to work for many applications including, notably, damage detection in jet engines (Danai and McCusker, 2010, Danai et al., 2009). Unfortunately, these methods both suffer from the same difficulties when it comes to detecting damage in more complex structure. Larger structures with many individual components require more sensors in order to accurately attribute the damage to a particular location or group of components. For example, if one sensor was placed at approximately every story in a high rise structure, these methods may be able to determine which story the damage has occurred on, but in order to pinpoint the damage to a certain member or connection in the structure, sensors would be

required on nearly every individual structural component in the building. Additionally, as the number of sensors increases the complexity of the simulations and the number of required computational runs to complete the analysis also increases.

For the inverse methods of damage estimation it may be known, from prior research, that not all of the sensors in a structural model are as important to the damage estimation as others (Yuen et al., 2001). In many cases, a sensor may not even pick up a detectable change in the dynamic response from the undamaged structure to the damaged structure. If a sensor is not able to pick up a change in the response, they are ultimately ineffective to the estimation routine (Danai and McCusker, 2010). By eliminating these unused sensors the analyses can be simplified without hindering the accuracy of the damage estimation procedure. Using a computer model, an engineer would be able to determine which sensor locations would be most crucial to the procedure and which locations are least likely to provide them with relevant data. This can help to reduce the number of sensors that are needed to be installed in the actual structure. A preferred suite of sensors would provide the damage estimation procedure with only the most important dynamic responses, allowing for simpler analyses and less computational runs (Danai et al., 2009).

The focus of this thesis is to present a method of simplifying damage estimation procedures by eliminated unused sensors without reducing the procedure's accuracy. Furthermore, analytically results will be used to verify the practicality of this sensor selection method with the indirect method. Finally, comparisons will be made to results from a scale model test database found in the NEES database and literature.

CHAPTER II

ANALYTICAL BACKGROUND AND METHODOLOGY

The sensor selection method presented in this thesis uses many of the same mathematical principles found in the direct method of damage detection. Therefore, to best understand the sensor selection method it is important to understand the principles of the direct method. Additionally, for the purposes of validation and verification, it will be essential to understand the principles of the inverse method as well. The direct and inverse methods are extremely powerful procedures used in the detection, isolation and even quantification of damage in virtually any type of damageable system. As long as a system has measureable outputs which are dependent on particular parameters, the direct and inverse methods can be used to detect changes (damage) in the parameters based on the measured outputs. In the case of a structure, a convenient parameter to consider is stiffness coefficients. Stiffness coefficients in a structure are used to quantify the stiffness of a particular member. If a member in the structure is damaged the stiffness of that member would be reduced, effectively decreasing its stiffness coefficient. These stiffness coefficients, and any changes that may incur, directly affect the outputs of the structure. In this case the outputs could be strains, forces or accelerations, recorded at various locations throughout the structure due to some sort of excitation or vibrations. If the stiffness of a member in the structure changes, the output record at some locations in the structure may also change. The direct and inverse methods analyze changes in the outputs to determine which parameters caused the changes. When used on a structure they can determine which members were damaged based on how the outputs were affected.

The Direct Method

There are many direct methods of damage estimation, however they all use similar mathematical theories. The fundamental principle of any direct method is to link specific patterns in the outputs to particular changes in the parameters. (Danai et al., 2011). When being used for structural applications the direct method detects unique patterns in the dynamic response of the structure and correlates them to different changes in the stiffness coefficients of the structural members. To put it simply, damage in one member will create a different change in the dynamic response than damage in another member. By training a computer program to recognize the patterns in the different dynamic responses and linking those patterns to corresponding damaged members it can create a database allowing it to predict in which member damage has occurred when damage does occur (Danai et al., 2011). In order for the direct method to create such a database a full record of dynamic responses must be obtained, each of which is the result of and is thusly associated with damage in a specific member of the structure. To get these responses without damaging members the actual structure a computer model is used to simulate damage at the expected locations. To record a dynamic response, damage is simulated at a certain location in the model, the model is excited with a known forcing function and the resulting accelerations are saved. The damage is moved to a different location and the process is repeated until damage has been simulated in every member. Rather than using accelerometers to record the response, as on an actual structure, a computer model uses a dynamic finite element to record how the structure would react if it were acted upon by forces or vibrations (Farrar, 1997). With all of the dynamic responses for each damage location the computer program can be trained to detect the

presence of damage in the actual structure based solely on its dynamic response to the same forcing function used on the model (Danai et al., 2011).

For the basis of this research, damage was simulated as a reduction in the assigned stiffness of one or more of the structural components in the model. A vector of those assigned stiffness values for the entire structure is given the notation $\bar{\boldsymbol{\Theta}}$. Minor damage occurrences may be simulated by a one percent reduction of stiffness while major damage may be represented by as much as a 20 percent reduction. Any change in the stiffness coefficient of a particular component, i, is give the notation $\delta\theta_i$. Additionally, all of the response measurements are taken as accelerations, as accelerometers would most likely be the easiest to install and take readings from in an actual structure.

Output Sensitivities

Unfortunately, these damaged responses cannot tell us much about the damage in the structure unless a response from the undamaged structure is recorded as well. In order for these damaged responses to give us any information about the damage in the structure they must be compared to their undamaged counterpart. It is also necessary for both the undamaged and damaged responses to be the result of the same known excitation function $\mathbf{u}(t)$ acting on the structure (Friswell, 2007) . The most important information from the responses is found in the *Output Sensitivity*. The output sensitivity is defined as the difference between the damaged response and the undamaged response normalized by the perturbation size (Danai et al., 2011). The output sensitivity can be calculated as

$$\frac{\partial \hat{y}_j}{\partial \theta_i}(t) = \frac{y_j(\mathbf{u}(t),\bar{\mathbf{\Theta}}+\delta\theta_i)-y_j(\mathbf{u}(t),\bar{\mathbf{\Theta}})}{\delta\theta_i} \quad (1)$$

Where $y_j(\mathbf{u}(t),\bar{\mathbf{\Theta}})$ is the undamaged response at location j due to the forcing function $\mathbf{u}(t)$ with a healthy stiffness coefficient vector $\bar{\mathbf{\Theta}}$. $y_j(\mathbf{u}(t),\bar{\mathbf{\Theta}}+\delta\theta_i)$ is the damaged response where $\bar{\mathbf{\Theta}}$ has been changed by a given perturbation, $\delta\theta_i$. (Danai et al., 2011). In order to calculate all of these output sensitivities quickly and efficiently a model is required that can be easily updated and changed to various damage configurations. Figure 1 displays two different dynamic responses from an eight story building model. Both responses are caused by a sinusoidal forcing function applied to the second story, but the first response is that of a healthy structure and the second had damage simulated in the fifth story. The output sensitivities, obtained using Equation 1, of the two responses in Figure 1 are provided in Figure 2. Although the responses look very similar, the presence of output sensitivity suggests that they are different. Figure 1 also illustrates the difference between the steady state and the transient response. The transient phase consists of the initial response to the forcing function. It can be very disordered and random. Shortly afterwards the response begins to fall into a steady repetitious pattern that is usually in sync with the forcing function. This portion of the response is known as the steady state response. The effect of both the transient phase and steady state phase on the output sensitivity is examined throughout this research.

Continuous Wavelet Transforms

Direct methods vary primarily in the process that is used for analyzing the output sensitivities and the method in which they train the computer to interpret this information. The difficulties that face almost all direct methods are the abilities to extract useful data

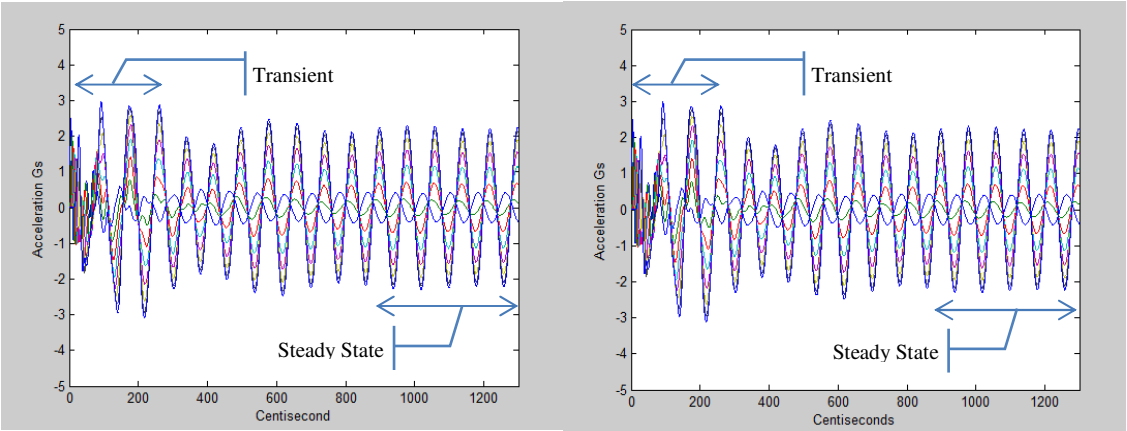

Figure 7 - Eight Story Building Response with Healthy Structure (left) and Damage at 5th Story (right)

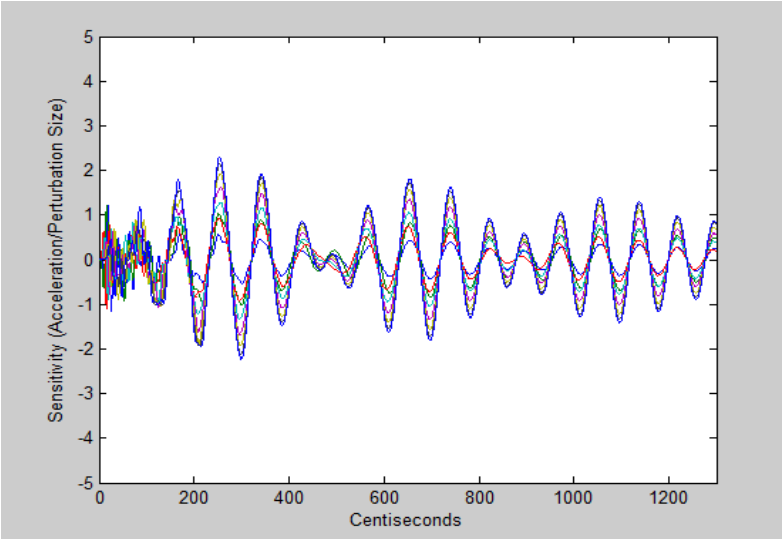

Figure 8 – Output Sensitivities of Eight Story Building due to Damage at the 5th Story

from the output sensitivities and/or differentiate a feature found in one output sensitivity from a feature found in another (Danai and McCusker, 2010). Many times the output sensitivities are minimal, making it difficult to find valuable shape changes let alone to differentiate shape changes from one output sensitivity to another. The Signature-Based Damage Isolation Method (SBDIM) was developed to address this issue. SBDIM is a process of estimating parameters by isolating unique regions of the output sensitivities

known as parameter signatures. The SBDIM uses continuous wavelet transforms (CWTs) to isolate these parameter signatures and prevents the difficulties that hinder most direct methods (Danai et al., 2011). The CWTs use their differential abilities to emphasize shape qualities such as slope and rate of slope change that occur in the output sensitivity. Using CWTs the output sensitivities can be transformed into a surface on a two dimensional time-scale domain which represents the output sensitivities unique shape attributes. This transformed output sensitivity details the times at which the most significant shape attributes occur in the original response as well as the scale of each attribute (Mallat and Hwang, 1992). The scale of a shape attribute is analogous to its frequency (Mallat and Hwang, 1992).

Because CWTs have the ability to represent shape attributes not only in the time domain, but also in the scale domain they make it much easier to differentiate one response from the others and emphasize their uniqueness (Danai and McCusker, 2009) The CWTs are created by the convolution of a wavelet function $\varphi_s(t)$ with the output sensitivity, $\frac{\partial \hat{y}_j}{\partial \theta_i}(t)$, as

$$W\left\{\frac{\partial \hat{y}_j}{\partial \theta_i}\right\}(t,s) = \frac{\partial \hat{y}_j}{\partial \theta_i}(t) * \varphi_s(t) = \int_{-\infty}^{\infty} \frac{\partial \hat{y}_j}{\partial \theta_i}(\tau)\varphi_s(t-\tau)d\tau \quad (2)$$

The wavelet function $\varphi_s(t)$ can be represented as $\frac{1}{s}\varphi(\frac{t}{s})$ in order to incorporate the scale parameter into the function of the wavelet as well as time (Mallat and Hwang, 1992). The wavelet function that is used to create a wavelet transform determines the characteristics that are ultimately described in the wavelet transform (Mallat and Hwang, 1992). A Gauss Wavelet function is the first derivative of the Gaussian smoothing function and

therefore it describes the slopes of the output sensitivities that are transformed. A Sombrero Wavelet function is the second derivative of the Gaussian smoothing function so therefore it describes the rate of slope changes in the output sensitivities (Mallat and Hwang, 1992). The Gauss and Sombrero Wavelets are displayed in Figure 3. Both the Gauss and Sombrero wavelet functions are excellent at emphasizing the shape attributes (i.e. slope and rate of slope change) in the output sensitivities and both work well for the SBDIM (Danai et al., 2011). Typically, only one type of wavelet function is required to transform the output sensitivities and create unique signatures.

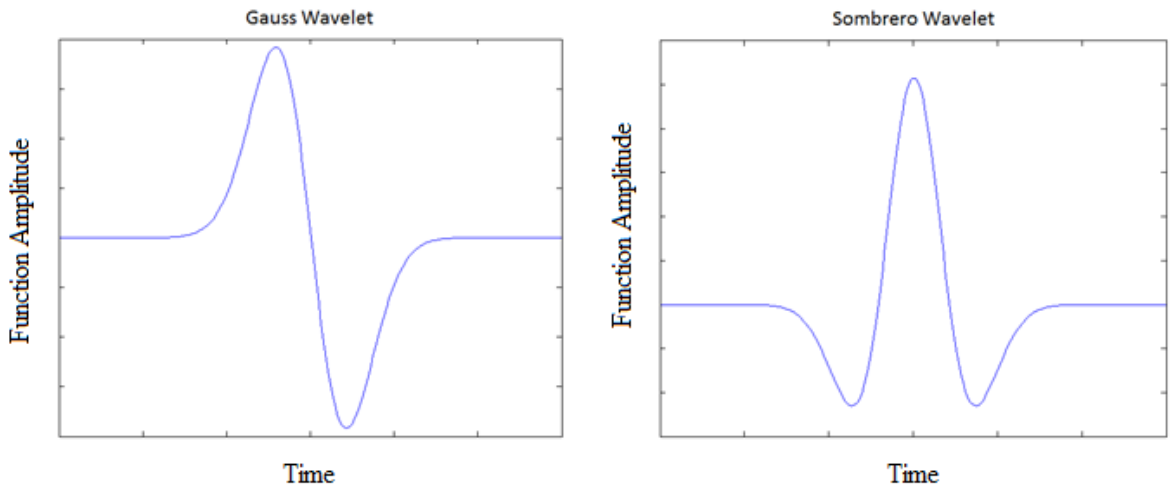

Figure 9 - Graphical representations of the Gauss and Sombrero Wavelets

An additional advantage of using the CWTs is that they negate the need to examine the more complex modal properties which are typically used in many other direct methods or sensor selection processes. Damage affects modal properties in the very same way that it affects the dynamic response. Instead of directly linking a change in response to damage configurations, other direct methods could link changes in the modal

properties to a certain damage configurations (Yang et al., 2004). The advantage of using modal properties is that it is traditionally easier to pick up changes in the modal frequencies than the dynamic response. However, with CWTs that is not the case. The CWTs pick up unique changes in the dynamic response more easily so that we are no longer forced to work with the structural modal characteristics. A glaring deficiently of modal properties is the lack of a time history such as you have when using a dynamic response (Danai et al., 2011). Unlike a method using the dynamic response of the structure, the outputs of a modal analysis are the modal frequencies and mode shapes. A dynamic response can have thousands of data points in its time history, each of which can change. On the other hand, a modal frequency is a single value and a mode shape has only as many data points as the structure has modes. Changes in the dynamic response may be more subtle, but a full time history allows for more uniqueness in the responses. Furthermore, the results that are yielded from a preferred sensor selection routine using modal properties seem to be overly complicated and are subject to error introduced in the transformation processes. In one example the preferred sensor locations in a structure was completely dependent on the number of sensors used and the number of modes considered in the analysis (e.g. Yuen et al., 2004).

Time Scale Domain

In order to achieve a time-scale domain, with two dependent variables (time and scale), the wavelet function must be able to be manipulated in two ways. The wavelet function can be translated along the output sensitivity signal which represents a convolution at different times. This allows various shape attributes from the output sensitivities to be characterized at specific times in the CWTs (Mallat and Hwang, 1992).

Being able to associate specific shape attributes at certain times in the response is a valuable way of flagging unique signatures. The other way that the wavelet function can be manipulated is by dilations to the scale of the wavelet. The wavelet functions can be widened or narrowed allowing them to pick up on very broad shape attributes, which occur over long lengths of time, and also very tiny features, which happen very quickly, all at exactly the same location (time) in the output sensitivity (Mallat and Hwang, 1992). For the current procedure, the wavelet is dilated to 75 different scales. Each of these 75 dilated wavelets is individually translated along the output sensitivity, resulting in 75 transformed output sensitivities. These 75 transformed output sensitivities make up the scale dimension in the time-scale domain. When put side by side they create a surface similar to the example in Figure 5.

The scale of the wavelets typically corresponds to the frequency of the response (Mallat and Hwang, 1992). A very wide wavelet will align nicely with longer period signals in the response but will be too large to pick up the much quicker frequencies. A very narrow wavelet will be able to align nicely with those much higher frequency signals. The clear advantage to a time-scale domain is that shape attributes for each output sensitivity can be characterized not only at specific times in the response but also on a varying scale (Danai and McCusker, 2009). Large, slow changes in shape associated with low frequencies will be displayed in the CWTs as well as the much quicker changes associated with high frequencies. Graphical representations of translation and dilation are shown in Figure 4.

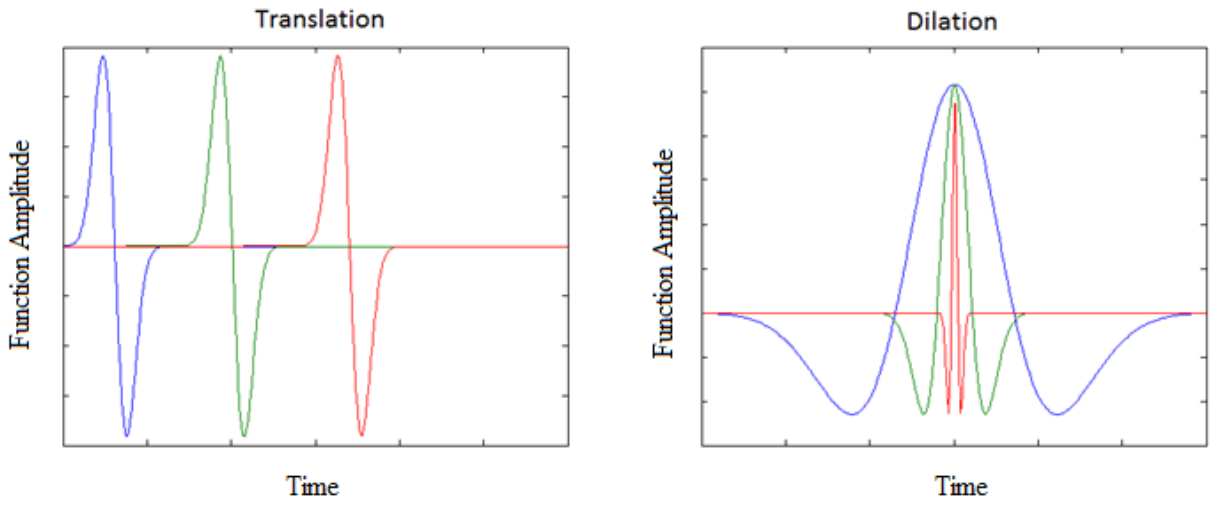

Figure 10 - Graphical representation of Translation and Dilation of a Wavelet

The advantage of the ability to isolate the very subtle differences in each output sensitivity using the time-scale domain allows us to more easily correlate which output sensitivities are affected most by different types of structural damage (Danai et al., 2011). The most predominant features found in the output sensitivities will create the largest spikes on the time-scale domain. That is, when there is a large difference between the undamaged response and damaged response it shows up as a drastic change in slope and/or rate of slope in the output sensitivity. The Gaussian and Sombrero wavelets, which are used to pick up slope and rate of slope changes respectively, will register these drastic changes as the highest and lowest points on a surface (Figure 5) in the time-scale domain. Therefore, the largest peaks and valleys in the surface on the time-scale domain represent the most significant differences between the undamaged and damaged responses. The locations of these high points and low points in the time-scale domain can be used to create a signature that is ideally distinctive to only one output sensitivity (Danai and McCusker, 2009).

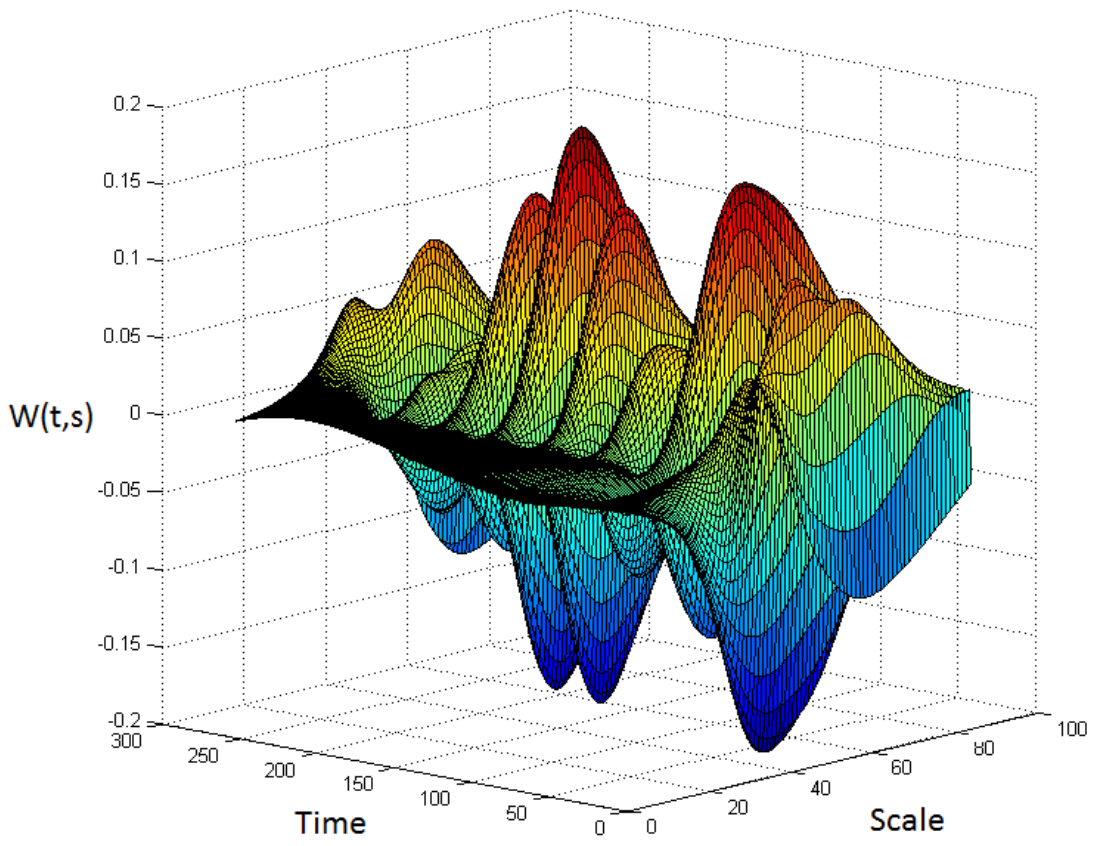

Figure 11 – Transformed Output Sensitivity Surface in the Time-Scale Domain from the Fifth Floor Accelerations due to Damage in the Fifth Story

Any regions on the transformed surface in the time-scale domain that have a significant uniqueness from those of any other response are known as signatures and play a crucial role in the damage estimation procedure (Danai and McCusker, 2009). A signature is unique to only one output sensitivity which is associated with (came from) only one damage location. However, some output sensitivities may not have unique regions in the time-scale domain and therefore will not have any associated signatures. An example of a signature taken from the surface in Figure 5 can be seen in Figure 6.

Component Signatures

Signatures taken from the output sensitivities are known as c*omponent signatures* Ω_{ji}. They are created by comparing one output sensitivity to each of the other output sensitivities recorded during the same finite element analysis but at different locations throughout the structure. For example, if there were ten possible sensor locations on a model structure there would be ten output records for each different damage configuration. These ten records would be used to create ten output sensitivities and then transformed using CWTs. Each of the ten transformed records would then be compared individually to the nine others in that suite using the following formula (Danai et al., 2011):

$$\left|\overline{W\left\{\frac{\partial \hat{y}_j}{\partial \theta_i}\right\}}(t_k, s_l)\right| > \eta_d \left|\overline{W\left\{\frac{\partial \hat{y}_q}{\partial \theta_i}\right\}}(t_k, s_l)\right| \ \forall\, q = 1, \ldots, P_s \neq j \tag{3}$$

where (t_k, s_l) represents an individual point on the surface $\overline{W\left\{\frac{\partial \hat{y}_j}{\partial \theta_i}\right\}}(t_k, s_l)$ in the time-scale domain, η_d is the *dominance factor* and P_s is the number of outputs from the output suite. The transformed responses are all normalized by the function (Danai and McCusker, 2009)

$$\overline{W\left\{\frac{\partial \hat{y}_j}{\partial \theta_i}\right\}} = \frac{W\left\{\frac{\partial \hat{y}_j}{\partial \theta_i}\right\}}{max_{(t,s)}\left|W\left\{\frac{\partial \hat{y}_j}{\partial \theta_i}\right\}\right|} \tag{4}$$

to prevent the amplitudes of the surface functions, which are insignificant, from overshadowing the locations of the peaks and valleys (Danai and McCusker, 2010). If the absolute value a certain point on the normalized surface is greater than the absolute value of that same point (same location) on any of the other normalized surfaces in the suite,

multiplied by a prescribed dominance factor, it is flagged and included in the component signature Ω_{ji} associated with that output sensitivity. The dominance factor represents the percentage by which a point in one transformed output sensitivity must be greater than the same point in any other transformed output sensitivity to be included in the signature (Danai and McCusker, 2009). A high dominance factor results in less data points in the signatures, providing more significance to the points that are included (Danai and McCusker, 2009). On the other hand, a low dominance factor may provide a better method of isolating the smaller changes in the output sensitivities. An example component signature is given in Figure 6. The signature was taken from the surface found in Figure 5.

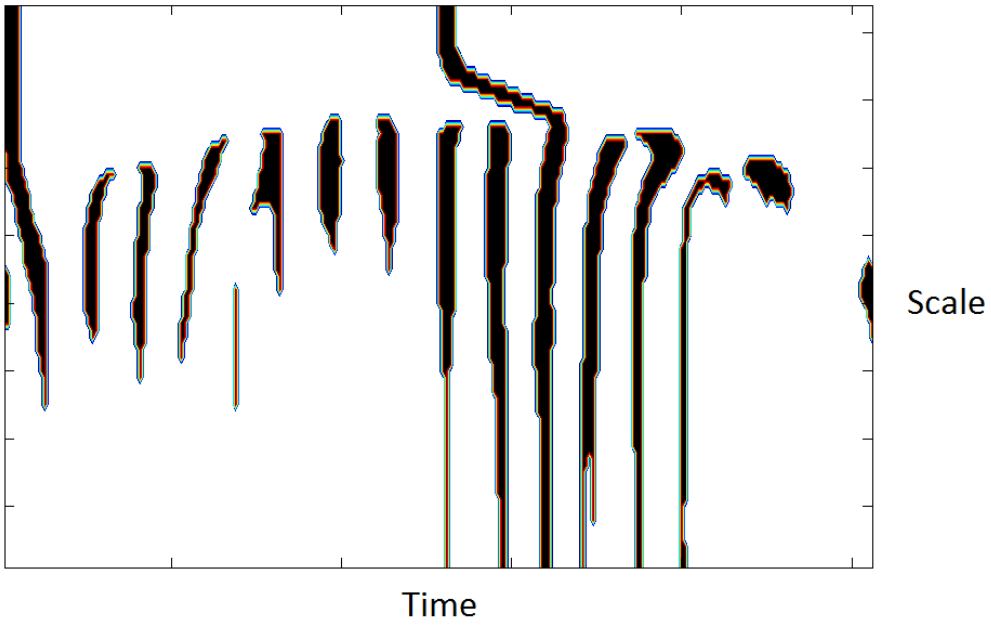

Figure 12 – Component Signature for the Fifth Floor Output Sensitivity due to Damage in the Fifth Story

A significant component signature represents a link between damage in a particular component and the effect that it has on the response at specific locations. In

other words, if a well-populated component signature is produced for a particular sensor location in the building, it means that that sensor location was able to pick up a definite change in the response of the structure due to damage in the component being investigated. Those component signatures are what give us the ability to identify damage based on the output of the sensors (Danai and McCusker, 2010). If the component signature has reasonable *identifiability,* that is they have enough points in order to identify a damaged component, they are assigned a value of 1 according to the equation (Danai et al., 2011):

$$\left|\frac{\partial \hat{y}_j}{\partial \theta_i}\right| = \begin{cases} 1 & \sum_{k=1,l=1}^{N,M}\left(t_k^j, s_l^j \in \Omega_{ji}\right) > d \\ 0 & \text{otherwise} \end{cases} \tag{5}$$

Where $\left|\frac{\partial \hat{y}_j}{\partial \theta_i}\right|$ is the binary value associated with the output sensitivity $\frac{\partial \hat{y}_j}{\partial \theta_i}$ depending on if it has identifiability or not. *d* is a prescribed positive integer that represents the number of points that must appear in the component signature in order for it to be considered to have proper identifiability. This prescribed value is known as the *signature size threshold* (Danai and McCusker, 2009), it can be increased to limit the number of signatures that are assigned identifiabilty to only the best, which are the most populated. It can also be decreased in the hopes that if more signatures are used then the estimation procedure will be more sensitive to very small amounts of damage (Danai and McCusker, 2009). If a output sensitivity is assigned a value of 1, it means that the sensor which recorded that response would be able to identify damage, but only if the damage occurred in the location associated with that output sensitivity. If the output sensitivity is given a value of 0, it does not have the ability to link the response to any one particular damage configuration in this analysis. However, an output sensitivity with no identifiability is still

useful, as you will see in the next section. A zero may not be able to identify where damage did occur but it can eliminate the locations where damage did not occur.

Influence Matrix

The results of the binary values that are assigned to each output sensitivity can be compiled into an *influence matrix* (Danai and McCusker, 2010) which visually displays the correspondence between damage in a particular component and its ability to be identified by different sensor locations. Three influence matrices, each coming from the same structure and input excitation but with different dominance factors, are displayed in Table 1. The structure that these influence matrices come from is a simple eight story structure, which for simplicity only has eight possible sensor locations; one at each floor. This structure also has only eight possible damage configurations considered, with the damageable components being each story as a whole. The values running vertically along the left side of the influence matrices are the parameters. In the case of our structural application, the parameters represent the components which can be damaged. For this particular case the parameters represent the story which can be damaged. The values along the top of the influence matrix represent the outputs, which in this case are the sensor locations. A value of one at any position in that matrix means that the sensor associated with that value can identify damage in the component that is also associated with that value. A zero means that that sensor cannot detect damage in that component (Danai and McCusker, 2010).

Table 1 - Sample Influence Matrices at Varying Dominance Factors for an Eight Story Structure

Parameters (Story Stiffnesses)	Outputs (Floor Accelerations) 1	2	3	4	5	6	7	8	Outputs (Floor Accelerations) 1	2	3	4	5	6	7	8	Outputs (Floor Accelerations) 1	2	3	4	5	6	7	8
1	1	1	1	1	1	1	1	1	1	1	1	1	1	1	1	1	1	1	1	1	1	1	1	1
2	1	1	1	0	0	0	0	0	1	1	1	0	0	0	0	0	1	1	0	0	0	0	0	0
3	1	1	1	0	0	1	0	0	1	0	1	0	0	0	0	0	0	0	0	0	0	0	0	0
4	1	0	1	1	1	0	0	0	1	0	1	1	1	0	0	0	0	0	0	1	0	0	0	0
5	1	1	1	1	1	0	0	0	1	1	1	0	1	0	0	0	0	0	1	0	1	0	0	0
6	1	1	1	1	1	1	1	1	1	1	1	1	1	1	1	1	1	1	0	1	1	1	0	1
7	1	1	1	1	1	1	1	1	1	0	0	1	1	1	1	1	1	0	0	1	1	1	1	1
8	1	1	1	1	1	1	1	1	1	1	1	1	1	1	1	1	1	1	1	1	1	1	1	1
	$\eta_d = 1.25$								$\eta_d = 1.50$								$\eta_d = 1.75$							

Damage Isolation

The influence matrix is the critical component which allows damage to be isolated using the direct method (Danai et al., 2011). To do this we compare the influence matrix, which was created entirely using a simulated model, against the signatures we calculate from the output sensitivities of the actual damaged model. Creating the damage signatures from the actual structure is very similar to creating the component signatures from the simulated model. The difference is that component signatures are created by simulating damage in every possible structural component while the damage signatures contain only the one actual damage situation that occurred in the structure (Danai et al., 2011). The component signatures correspond to many known simulated damage configurations while the damage signatures correspond to a single unknown damage configuration which are to be determined. The output sensitivities from the damaged structure are calculated by (Danai and McCusker, 2009):

(6)

where $y_j(t, \mathbf{u}(t))$ is the dynamic response recorded from the potentially damaged structure and $y_j^n(t, \mathbf{u}(t))$ is the normal response before the damage occurred. It is important to note that the forcing function, $\mathbf{u}(t)$, is the same forcing function used on the simulated structure (Friswell, 2007). These output sensitivities are transformed into a time-scale domain by a convolution with the exact same wavelet function as the simulated output sensitivities were (Danai et al., 2011). Similarly, a signature R_j is created for each output sensitivity based on the condition (Danai et al., 2011)

$$\left|\overline{W\{\epsilon_j\}}(t_k, s_l)\right| > \eta_d \left|\overline{W\{\epsilon_m\}}(t_k, s_l)\right| \ \forall\, m = 1, \ldots, P_s \ \neq j \tag{7}$$

where $\overline{W\{\epsilon_j\}}$ is the transform of output sensitivity $\epsilon_j(t, \mathbf{u}(t))$ normalized to negate effects of amplitude. The signature R_j is known as the damage signature as it relates to the actual damage condition. Finally, the signatures are assigned a binary value of 1 or 0 based on the condition (Danai et al., 2011)

$$|\epsilon_j| = \begin{cases} 1 & \sum_{k=1,l=1}^{N,M} \left(t_k^j, s_l^j \in R_j\right) > d \\ 0 & \text{otherwise} \end{cases} \tag{8}$$

The results from this condition do not create a full matrix, like they did for the influence matrix, but rather a single vector representing which sensors were affected by the unknown damage and which were not (Danai et al., 2011). An example of this vector is given by Table 2 from the same simple eight story structure used earlier. Although in a true structure the damage would be unknown to us, for proof of concept we chose the location that the damage occurred to verify that the procedure was isolating damage to the correct location. Application to an actual structure would be dependent on the variations between simulated and actual damage responses. The vector in Table 2 is the

result of damage in the fifth story, calculated with a dominance factor of 1.5. To determine the most likely location in which damage has occurred, we compare the signature vector, found using the damaged response, to the influence matrix, found using the simulated responses using the equation (Danai et al., 2011)

$$\widehat{\Delta C_m} = \frac{\sum_{j=1}^{P_S} |\epsilon_j| \times \left|\frac{\partial \hat{y}_j}{\partial \theta_m}\right|}{\sqrt{\sum_{j=1}^{P_S} (|\epsilon_j|)^2} \sqrt{\sum_{j=1}^{P_S} (\left|\frac{\partial \hat{y}_j}{\partial \theta_m}\right|)^2}} \tag{9}$$

This equation compares the signature vector to the influence matrix column by column. The more similar the vector is to a column, *m*, the higher the value $\widehat{\Delta C_m}$ will be. An exact match between the vector and a column will return a value of 1 (Danai et al., 2011). The highest value represents the most conclusive location that damage has occurred (Danai et al., 2011). For example, in the vector Table 2 is an exact match for the fifth column of the matrix in Table 1. This results in a value of 1 at the fifth floor, the highest that was returned, which easily concludes that the damage was in the fifth floor. The actual damage on story five created the same signatures as the simulated damage on story five which is why the vectors match. The results of equation 9 for each of the other floors are shown in Table 3. The values of 0.866 and 0.707 represent that there was some similarities between the vector and other columns in the matrix which is expected. With only ten outputs it is not uncommon for six or seven of the binary values to match which will return a fairly high estimate. But, the highest estimate, especially an estimate of 1, is almost definitively the location that damage has occurred. None of the other results returned a value of 1 so it can be said that the procedure accurately predicted the damage at the fifth story. It was easy to determine that the vector was an exact match to the fifth

story through visual inspection because of the simplicity of this example, however, as the number of sensor locations increase as well as the number of damage location it becomes increasingly difficult. We must rely purely on the results to tell us the likelihood that damage happening in any one location.

Table 2 - Binary Vector Created from the Response History of the Damaged Structure

Acceleration Output Sensors	Binary Vector Obtained from Damaged Structure
Floor 1	1
Floor 2	1
Floor 3	1
Floor 4	0
Floor 5	1
Floor 6	0
Floor 7	0
Floor 8	0

Table 2 - Damage Estimates given by Equation 9

Damage Estimates for each Story	
Story 1	0.707
Story 2	0.866
Story 3	0.707
Story 4	0.750
Story 5	1.000
Story 6	0.707
Story 7	0.408
Story 8	0.707

Direct Method Results

The following are results obtained reported in Danai et al., 2011 which detail the efficiency and applicability of the Signature Based Damage Isolation Method (SBDIM) for the use on civil structures. The SBDIM was a direct method developed by Professor Danai. These results include the effects of excitation functions, damage location, damage severity, response type and noise.

For the initial case of damage isolation the output sensitivity sensitivities were obtained according to equation 1 in response to a sinusoidal excitation of 0.64 Hz. A frequency of 0.64 Hz was chosen because it was the average of the first and second modal frequencies of the sample structure that was used, 0.442 Hz and 1.182 Hz respectively. The parameter sensitivities were found using a perturbation size $\delta\theta_i = 0.01$ in the stiffness coefficients from the "healthy" response. The baseline "healthy" response was obtained with all elements in the structural model set to a modulus of elasticity of 345 MPa. The sensitivities were transformed and the component signatures were obtained for four dominance factors of $\eta_d = 1.25$, 1.5, 1.75, and 2. The influence matrices for those four dominance factors were then created with a signature size threshold of $d = 5$. The damaged signature was estimated by calculating the output sensitivity of the damaged structure. Since there was not an actual nine story structure to record the damaged response, it was also obtained from the simulated model. Damage was simulated in the model by a 20% reduction in the effective story stiffness by decreasing the modulus of elasticity of the structural members on that story. The damage signature was created for the same four dominance factors and signature threshold size as the influence matrices.

To determine the effects that excitation location has on the SBDIM direct method, a forcing function was applied to each of the nine floors individually and the direct method was performed for each of the excitations. Additionally, to determine the effects of damage location in the structure the direct method was performed for simulated damage in all nine stories. In total there were 81 direct methods performed to account for every excitation floor and damaged story configuration. Furthermore each direct method was performed for both a steady state and transient response. The results of the damage isolation are found in Table 5.

Table 4 – Damage Isolation Accuracies for the Nine Story Model using the Direct Method

		Story Damage Location																	
		1	2	3	4	5	6	7	8	9		1	2	3	4	5	6	7	8	9
Excitation Floor	2	1	1	1	1	1	1	1	1	1		1	1	1	0.5	1	1	1	0	1
	3	1	1	1	1	1	1	1	1	1		1	1	1	1	1	1	1	1	1
	4	1	1	1	1	1	1	1	1	1		0	1	1	1	1	1	1	1	1
	5	1	1	1	1	1	1	1	1	1		1	1	1	1	1	1	0	0	1
	6	1	1	1	1	1	1	1	1	1		1	1	1	1	1	1	0	0	1
	7	1	1	1	1	1	1	1	1	1		0	1	1	1	1	1	1	1	1
	8	1	1	1	1	1	1	1	1	1		1	1	1	1	1	1	1	1	1
	9	1	1	1	1	1	1	1	1	1		1	1	1	1	1	1	1	1	0
	Roof	1	1	1	1	1	1	1	1	1		1	1	1	1	1	1	1	1	0
		Transient Response Accuracy = 100%										Steady-State Response Accuracy = 88%								

In Table 4 a value of 1 represents a correct diagnosis while a value of 0.5 represents a split diagnosis and a value of 0 represents a misdiagnosis. A split diagnosis occurs when the highest damage estimation value returned by the isolation procedure is identical to one or more of the other returned values. This means that the damage

isolation procedure was not able to predict one definitive location where the damage occurred, but rather two locations where the likelihood of damage was split between them. A misdiagnosis occurs when the highest damage estimation value does not coincide with the correct damage location. It is evident from Table 5 that the SBDIM direct method was perfect for transient responses while it was less accurate for steady state responses.

The question then existed if the SBDIM would be affected by a change in the excitation frequency. The same procedure was performed again, this time with a different excitation frequency of 1.50 Hz (the average of the second and third modal frequencies, 1.182 Hz and 2.031 Hz respectively). The results of this case can be found in Table 5. The SBDIM was again perfect for transient responses but slightly less accurate for steady state responses. It is interesting to note that the locations of the misdiagnosis in Table 4 and Table 5 are mostly different, with higher modes missing damage at lower stories and lower modes missing damage at higher stories in general. Although using steady state response may not be as accurate as desired, these results suggest that two SBDIM procedures can be performed at different frequencies to improve the accuracy of the procedure. Both Tables 4 and 5 use a 20% reduction in the effective story stiffness to simulate damage. Table 6 presents the results of the direct methods which an excitation frequency of 0.64 Hz and a reduction in stiffness of only 10% to evaluate the accuracy with different damage states. The results are almost identical to Table 4 with 20% damage. Other than a slight increase in the accuracy using steady state responses, almost all of misdiagnoses occurred at the same locations which suggest that the severity of damage has only a very small effect on the results.

Table 5 – Damage Isolation Accuracies using an Increased Excitation Frequency

Excitation Floor	Story Damage Location																		
	1	2	3	4	5	6	7	8	9		1	2	3	4	5	6	7	8	9
2	1	1	1	1	1	1	1	1	1		1	0	1	1	1	1	1	1	1
3	1	1	1	1	1	1	1	1	1		1	1	1	1	1	1	1	1	1
4	1	1	1	1	1	1	1	1	1		1	0	1	1	0	1	1	1	1
5	1	1	1	1	1	1	1	1	1		1	0	1	0	1	1	1	1	1
6	1	1	1	1	1	1	1	1	1		1	0	1	1	1	0	1	1	1
7	1	1	1	1	1	1	1	1	1		1	0	1	1	1	1	1	1	1
8	1	1	1	1	1	1	1	1	1		1	0	1	1	1	1	1	1	1
9	1	1	1	1	1	1	1	1	1		1	0	1	0	1	1	1	1	0
Roof	1	1	1	1	1	1	1	1	1		1	1	1	1	1	1	1	1	0

Transient Response
Accuracy = 100%

Steady-State Response
Accuracy = 84%

Table 6 - Damage Isolation Accuracies using a 10% Reduction in Stiffness to Simulate Damage

Excitation Floor	Story Damage Location																		
	1	2	3	4	5	6	7	8	9		1	2	3	4	5	6	7	8	9
2	1	1	1	1	1	1	1	1	1		1	1	1	0.5	1	1	1	0	1
3	1	1	1	1	1	1	1	1	1		1	1	1	1	1	1	1	1	1
4	1	1	1	1	1	1	1	1	1		1	1	1	1	1	1	1	1	1
5	1	1	1	1	1	1	1	1	1		1	1	1	1	1	1	0	0	1
6	1	1	1	1	1	1	1	1	1		1	1	1	1	1	1	0	1	1
7	1	1	1	1	1	1	1	1	1		1	1	1	1	1	1	1	1	1
8	1	1	1	1	1	1	1	1	1		1	1	1	1	1	1	1	1	1
9	1	1	1	1	1	1	1	1	1		1	1	1	1	0	1	1	1	0
Roof	1	1	1	1	1	1	1	1	1		1	1	1	1	1	1	1	1	0

Transient Response
Accuracy = 100%

Steady-State Response
Accuracy = 91%

Finally, noise was added to the responses in order to examine the effect it would have on the accuracy of the procedure. Even a small amount of noise can be a significant problem when using wavelet transforms if they happen to pick up shape characteristics that were created by noise and not by damage. Noise was added to the recorded responses at differing levels known as the signal to noise ratio (SNR) and then low-pass filtering was used to reduce the jaggedness of the responses. The results of the diagnosis accuracy are shown in Table 7 which uses an excitation frequency of 0.64 Hz and a 20% reduction in the overall stiffness of the story. As expected noise does considerable damage to the accuracy of the isolation procedure even at low SNRs. There are more advanced methods of noise removal but were beyond the scope of the current research. The values in Table 7 range from zero to nine, each representing the sum of accurate diagnoses at each sensor location. A value of nine signifies that the sensor at that location correctly diagnosed the damage for all nine excitation locations, while a value of zero means that the sensor misdiagnosed the damage for all nine excitation locations.

Table 7 - Total Damage Isolation Accuracy for Excitations at Each Floor when Noise is Included

	Excitation Floors																			
Signal to Noise Ratio	2	3	4	5	6	7	8	9	Roof	Overall Accuracy	2	3	4	5	6	7	8	9	Roof	Overall Accuracy
80-100	6	8	8	9	8	7	7	8	8	76%	5	3	3	4	2	3	6	5	7	42%
60-85	6	8	8	9	8	7	7	8	8	76%	5	3	3	5	2	2	5	6	8	43%
40-65	7	9	8	8	9	8	8	7	9	81%	2	2	2	2	2	3	3	5	6	30%
20-45	3	8	6	5	5	3	5	6	7	53%	2	1	1	1	2	2	4	2	4	21%
0.1-25	1	1	1	1	1	1	2	2	2	13%	1	1	1	1	1	1	2	0	1	11%
	Transient Response										Steady-State Response									

The SBDIM is a conceptually proven method of damage isolation, however, the focus of this thesis is on sensor selection which is a more difficult procedure using the direct method. Since the component signatures are created by comparing the sensor outputs, the component signatures would ultimately change if one or more of the sensors were removed from the analysis. Signatures are created with unique output sensitivities, if two output sensitivities match they are not unique and do not create output sensitivities. But if one of those two sensors was removed a new signature would appear and most likely change the influence matrix. Sensors can be chosen for the direct method but it requires repeating the procedure to verify that these are still the preferred sensors even when the others have been removed. This process could work but is time consuming and costly; the goal of this thesis is to reduce the analysis time. A simpler way of choosing sensors can be performed if the techniques used to create signatures in the SBDIM are altered slightly and the inverse method is used.

Sensor Selection

The direct method compared the output sensitivities from different sensors all from one damage configuration to create the component signatures. Therefore, these component signatures detailed which of the possible sensor locations were most affected by that particular damage configuration. Because each sensor was compared to all the rest, no sensor could be removed without changing the signatures. However, if the sensors are not compared to other sensors, but rather the other outputs from the same sensors due to each damage configuration, sensors could be removed without effect. If the outputs of one sensor were compared against the other outputs of that same sensor for

the perturbation of each of the different parameters then the signatures would not be dependent on how many sensors are used. These new signatures detail which damage configurations can be picked up by that sensor. This is perfect for the inverse method because the inverse method uses the sensor outputs to estimate the parameters. The apparent preferred sensors are those that can detect and estimate all of the possible parameters.

Determining the preferred sensor locations is similar to the direct method in every way but one, which is that now the output sensitivity surfaces are compared. The output sensitivities must be recorded from each sensor for all of the perturbed parameters. The output sensitivities must then be transformed using CWTs as described above. The sensor outputs can then be compared to the other outputs from the same sensor using the equation

$$\left|\overline{W\left\{\frac{\partial \hat{y}_j}{\partial \theta_i}\right\}}(t_k, s_l)\right| > \eta_d \left|\overline{W\left\{\frac{\partial \hat{y}_j}{\partial \theta_q}\right\}}(t_k, s_l)\right| \ \forall\ q = 1, \ldots, R_s \neq j \tag{10}$$

where (t_k, s_l) represents an individual point on the surface $\overline{W\left\{\frac{\partial \hat{y}_j}{\partial \theta_i}\right\}}(t_k, s_l)$ in the time-scale domain and R_s is the number of parameters which were perturbed. Finally, the significant signatures are flagged according to Equation 5 and an influence matrix is created. However, to distinguish this matrix from the original influence matrix it shall be known as the *parameter signature matrix.*

The best locations to position sensors in the structure are determined from an interpretation of the parameter signature matrix (Danai and McCusker, 2010). If one sensor location has many signatures, represented by binary values of 1 in the parameter

signature matrix, it could be a preferred sensor location. For example, if the parameter signature matrix yields that one sensor is able to pick up a change in stiffness for all or even most of the damage locations then it would most likely be a preferred sensor. A sensor in that location would be able to detect a change in the dynamic response caused by damage no matter where damage occurred. On the other hand, if a sensor location has few or no values of 1 in the parameter signature matrix it might not be a preferred sensor location. A sensor location that yields only one or two values of 1 in the parameter signature matrix is only able to detect damage if damage occurs in those one or two locations. It might be beneficial to place a sensor in a different location that has more 1's in the parameter signature matrix. However, if a certain sensor is the only sensor able to detect damage in a certain location then that sensor is necessary in the occurrence that damage happens in that location. The apparent preferred sensor suite does not require every possible sensor, but it does require the minimum number of sensors that can identify damage in every possible damage location. Choosing the best and most cost efficient sensor suite requires positioning sensors so that damage can be readily identified no matter where it occurs without being overly redundant (Yuen et al., 20011).

Using the parameter signature matrices we can easily choose the preferred locations to place sensors in the structure. The most important requirement in choosing the sensor suite is that each parameter (damageable component) is represented with at least one value of 1 in whatever suite you choose. Therefore, the minimum required sensors are those that can populate each column of the parameter signature matrix with a least one value of 1. As long as the suite that is chosen has populated every column with a value of 1 at least one of the sensors will always be able to identify damage not matter

where the damage occurred. If a column in the parameter signatures matrix has no values of 1 for any of the sensors, this means that no sensor is able to pick up a change in the response and the dominance factor may need to be reduced. Reducing the dominance factor decreases the scarcity of the parameter signature matrix, however, it also makes it less substantial and betters the chances of a misdiagnosis (Danai and McCusker, 2010). It is most preferable to choose a sensor suite using the highest dominance factor possible which still populates each column with at least one 1.

The method detailed above provides a way for an engineer to determine the preferred sensor locations in a structure that are most sensitive to changes in the dynamic response due to damage. However, selecting preferred sensors is meaningless without verifying that this method can actually minimize the number of sensors while still allowing damage estimation routines to accurately isolate or estimate damage.

Inverse Method of Damage Estimation

The inverse method of damage estimation, unlike the direct method, has the ability to estimate the severity of the damage as well as isolating its location (Friswell, 2007). Knowing the severity of the damage is a clear advantage to the inverse method, however this process can require more computational effort (Friswell, 2007).

The inverse method modifies the stiffness coefficient of components in a structural model over numerous iterations until the dynamic response of the model matches the dynamic response of the damaged structure. The idea being that if the dynamic response of the model is the same as the dynamic response of the structure, the physical properties of the model and the structure must be the same (Friswell, 2007). This

includes the stiffness of all the structural components. If a structural member is damaged its stiffness will have decreased; this decrease will manifest itself in the updated model as each iteration modifies its characteristics to converge on those in the structure (Friswell, 2007). The iterative procedure used in this research which continuously modifies our model to determine the unknown stiffness parameters is the well-known Gauss-Newton non-linear least squares. This procedure is a form of non-linear regression that fits a non-linear function, which depends on a certain number of parameters, to a known set of data points (Hartley, 1961). The goal of the procedure is to determine the ideal set of parameters such that the curve fits the known data points most closely (Hartley, 1961). In our case the set of known data points is the response of the actual damaged structure and the non-linear function is the response of the model which is dependent on the parameters of component stiffness. Through non-linear least squares we are attempting to determine the ideal set of component stiffness (parameter) that fits the model response (non-linear function) to the damaged structures response (known data points) (Hartley, 1961).

A certain structure may have n number of sensors which therefore produces n outputs for each dynamic response that is recorded. Each output consists of k data points, each data point representing acceleration at a constant time interval throughout the time history of the response. Furthermore, the response of each output is dependent on m number of parameters given by the symbol θ. As the parameters change the outputs change. Each output y_h consists of the data points $x_{1h}, x_{2h}, \cdots, x_{kh}$ (where h = 1, 2, … , n). It is the purpose of non-linear least squares to determine a regression function

$$f(x;\theta) \equiv f(x_1, \cdots, x_k\,;\, \theta_1, \cdots, \theta_m) \tag{11}$$

with a parameter vector θ_i such that the function matches the observed outputs y_h. This is done by finding the difference between the observed outputs and the regression function, and minimizing it. The first regression function uses a trial set of parameters which are continually updated through the minimization process to determine the actual parameters.

To minimize the differences between the observed outputs and regression function the sum of the squares of the differences, $= \sum(y - f)^2$, must be minimized itself. Q is also a variable function of the parameter vector θ_i and therefore must be minimized as a function of these parameters.

$$Q(\theta) = \sum_{h=1}^{n} (y_h - f(x_h\,;\,\theta))^2 = Min \tag{12}$$

It is assumed that the following functions are continuous for all θ:

$$\frac{\partial f}{\partial \theta_i} = f_i(x, \theta); \qquad \frac{\partial^2 f}{\partial \theta_i\, \partial \theta_j} = f_{ij}(x, \theta) \tag{13}$$

Therefore it can be said

$$\frac{\partial Q}{\partial \theta_i} = Q_i(x;\,\theta) = -2 \sum_h (y_h - f(x_h\,;\,\theta)) f_i(x_h\,;\,\theta) \tag{14}$$

$$\frac{\partial^2 Q}{\partial \theta_i\, \partial \theta_j} = Q_{ij} = -2 \sum_h (y_i - f(x_h\,;\,\theta)) f_{ij}(x_h\,;\,\theta) + 2 \sum_h f_i(x_h\,;\,\theta)) f_j(x_h\,;\,\theta) \tag{15}$$

In order to update the parameters we must compute corrections to the parameters which we determine from solving the equations

$$2\sum_{j=1}^{m}\{\sum_h f_i(x_h\,;\,{}_0\theta)f_j(x_h\,;\,{}_0\theta)\}\,D_j = \;Q_i(x;\;\theta) \tag{16}$$

where $Q_i(x;\;\theta)$ is given by equation 13. The equations in (16) were found by substituting a multiple 1st order Taylor expansion of $f(x,\theta)$ into (12). This set of linear equations has a determinant of rank *m,* thus it can always be solved. Solving this set of linear equations yields a vector *D* which is proportional to the correction needed to update the parameter vector θ_i. In order to determine at which proportion the corrections should be adjusted we consider the equation

$$Q(v) = Q\big(x,\;{}_0\theta + v\,D\big), \qquad for \qquad 0 \le v \;\le 1 \tag{17}$$

where *v'* will be used to donate the value of *v* such that $Q(v)$ is a minimum. Therefore the new parameter vector will be defined as

$${}_1\theta = \;{}_0\theta + v'D \tag{18}$$

With this new vector of parameters the iterative process can begin again resulting in a new vector ${}_2\theta$ and so on until the parameter values converge to constant values. In time as the iteration is performed the new parameter vector will yield a minimized function of $Q(x,\theta)$ such that

$$Q(x,{}_\infty\theta) \;\le\; \cdots \le Q\big(x,\;{}_1\theta\big) \le\; Q\big(x,\;{}_0\theta\big) \tag{19}$$

To start, a record of the damaged structures dynamic response is necessary. Ideally, a sensor suite will have been chosen for the structure and the response recorded using those sensors. A dynamic finite element analysis must be performed on a computer model of the structure to get its response. Again, it is necessary to use the same forcing

function for both the actual structure and each analysis of the model. The starting values of the component stiffness in the model are not critical for the procedure, however, the closer they are to the actual values in the structure the quicker the convergence. Without knowing which components stiffness have been decreased the stiffness associated with a non-damaged structure could be used as a reasonable starting point. If some knowledge of damage is available a better estimate for component stiffness can be made. Each non-linear least squares analysis will return new values of the component stiffness which must be put back into the model so that a finite element analysis and non-linear least squares analysis can be performed again. As the method converges each iteration will return a more accurate stiffness until the procedure converges to the actual stiffness. The accuracy of this method can be determined by taking the cumulative differences between the final models response and the damaged structures response (Hartley, 1961). If the model's response fits to the damaged response closely the cumulative difference between the responses will be minimized. Depending on the cumulative difference value we can judge the accuracy of the component stiffness. A component that has stiffness similar to a healthy structure is obviously healthy, while a component with a decreased stiffness would be considered damaged. The percent that the stiffness decreased from that of a healthy stiffness is an indication of the severity of the damage in that component.

CHAPTER III

CASE STUDIES

The analytical case studies of this thesis focus mainly on the findings associated with adapting the sensor selection process and the inverse method for the use on civil structures. Danai et al. 2011 reported work that has been done to adopt the direct method for the use on civil structures, results of which were included in the introduction as supplemental background information for this thesis.

Two structures to be used as the sample buildings, chosen for their prior usage on projects in the field of sensor selection and seismic research, were modeled using the structural analysis program OpenSees. The first structure is a simple, eight-story frame. The second is a slightly more complex, multi-bayed, nine-story structure. These structures were ideal for this project because they could be modified quickly for whatever purpose was required in the project but they were simple enough that a finite element analysis could be performed reasonably quickly. Additionally, the nine-story structure offered realistic characteristics of an actual structure, while the eight story building offered more optimal dynamic characteristics.

After a thorough investigation of this method with the purely analytical models, it was further tested on data from physical models. These physical models added the variables of noise and modeling error which were not accounted for with the analytical models but would be present during real world testing. The research utilized reported results from previous research which had excited a structure both pre and post damage. A downside of using existing test data is that there was no control of the structure or how

it was tested, the only usable information was the data that was reported by the researchers at the time the project was performed.

The physical model data was obtained from the Network for Earthquake Engineering Simulation (NEES) database of archived projects. The project that was chosen was a study originally preformed to investigate the interactions between a reinforced concrete frame and shear wall during strong earthquake excitations. The project was performed during May of 1979 at the University of Illinois at Urbana-Champaign. All available information about the project including publications, recorded data, drawings and photographs can be found in the NEES database at http://nees.org/warehouse/project/1019. The particular project was chosen from the many available in the NEES database because it provided the dynamic responses of the test structures to various magnitudes of earthquake excitations both before damage occurred and subsequently after different stages of damage. Additionally, that project provided detailed drawings of the damage that occurred in the structures after each excitation which would be useful when verifying the results of the damage estimation procedure. Finally, the structures which the research team used were relatively simple models that were applicable for use in this current sensor selection project. The research team designed and built four tenth scale reinforced concrete structures which were outfitted with a full set of accelerometers, LVDTs and stain gages to record accelerations, displacements and forces at multiple locations on each floor.

The previous research provided the necessary damaged responses of the structures which could ultimately be used by the damage estimate procedure to approximate where the damage occurred. But since this current research is focused on minimizing the

required sensors to correctly estimate damage the sensor selection process needed to be performed first. An analytical model which matched the physical model as closely as possible was developed in OpenSEES based on the specifications which were provided in the available publications. Using the newly created analytical models of the structures, preferred sensors could be chosen. Next, using only the responses generated by those preferred sensors on the physical model the damage in the structure was estimated. By verifying that the damage estimated by the damage estimation routine matched the actual damage that was reported in the previous research it could prove that the preferred sensor suite is a better fit to estimate damage than other sensors.

Eight Story Model

The eight story model (Figure 7) is a two-dimensional single-bay structure. The model characteristics were taken from a previous sensors optimizations study (Yuen et al. 2001) which investigated modal characteristics rather than the dynamic response. The original model from Yuen et al. was a simple mass-spring structure which was modified for this project to a simple frame structure. Although the shape of the model was updated the dynamic properties were kept the same, most importantly the stiffness to mass ratio of 1160 s^{-2} which creates a fundamental natural frequency in the structure of exactly 1.00 Hz

Each story in the structure consists of two massless columns of identical stiffness connected laterally by a rigid girder. The rigid girder was assigned a lumped mass which was equivalent for each story. The columns in the structure were fixed to the rigid girders with a moment connection at each end. The columns on the bottom story were fixed to

the ground. The girders assigned infinite rigidity so that the stiffness of each story was independent of the stiffness any other story. Therefore, if the column stiffness of one story was decreased to simulate damage it would not change the column stiffness on any other story. The structural modeling was done in OpenSees using completely elastic beam elements for all of the structural members. Each of the columns was assigned a 3.05 m (10 ft) length and a modulus of elasticity of 200 GPa (29000 ksi). The girder span between the columns was 9.14 m (30 ft). The girders were assigned infinite rigidity by constraining the rotational degrees of freedom at each of the girder-column connections. Each column was assigned an area of 929 cm^2 (144 in^2) resulting in a moment of inertia of 71,925 cm^4 (1728 in^2). Because the columns were fixed at each end the resulting stiffness of each column was 30.47 MN/m (174 kips/in). Because each story had two columns, the effective stiffness of each story was twice that of a column, or 60.94 MN/m (348 kips/in). Each of the rigid beams was assigned a mass of 52,540 kg (0.3 kip-s^2/in) and the columns were left massless. The resulting stiffness to mass ratio of each story was 1160 s^{-2} which produced a fundamental natural frequency in the structure of exactly 1.00 Hz.

Damage was introduced to this model as a reduction in the overall stiffness of an entire story. Therefore there were eight possible damage locations in this structure. The stiffness of a story was decreased by reducing the Modulus of Elastic (E) of both columns by a prescribed amount. The stiffness reduction is not cause specific and could represent distributed damage throughout a story or localized damage. Damage could be due to an extreme event or long term deterioration. The conceptual application is applied to a

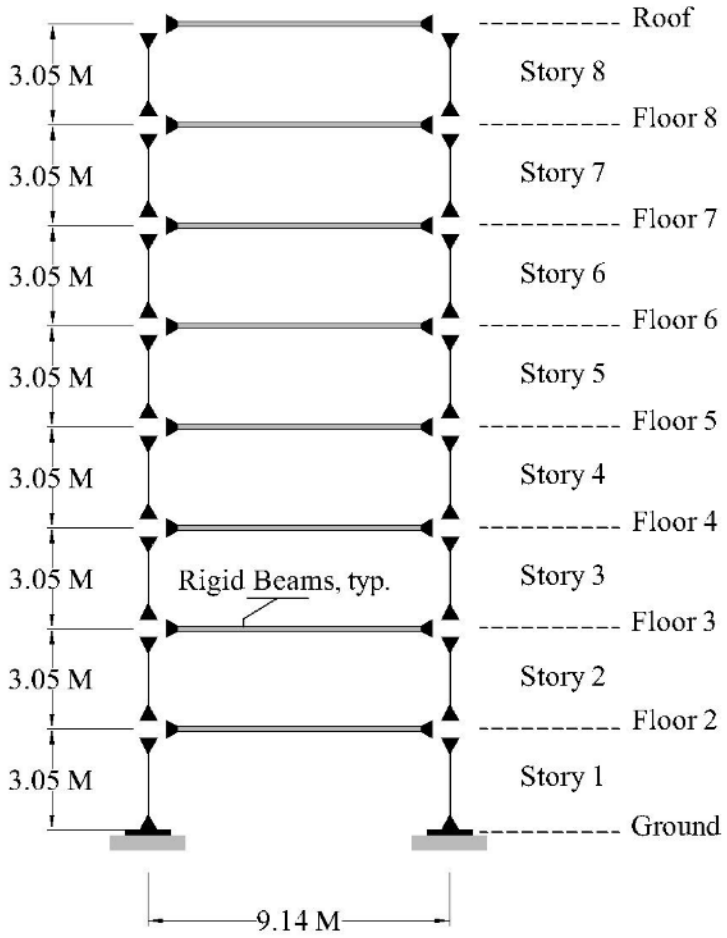

Figure 7 - The configuration of the eight story building model

situation where a building is instrumented and readings are taken for a baseline initial ``non-damaged" condition (such as immediately after construction, but could be any point prior to measured damage) and a post damage reading. One possible option, and the most likely option for practical applications, was to excite the structure using an eccentric mass shaker such as those available as part of the Network of Earthquake Engineering Simulation facilities at UCLA (http://nees.ucla.edu/shakers.html). To simulate the eccentric mass shaker, lateral sinusoidal time series forcing functions were applied at individual nodes of the model. These forcing functions were applied at a specific

magnitude, frequency and duration to produce a dynamic response in the structure. Another option was to use ground excitation such as an earthquake record. Although this option may not be practically feasible it was still beneficial to examine from a conceptual standpoint.

SAC Nine Story Model

The second model that was used as part of this research was a nine-story building frame with a basement. The structure that this model was taken from was developed as part of the SAC Phase II research initiative as described by Ohtori et al., 2005 as a reference for benchmark structural evaluations. While the eight story model used non-specific physical properties to achieve an optimal natural frequency, the physical properties of this model reflects those of material that would be used in an actual structure.

The SAC building consists of perimeter steel moment frames designed to meet seismic design requirements in Los Angeles, California. The model that was used in this project was a single North-South moment resisting frame of the SAC structure as shown in Figure 8. The modeled masses on the frame (one of two frames that would be provide for the North-South direction lateral resisting system) were 4.825 x 10^5 kg (2.75 kip-s^2/in), 5.050 x 10^5 kg (2.88 kip-s^2/in), 4.945 x 10^5 kg (2.81 kip-s^2/in) and 5.350 x 10^5 kg (3.05 kip-s^2/in) for the first floor, second floor, third to nineth floors and roof, respectively. Column splices shown in the figure were included as weighted averages of the above and below column properties within the story height, similarly to Ohtori et al., 2005. Column sizes and girder sizes vary throughout the height of the building,

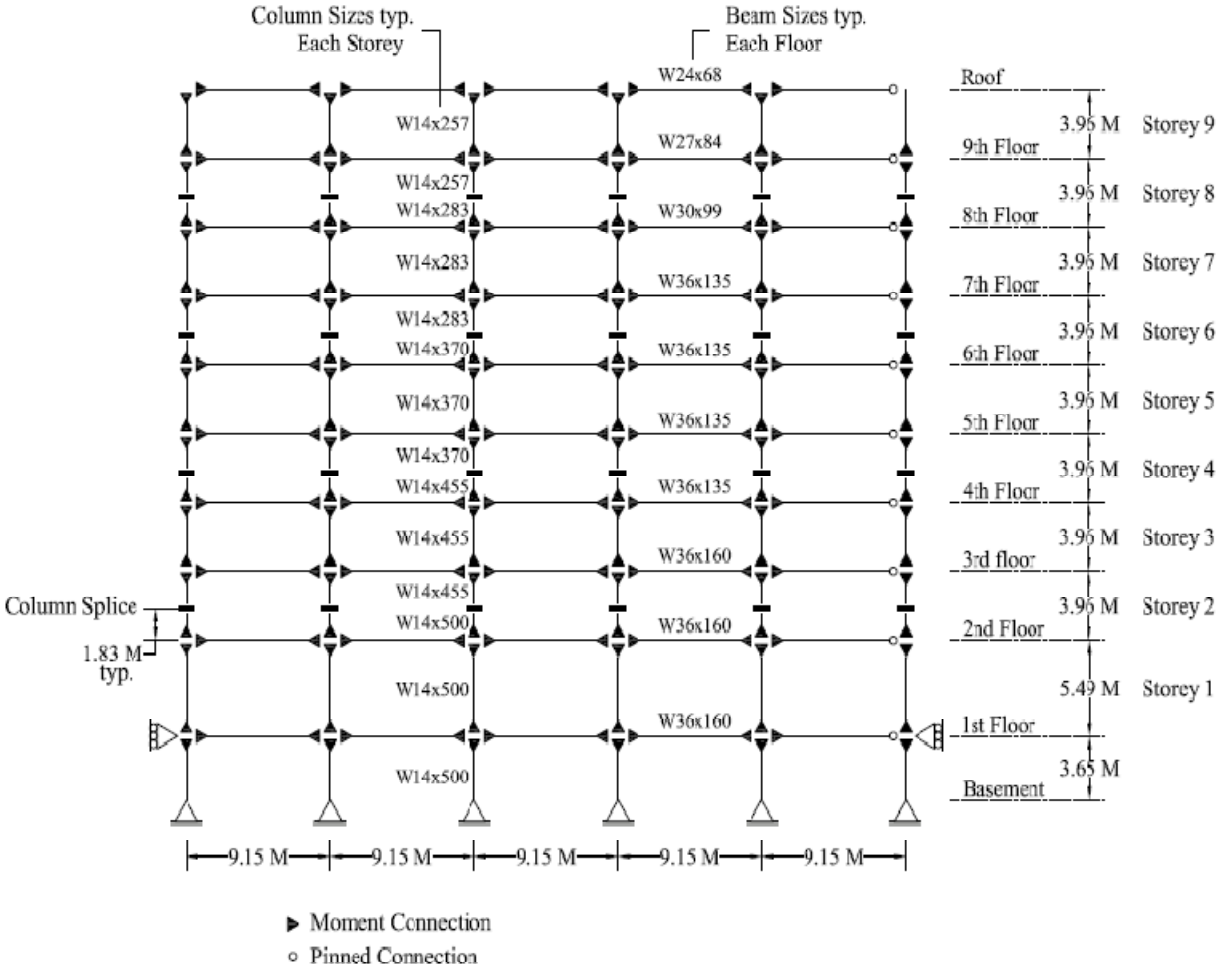

Figure 8 - The configuration of the SAC nine story building model

remaining similar at each floor level. Column and girder steel is modeled with a modulus of elasticity of 345 MPa (50.0 ksi), with non-linear material properties (strain hardening included), and non-linear geometric (P-Delta analysis) included in the analysis. Beam and

column elements were modeled as fiber element W sections using nonlinear beam-column elements which allow for spread of plasticity in members. It is important to note that non-linear behavior was included in the model to capture behavior under full seismic loads being considered in other phases of the research project. However, all analysis for damage isolations reported in this paper is within the material elastic range of behavior. This was verified by comparing results to models with elastic material behavior and first-order analysis.

Similar to the eight-story model, this model was excited using forcing functions which were positioned at nodes throughout the structure to simulate eccentric mass shakers. Ground motion was also used to simulate an earthquake event, but in a limited capacity as it would not be practical for real world applications.

Sensor Selection with the Inverse Method

The method of sensor selection that is used in this research relies on the parameter signature matrix to determine the sensor suite. Since the influence matrix is found using the direct method it will therefore be related to the direct method. If a sensor suite was to be chosen for the direct method, the suite that provided identifiability throughout the entire structure should result in the highest likelihood of the direct method isolating damage. However, the inverse method itself is not directly related to the parameter signature matrix. Although the suite is the group of sensors which are most influenced by damage, the inverse method does not necessarily require exactly that suite in order to work such as the direct method would. The preferred sensors are more of a suggestion

when it pertains to the inverse method rather than a requirement as with the direct method.

The inverse method may be able to estimate damage using fewer sensors than is suggested by a preferred suite or it may require more. The reason that this can occur is because the parameter signatures, which are used to create the parameter signature matrix, are created using only the most unique characteristics in the output sensitivities. If two sensors record responses with similar output sensitivities those output sensitivities will mask each other because they are not unique and therefore would not show up in the signatures. The direct method requires the unique output sensitivities in order to work which is why it is so dependent on the influence matrix, but the inverse method can work with even the small and repetitive changes that may not show up as unique signatures. However, this doesn't mean that the parameter signature matrix is not important to the inverse method. It is intuitive to think that more unique signatures will allow the inverse method to converge to the correct parameters quicker and more accurately. It can also be assumed that sensors with unique changes must also have smaller changes which did not show up as a signature but can still help the inverse method converge. It is the primary purpose of this research to determine the validity of these assumptions and determine the usefulness of the parameter signature matrix when choosing a sensor suite for use with the inverse method.

Additional Cases

Supplemental case studies were also performed in this project to investigate the many factors that can affect the outcomes of the sensor selection and damage estimation

procedures. The investigation of these factors was to determine valuable insight into the feasibility of implementing these procedures for real world applications. These factors include how and where the structure is excited in order to create the dynamic response, the use of transient versus steady state responses and the severity of damage.

Excitation Functions

A wide range of forcing functions were evaluated in order to determine which forcing functions were optimal for both the structure and the estimation procedures. Included in these forcing functions were simple sinusoidal waves with a constant frequency, sinusoidal sweeps over a wide frequency range, impulses and a number of earthquake records. Furthermore, the forcing functions could be applied to ground motion or at any of the floors in the structural models.

For the sensor selection or damage estimation procedures to work properly, an identical excitation function must be used to obtain the undamaged and the damaged responses. The excitation functions that can be applied to a computer model are nearly unlimited, but they are limited in application to an actual structure. The placement of a vibration generator in a structure is limited by the space and accessibility in the structure, while the frequency and amplitude of the vibrations are limited to the capacity of eccentric mass shaker. Secondly, ground motion can be eliminated as a means of exciting the damaged structure because it is impossible to predict the time or response of the earthquake before it occurs or obtain identical excitations at different points in time. Therefore, the most practical excitation configuration would be a sinusoidal forcing function. In an existing building the roof would be the most accessible location to place a

vibration generator though would most likely need a crane in order to lift it into position. However, as the research has shown, this is not always the ideal configurations for these models. If a structure were designed to accommodate a lifelong monitoring plan a wide range of excitation source locations could be designed for implementation.

It can be shown that the preferred sensor suite for a structure varies depending on the excitation type. By changing the placement of the forcing function as well as other characteristics such as its frequency, the parameter signature matrix change, and therefore so does the sensor suite. It has also been determined that some excitation functions create a more preferred sensor suite than others. Table 8 shows two parameter signature matrices, both created with a dominance factor of 1.5 for an excitation at the second floor and an excitation at the roof of the nine story model. It is shown in the table that a full range of damage detection (unique signatures) requires only sensors at floor three, six and seven while using a second floor excitation. However sensors at three, four, six and eight are required to detect damage while using roof excitations. It is also possible to select other combinations of floors which would also provide a sensor suite.

Table 8 - Sensor Suites for Excitations at the Second Floor and the Roof

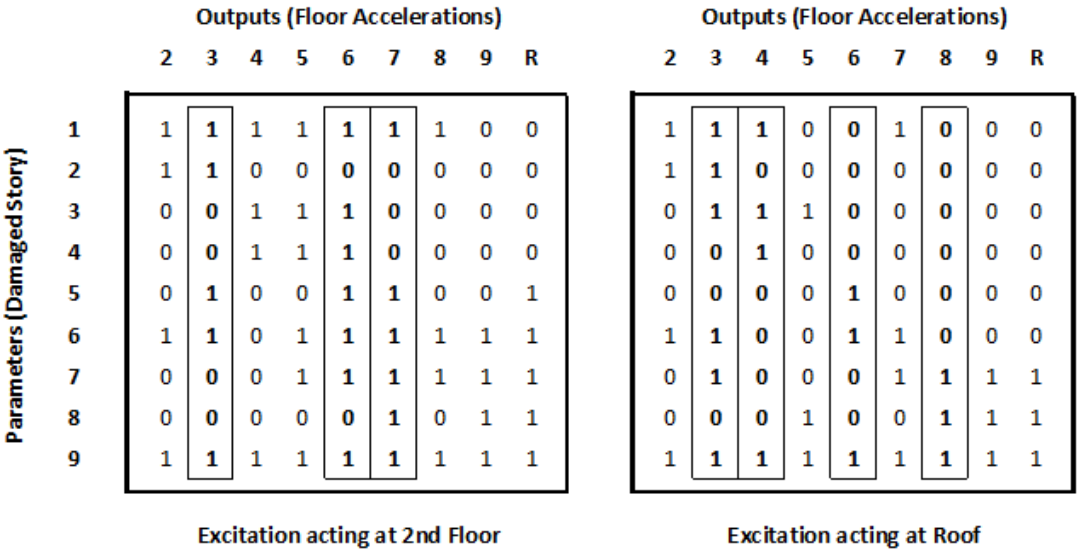

Another determination which needs to be considered when performing damage estimation is what type of response will be used. From a practical stand-point the steady state response is much easier to acquire in the field with confidence of repeatability. However, because of the uniqueness of the transient response, it provides the estimation procedures with data which is better for isolating and estimating damage. The problem with the transient response is the difficulty of recording a consistent transient response from the actual structure that can closely match the response of the computer model.

A transient response has a seemingly random and non-repetitive pattern of motion while the steady state response is consistent and unchanging. Therefore, the output sensitivity that occurs in the transient region is also non-repetitive while the output sensitivity from the steady state region of a sine wave falls into a cyclical pattern. A transient response will yield more unique parameter signature which provides the sensors with better identifiability. This does not mean that a steady state response will not

provide identifiability, and therefore could still be used. The reason that a transient response is so hard to properly acquire is because of the variability of the vibration generators. On a computer model a force can be applied instantly at any amplitude and in any direction, however a vibration generator does not have those capabilities. They cannot apply force instantaneously and must accelerate from a static position before being able to apply the desired amount of force. Applying a forcing function to the simulated model that can exactly match the forces created by a vibration generator in the initial instances is very difficult but critical to the procedure. Steady state is preferred because a response will always reach a constant steady state no matter how different the initial stages of the forcing functions began. However, it would also be considered transient to capture data as a temporal section of data during which the excitation is changing, such as a transition from one steady state excitation to another.

The frequency of the forcing function also has an effect on the optimum sensor suite. However, precautions must be taken not to excite a structure at or near a modal frequency which could incite resonance and possibly cause more damage in the way of plastic deformations in the structure. To prevent this, the model structures were only excited at frequencies which occurred at the median of any two adjacent modal frequencies i.e. the average frequency of the first and second modes, the second and third modes etc. In an attempt to eliminate the need to run analyses at each individual frequency a sine sweep function was also modeled. The function continuously increased frequency as it gradually swept through each desired frequency range in one analysis. The sine sweep provided some valuable information. It was determined that the frequencies beyond the third mode were so high that the finite element analysis could not

get an accurate representation of the dynamic response. The analysis used time steps of .01 s while the modal periods associated with higher modes became just as small or even smaller. In order to achieve an accurate record of the response the time steps in the finite element analysis would need to be refined greatly which was too costly in a computational perspective to be feasible. Because the responses yielded by excitation frequencies greater than the third mode were not representative of what the actual responses would be, the parameter signature matrices that were created using those responses were not useful in damage identification.

In order for the swine sweep to be effective it must be adapted to sweep through only the frequency range of the first three modes of the structure. There are two apparent benefits that can be gained by using a sine sweep. The first is that if the sweep is gradual enough it can incite a response that is very close to steady state for a wide range of frequencies all in one analysis. The response will reach steady state (or be very close to it) when the frequency of the sweep is below the first mode, between the first and second modes and between the second and third modes. Instead of exciting the structure with three different constant frequencies individually, the same responses can be obtained with one excitation. However, the sweep must be gradual enough so that the response is able to reach steady state before the frequency changes too significantly. The second benefit occurs when the frequency sweep is too quick to allow steady state to develop. If steady state cannot occur, then the response is a true transient response. Transient responses are generally more difficult to control in an actual application and replicate however using a sine sweep at a designated rate would be feasible.

Physical Test Models

The test structures that were utilized in the physical test data phase of this project where taken from a previous research project entitled "Experimental Study of Frame-Wall Interactions in Reinforced Concrete Structures Subjected to Strong Earthquake Motions" (found in the NEES database at http://nees.org/warehouse/project/1019) performed at the University of Illinois of Urbana-Champaign by Daniel P. Abrams and Mete A. Sozen. While the focus of this previous project was not on sensor selection or damage estimation, the data that was recorded and archived were nearly ideal for the purposes of this project. The models used were large and detailed enough to be a fairly accurate representation of a real world structure while not being too complex to complicate modeling or analysis. Additionally, the data that were provided included detailed dynamic responses of each structure to various earthquakes both before and after damage occurred at multiple locations throughout the structures. This data was thought appropriate to be used in, and to verify, the damage estimation procedure as long as the sensor selection procedure could be accurately performed using the analytical models.

The purpose of the original research performed by Daniel P. Abrams and Mete A. Sozen was to study the response of reinforced concrete structures that were subjected to various earthquake motions. Additionally, during their research they began to investigate superior methods of analysis in the design of structures in the non-linear response range. The study consisted of subjecting the reinforced concrete structures to simulated earthquake motions from a shake table and recording the floor acceleration responses and other global response characteristics. Four reinforced concrete structures were tested during the investigation. All of the four structures had the same geometry, consisting of two ten-story three-bay frames in parallel with a slender structural wall. The structures

varied only in the arrangement and amount of reinforcing steel designed in the structures and therefore the expected levels of damage to be sustained under high excitations. The dynamic responses of the structures were captured at each floor during ground motion excitation using accelerometers, LVDTs and strain gauges to measure accelerations, displacements and resisting forces respectively. Results observed from the original research verified that a newer method of calculating the design strengths of reinforced concrete members was accurate while conventional methods were too conservative. Additionally, a simpler method of determining displacement maxima using a linear response model with arbitrarily softened members was proven to be acceptable.

The four test structures were designed and built at the University of Illinois at Urbana-Champaign by the project team. All four test structures had the same geometry, however two structures were designed with less reinforcement and designated as the lightly reinforced models and the other two structures were designed with greater reinforcement and designated as the highly reinforced models. The geometry of each structure consisted of two 2-dimentional frames and a single slender structural wall acting together in parallel to resist lateral forces and motion. Each frame was ten stories tall with an individual story height of 229 mm (9.02 in) for a total height of 2.29 m (7.51 ft). Each frame also consisted of three bays with an individual bay length of 305 mm (12.0 in). The frame columns had a depth of 51 mm (2.0 in), the frame beams had a depth of 38 mm (1.5 in) and the thickness of the entire frame was also 38 mm (1.5 in). The structural wall had a total height of 2.29 m (7.51 ft), a depth of 203 mm (7.99 in) and a width of 38 mm (1.5 in) (Figure 9). The two frames were placed 914 mm (36.0 in) apart in parallel with a single structural wall placed directly in the center, also in parallel. Both the frames and

the walls were fixed to the base of the shake table. A description of the anchorage used to fix the base of the structure to the shake table can be found in Figure 10. The frames and wall of each structure were connected by a 465 kg (2.65 lb-s^2/in) rigid steel diaphragm at each floor level so that the lateral displacements would be equivalent in both the frames and wall. The rigid diaphragm for a single floor was connected to the frames at each of the eight beam-column intersections on that floor level. It was also connected to both sides of the structural wall at that floor level. It is important to note that even though the connections between the diaphragm and frames were fully fixed translationally, they did not provide any resistance to joint or wall rotations.

Any differences between the test structures were entirely in the design of the steel reinforcement. The reinforcement designs were specifically chosen for the purposes of the original project. The two heavily reinforced structures were designed in accordance

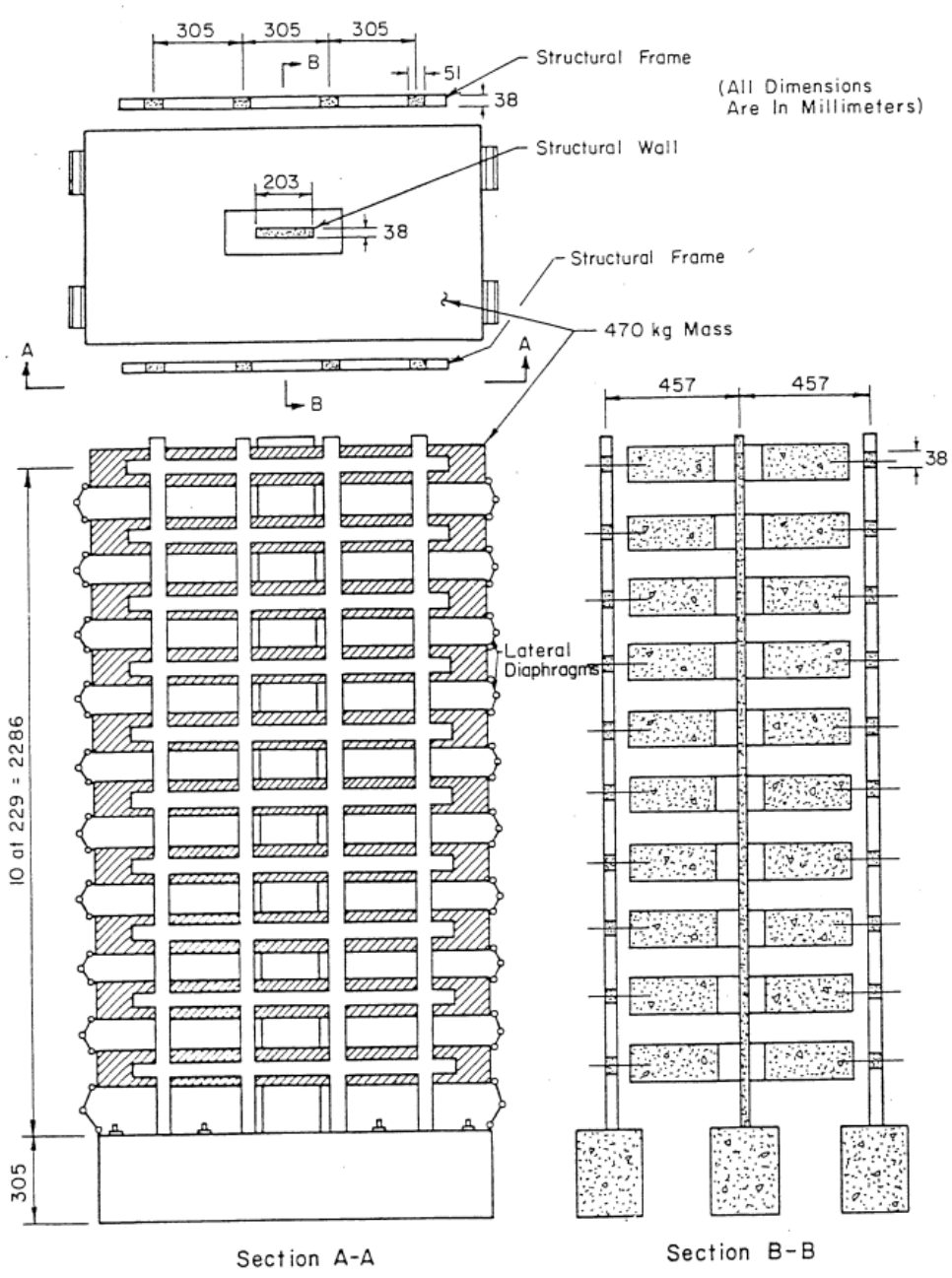

Figure 9 - Dimensions of Physical Structure (Sozen, 1979)

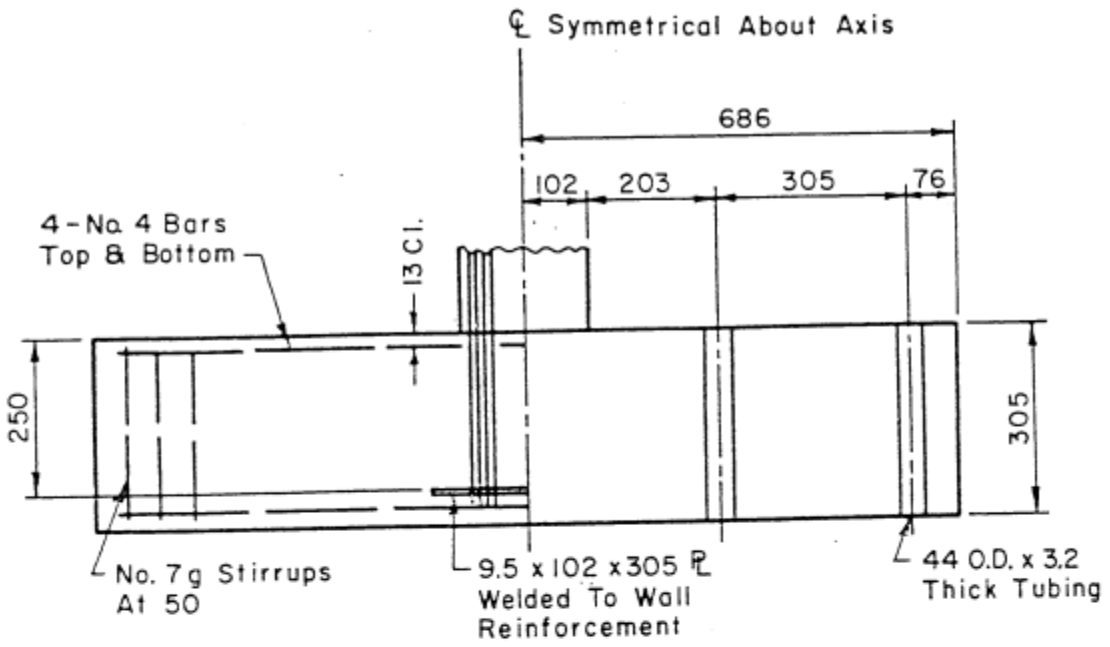

Typical Wall Base Anchorage

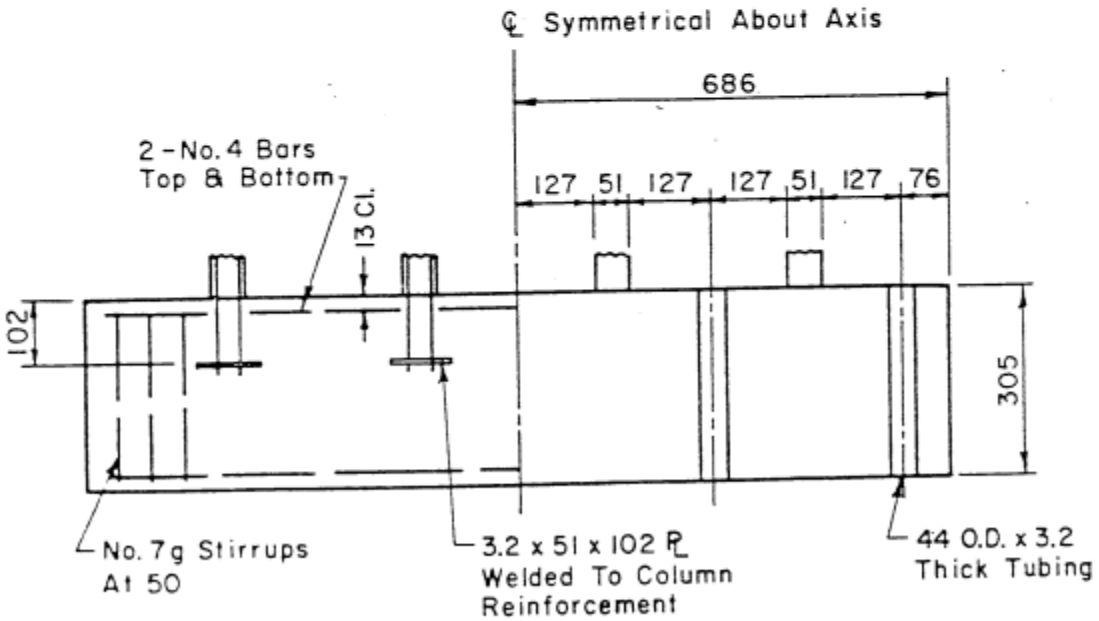

Typical Frame Base Anchorage

(All Dimensions In Millimeters)

Figure 10 - Typical Base Anchorage (Sozen, 1979)

with the standard design processes of the time and determining element stiffness based on cracked section properties. The other two structures, which were considered lightly reinforced, were designed using arbitrarily reduced element stiffnesses in order to induce nonlinear behavior in certain members of the structure as well as promote a more "economical distribution of strength." Both of the lightly reinforced structures were designed with the same reinforcement scheme making them identical structures. Similarly, the heavily reinforced structures were both identical as well. The major differences in the reinforcement design between the heavily and lightly reinforced structures took place in the structural wall, however there were slight differences in the reinforcement of the frames as well. The lightly reinforced wall simply had four No. 2 gage bars the entire height of the wall with No. 16 gage stirrups. The heavily reinforced wall had sixteen No. 2 gage bars for the first four floors, eight No. 2 gage bars from floors four to six, and four No. 2 gage bars for the remaining height of the wall with additional No. 16 gage stirrups in the first four stories. The reinforcement in the frames consisted entirely of No. 13 gage wire with No. 16 gage stirrups however the amount of reinforcement varied based on the floor level and in which structure it was being used. A detailed description of the wall and frame reinforcement schedules for both the lightly and heavily reinforced structures can be found in Figures 11, 12, and 13.

The primary base motions that were used to excite the structures were the north-south component of the 1940 Imperial Valley Earthquake measured at El Centro, California and the N21E component of the 1952 Tehachapi Earthquake measured at Taft, California. The El Centro ground motions were applied to one of the lightly reinforced structures and one of the heavily reinforced structures. After exhaustive testing was

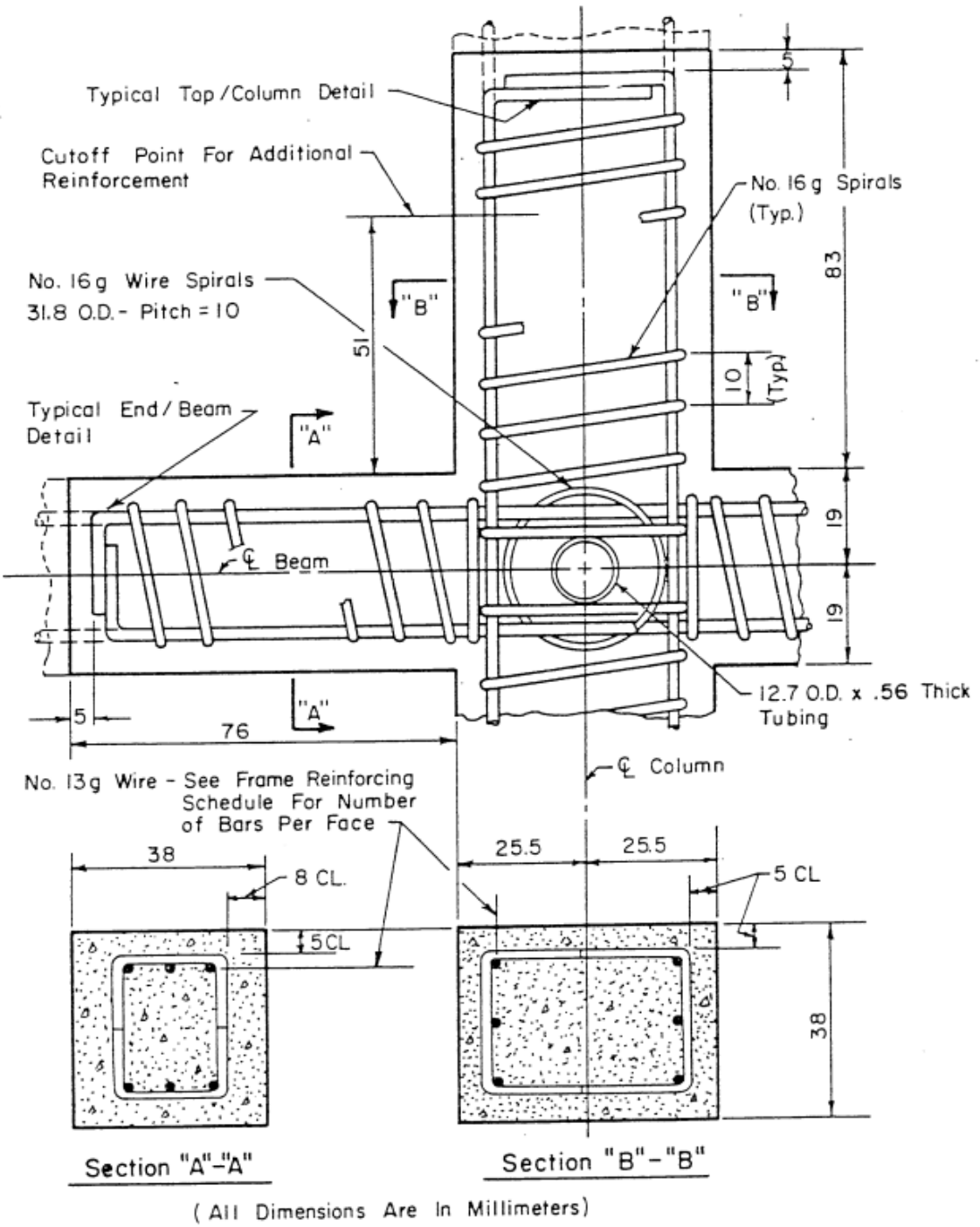

Figure 11 - Frame Reinforcement Schedule (Sozen, 1979)

FRAME REINFORCING SCHEDULE

Number Of No.13 g Wires Per Face

Story Or Level	Structure With Heavily Reinforced Wall			Structure With Lightly Reinforced Wall		
	Beams	Exterior Columns	Interior Columns	Beams	Exterior Columns	Interior Columns
10	2	2	3	2	2	2
9	3		3	2		
8	3		2	2		
7	3			3		
6	3			3	2	
5	3			3		
4	2			3	3	
3	2			3		
2	2	2	2	2	3	2
1	2			2		

Figure 12 - Amount of Frame Reinforcement Wire Per Face Per Floor (Sozen, 1979)

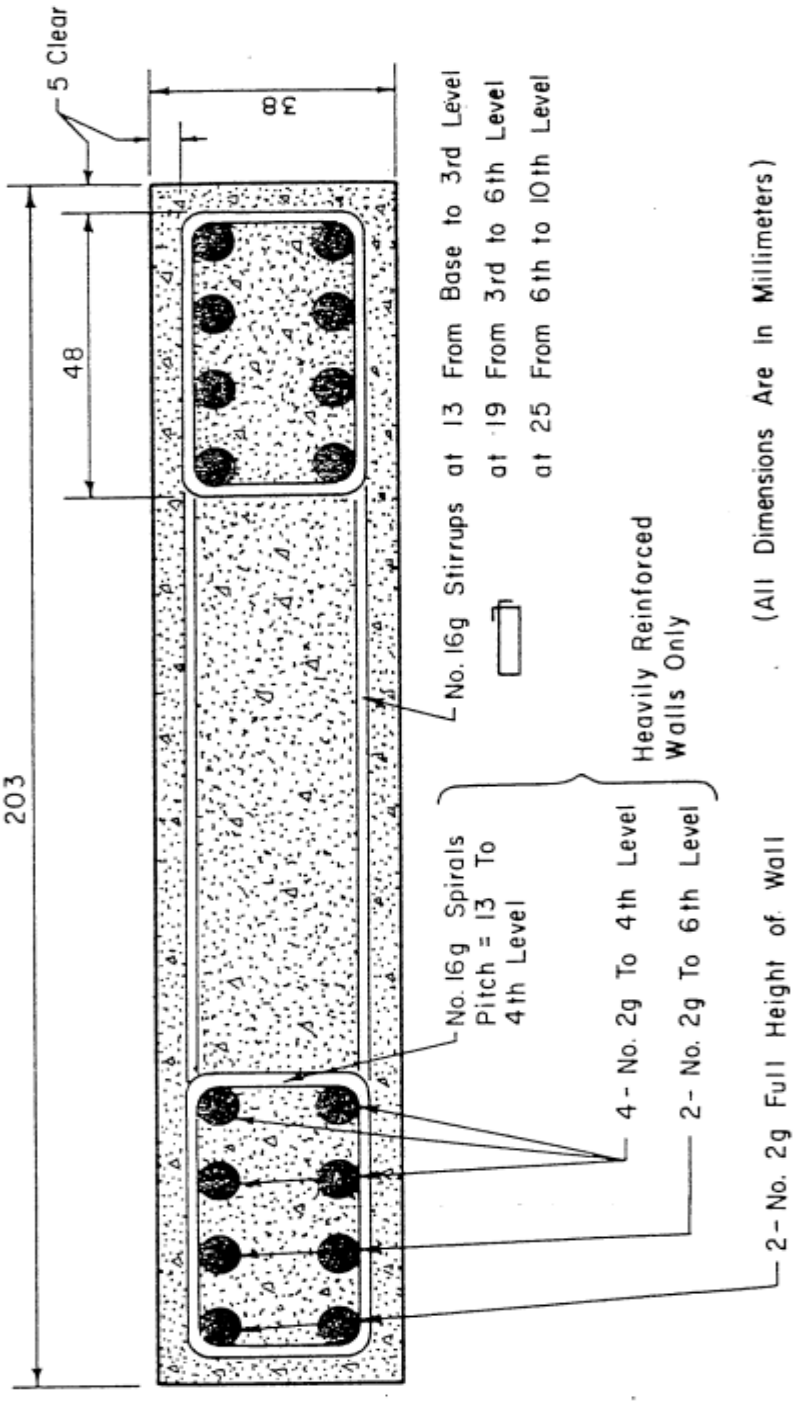

Figure 13 - Wall Reinforcement Schedule (Sozen, 1979)

completed on the first two test structures using the El Centro record, the remaining two structures were then excited similarly with the Taft ground motion record. However, before the structures were excited by any ground motion records the estimated natural frequencies of the structures was determined and the records were modified such that the frequency content of the records better matched the natural frequency of the structures. This was done by compressing the time scale of both records by a factor of 2.5. The intensity of the initial ground motion excitations was chosen such that the stress in the reinforcing steel of the models would approach but not surpass the yield stress. This was apparently determined based on testing of an analytical design model. The intensity of subsequent tests was increased by two and then three times that of the initial tests in order to produce significant yielding and non-linear behavior. Additionally, directly following the earthquake simulations, a low-amplitude steady-state ground motion was applied to the structures, but only for those being tested with the Taft Earthquake. Finally, before and after each ground motion test the structures were subjected to low-amplitude impulses to study their free vibrations responses. The data obtained from this previous research provided numerous response records at multiple damage states due to multiple excitation inputs. Therefore, this would allow for investigations to be performed on the effects of excitation type and amount of damage. It is important to remember that even though many responses are being investigated only one response from the damaged structure is ideally required in order to estimate the damage.

To begin verifying the preferred sensor selection method using physical test data it was crucial to first create an accurate and reliable replication of the physical models in an analytical form. As was discussed earlier, an analytical model is needed for the

preferred sensor selection process because parameters in the structure, in this case story stiffnesses, are required to be perturbated. It is extremely important that the analytical model match the physical structure as closely as possible in order for the entire process to work accurately.

An analytical model of the test structures was built by the original research team but was used primarily for design purposes to estimate maximum displacements and stresses during excitation. Since that design model was created prior to the test structures being built it was likely that the stiffnesses of some members or the moduli of elasticity of some materials in the test structures differed from that of the analytical model. However, even a slight difference between the physical model and analytical model could result in a large enough difference in the dynamic responses that the preferred sensors chosen using the analytical model many not accurately reflect the actual preferred sensors of the physical structure. Therefore it is critical to create the analytical model using the as-built specifications of the physical structure and matched to the dynamic properties of the undamaged structure rather than simply the design specifications.

A number of different models were created and used for this phase of testing. These models ranged from very simple to fairly complex in order to evaluate the model complexity required for sensor selection. The ideal model, it was thought, would be one that closely and consistently replicated the dynamic response of the physical structure regardless of the input excitation but was also as simple as possible to reduce analysis time during sensor selection or damage estimation. The first models were simple two-dimensional models which combined the two frames into one and placed the wall in series with the frame. This was the configuration of the analytical model from the

original project. The more complex models captured the physical three-dimensional characteristics of the actual tested structures. Each of these models consisted of a variety of element types ranging from linear to non-linear beam-columns, joint connections, diaphragm connections and fixities. A more detailed description of the models is presented in the following sections. All analytical models of the test structures were created using OpenSees structural analysis software.

Two-Dimensional Models

The geometry of the two-dimensional models was based on the configuration of the analytical model created for the original project. A drawing of that model can be found in Figure 14. The models consisted of a single ten-story three-bay frame and a single ten-story structural wall having the same dimensions as the frames and walls in the actual structures. Although the actual test structure set-up was a three-dimensional configuration, motion was only applied in a single lateral direction parallel to the major axis of the frames and wall and therefore the elements of the analytical model could be compressed into a single two-dimensional plane, i.e., the frames and wall could be set up in series rather than parallel without affecting the response. Additionally, instead of using two frames, a single frame with double the stiffness would ideally provide the same response for the reason listed above.

The simplest of the two-dimensional models was a completely linear elastic model with fully fixed connections at the base of the frame and wall. The frame and wall were connected by rigid beam elements at each floor in order to ensure equal lateral displacements between the frame and wall. The rigid beams utilized pin-pin connections

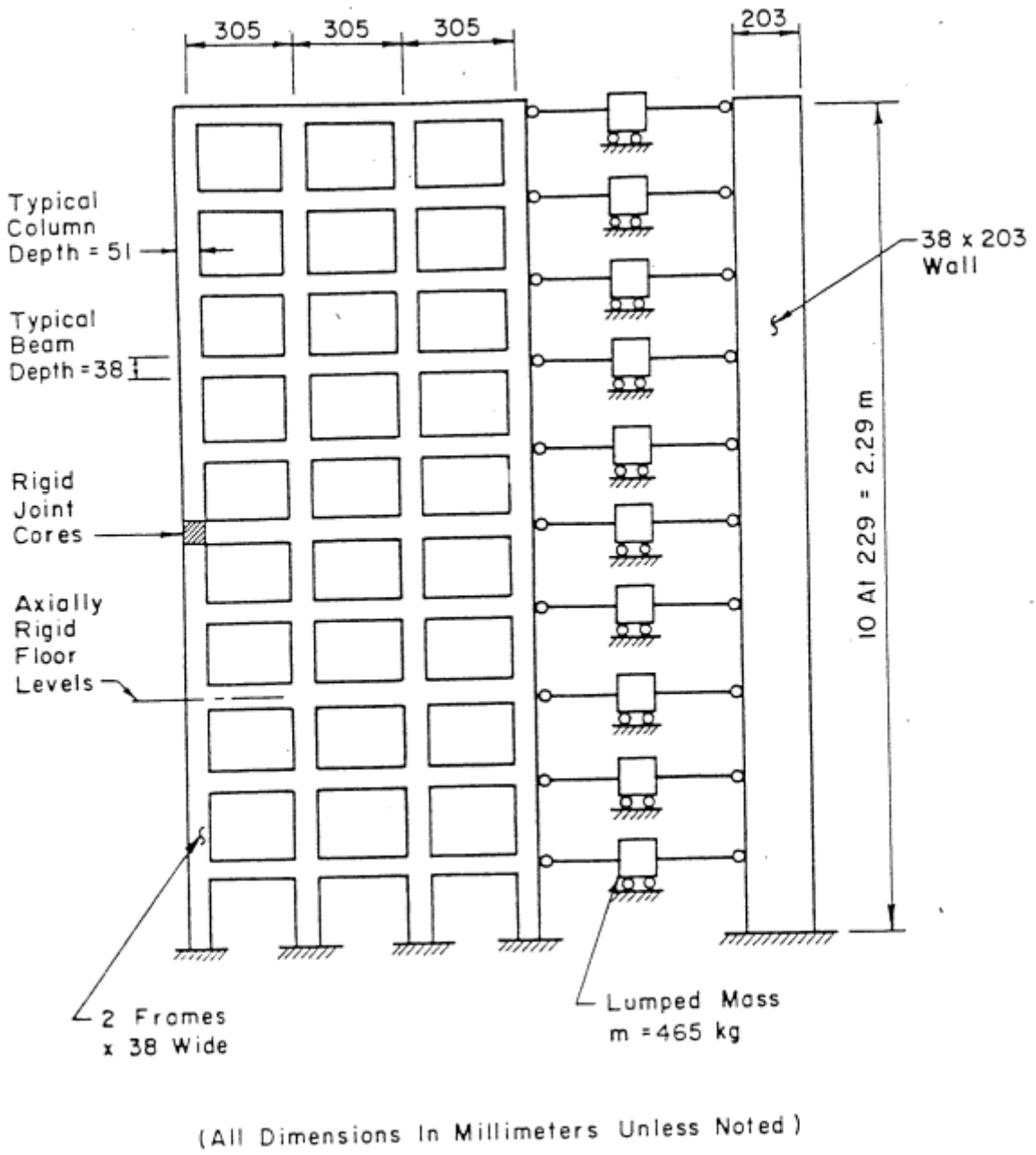

Figure 14 - Description of Analytical Model from Previous Research (Sozen, 1979)

to eliminate the transfer of moment and a 465 kg (2.65 lb-s^2/in) mass was lumped at the center of the rigid beam to represent the mass of the rigid diaphragm. The beams and columns of the frame were modeled using linear-elastic beam column elements. A simple

investigation was performed to determine the best way to model the structural wall in OpenSees. Three simple wall-only models were built using quad elements, brick elements, and elastic beam column elements in OpenSees. An additional wall-only model was built in SAP2000. By comparing results after applying simple loads and excitations to both the OpenSees models and the SAP2000 model it was determined that the elastic beam column element wall model captured the most accurate responses in respect to deflections and accelerations of the SAP2000 model. From the comparison, it seemed as though the quad and brick elements were not intended for the purpose in which they were being used to model the wall. Therefore, elastic beam column elements were used to model walls.

The characteristics of the frame and wall elements were chosen based on the information provided about the test structures in the original project report. The cross-sectional area of each element was determined based on reported test structure dimensions. The strong axis moment of inertia that was assigned to each element was a transformed moment of inertia calculated based on the amount and placement of the steel reinforcement in the concrete, the ratio of steel modulus of elasticity to concrete modulus of elasticity, and cracked section properties of the cross section. The steel and concrete moduli of elasticity were determine by the original project team through testing and reported in the publication. Since the moment of inertia assigned to each element was a value transforming a composite steel-concrete material into an equivalent concrete-only material the compressive modulus of elasticity for each element could simply be that of the concrete used in construction. However, the tensile modulus of elasticity was require to be a highly reduced value such that the resulting tensile section of the element would

be approximately equivalent to that of only the steel reinforcement acting in tension as concrete has very little tensile strength. Finally the weight per unit length of each element was estimated and assigned to each member to account for the mass of the structural elements.

The stiffness of the single frame in the model was doubled in order to account for both frames in the test structures. The stiffness of the frame was doubled by factoring the moments of inertia in all frame elements by a value of two.

Since much of the cracking and damage that occurred in the actual structures was located in or around the beam column joints, a slightly more complex model used beam with hinges elements in the frame and another used them in both the frame and wall. The beam with hinges element is exactly the same as a linear elastic beam column with the exception of two small non-linear regions at each end of the element. These non-linear regions can be defined with a variety of preset stress-strain curves or a unique user defined stress-strain relationship. The first stress-strain relationship that was chosen is that of an elastic perfectly plastic material as the compressive modulus of elasticity is known and the approximate yield strength of each element can be found using a moment-curvature relationship, yet the stress-strain relationship beyond yielding is difficult to determine and define. An additional alternative is a basic concrete stress-strain curve in compression with a user defined concrete yield strength and modulus of elasticity, and an elastic perfectly plastic stress-strain curve in tension to represent reinforcing steel.

An additional method that is conceptualized to model inelastic behavior around the joints is to model the beams and columns as completely elastic and creating joint

elements at the beam column interfaces. The joint elements in OpenSees consist of a shear panel at the center of a joint and a small interface between the joint and beam or column elements which contains springs to resist lateral, shear, and moment forces. Determining the characteristics of each spring in order to accurately model each joint, however, is more suited to projects where direct testing or calibration of the joint is available. Therefore, the beam with hinges element was utilized in the project.

Finally, a completely non-linear model was created using displacement-based beam column elements in both the frame and wall. These elements capture the spread of inelastic behavior throughout the entire length of the elements rather than in just two hinge locations at the end of each element. Similarly to the hinge elements, the stress-strain relationship of the element material can be characterized by a unique user defined curve or by a preset curve. Again, the most appropriate material types for the model are elastic perfectly plastic in both compression and tension and a concrete curve in compression and elastic perfectly plastic in tension.

Additional alterations were made to some models in order to achieve a more accurate response. However, if there was no positive result in the accuracy of the response due to the alteration of the model, it was generally reverted back to the original configuration. For example, instead of simply using pins to connect the rigid diaphragm to the frame and wall, springs were added to represent a small amount of rotational resistance created by the rigid diaphragm connections. Another example was to remove the entire bottom story of the structure from the model and using first story response as the input "ground" excitation. Although the publication claimed that structures were fully fixed to the base of the shake table there was the possibility of slippage between the

shake table and structure, especially with such large and heavy models. To eliminate the possibility of slippage between the shake table and model, the entire first floor of the structure was removed from the analytical models and the resulting models (floors two through ten) were excited at the second floor (which was now the lowest floor in the models) with the response that was recorded at the second floor of the actual structure.

In a further attempt to increase the reliability of the model, the parameter estimation routine was used to try and better determine the actual stiffness of each story in the structure. The story stiffnesses in the models were initially defined by the material and section properties assigned to each element. These material and section properties were either given or calculated using values found in the original project publication. However many of these values are based on design calculations which could possibly vary from the constructed structures, or they could differ slightly from floor to floor. In an attempt to get a better estimate of the actual stiffness parameters the model with the estimated parameters was input into a parameter estimation routine with the response from the actual structure. The model provided an estimated response of the structure and tries to match that response using estimated parameters to the structure's actual behavior. This is the same procedure used during damage estimation, however, instead of fitting a healthy response to a damage response to get the damaged parameters, it fit the estimated response to the actual response to get the actual initial parameters.

Three-Dimensional Models

The two-dimensional models make use of a fairly valid assumption that the actual three-dimensional structure can be compressed into a single two-dimensional plane and

still provide an accurate response. The accuracy of the response from these models may not, however, be sufficient enough for this project to work. To minimize the differences between the test structure response and the model response, use of the actual form of the structure in a three-dimensional model was evaluated. The advantage of the two-dimensional model was the simplicity which led to quick analyses. The three-dimensional models add an additional dimension and nearly double the amount of required elements which significantly increases analysis time. The advantage being that it could improve the accuracy of the modeled response.

The three-dimensional models were creating using the exact dimensions of the test structures, including distance between the frames and wall. Each model consisted of two three-bay ten-story frames in parallel separated by a single structural wall. Again, all base restraints were fully fixed. A rigid diaphragm was modeled at each floor of the structure with is 465 kg mass lumped at the very center of the diaphragm. The diaphragm was modeled to ensure equal displacements in the lateral and horizontal directions at each floor of the structure. Each floor consisted of nine nodes which were constrained by the rigid diaphragm command, one on the wall and four on each frame. The four nodes on each floor of the frame existed at the beam column intersections. The rigid diaphragm was initially modeled such that it did not provide any rotational resistance to the structure.

A similar progression to the two-dimensional models was used while creating the three-dimensional models, starting from the simplest form and building on each model to create a more complex iteration. The first model was a created using entirely elastic beam column elements for both the frames and wall. A second model replaced the elastic beam

column elements in the structure with beam with hinges elements. The hinge portions of the elements were assigned an elastic perfectly plastic stress strain curve with the appropriate moduli of elasticity and yield stresses to represent concrete and steel during compression and just steel during tension. The hinges were alternatively assigned a concrete stress strain curve during compression and an elastic perfectly plastic steel curve during tension. Finally, an entirely non-linear model was created using displacement-based beam column elements throughout the structure. These elements were assigned the same material properties as the hinge elements in the previous model, however these elements were able to capture the spread of inelastic behavior throughout the entire element rather than just at the connections.

Also similar to the two-dimensional models were the modifications that were made to the models throughout the testing process in order to increase the accuracy of the response. For example, adding springs to account for rotational resistance caused by the rigid diaphragm. Removing the entire first story of the structure to eliminate the possibility of slippage between the base of the structure and shake table. Adjusting variables such as the compressive moduli of elasticity on a trial and error basis in an attempt to improve the accuracy of the response. Even using the parameter estimation procedure to better estimate the stiffness parameters used in the model.

CHAPTER IV

ANALYTICAL RESULTS

The following results display the data obtained while attempting to determine how to best configure the sensor selection procedure for the most favorable results in practical applications. Much of what was done was to determine which conditions are optimal in order to get the most consistent and accurate results. The results provided effectively show the analytical validity of the method as well as its limitations.

Steady State Response

The first part of this analysis examined the use of the steady state responses to create the parameter signature matrices and estimate damage. Steady state responses were investigated first in the hopes that transient responses could be avoided if steady state response worked well enough with this method. This portion of the research was performed entirely on the eight story structure. Each finite element analysis was performed over a 40 second time period; the steady state phase began at approximately 15 seconds but varied slightly for each response. The parameter signature matrices and estimation procedures were all run using a 10 second portion of the responses from 25 to 35 seconds.

The parameter signature matrices were created according to Equation 10 using Guass wavelet transforms and a signature size threshold of d = 5. The perturbation size that was used to determine the parameter sensitivities was $\delta\theta_i = 0.01$. A large set of parameter signatures matrices were created for a wide variety of dominance factors,

excitation locations and excitation types. A portion of those matrices are displayed in Table 9. The 12 matrices shown in Table 9 were created for three excitation locations. These locations were the second floor, the roof and the ground. The excitation function was a simple sine wave excitation with a period of 0.800 s and amplitude of 44.5 KN (10 kips) that excited the structure over a 40 s time window to create the dynamic response. Four parameter signature matrices were created for each excitation location, for dominance factors of 1.1, 1.2, 1.3 and 1.4.

Even from the small sample of data displayed in Table 9 it is easy to see that steady state response do not provide very dense parameter signature matrices, even at relatively low dominance factors below 1.3. An ideal sensor suite would be the group of sensors that, when combined, is able to provide a value of 1 for each of the parameter stiffness in the structure. In the direct method this is a requirement, while in the inverse method it is not. It is still expected to be greatly beneficial to the inverse method to have as many parameters represented in the sensor suite as possible. The ground excitation parameter signature matrices are the only matrices that are able to meet that standard for any dominance factor. Even at a very low dominance factor of 1.1 the roof and second floor excitations were not able to record a unique signature for a change in the fourth story and third story stiffness respectively. This is evident because of the absence of 1's in those two rows of the respective signature matrices. These matrices would not be able to be used with the direct method. The inverse method did still work for these excitation locations, as it will be shown, however it did require nearly all of the sensors in order to correctly estimate the damage. As a practical example of sensor selection, the preferred sensors for the ground excitation case would be at floor three, four, five and six. These

Table 9 - Parameter Signature Matrices for Ground, Second Floor and Roof Excitations using Steady State Responses

		(a) Ground Excitation								(b) 2nd Floor Excitation								(c) Roof Excitation							
		Outputs (Floor Accelerations)								Outputs (Floor Accelerations)								Outputs (Floor Accelerations)							
		2	3	4	5	6	7	8	R	2	3	4	5	6	7	8	R	2	3	4	5	6	7	8	R
Parameters (Story Stiffness)	1	1	1	1	1	0	0	0	1	1	1	1	1	1	1	1	1	1	1	0	0	0	0	0	0
	2	1	1	0	0	1	0	0	0	1	1	1	0	0	0	0	0	0	1	0	1	0	0	0	0
	3	0	0	1	1	0	1	0	0	1	0	1	1	0	0	0	0	0	0	0	0	0	0	0	0
	4	0	1	0	1	1	0	0	0	0	0	0	0	0	0	0	0	0	0	1	0	0	0	0	0
	5	0	0	1	1	1	1	0	0	1	0	0	0	1	0	1	1	1	0	1	0	0	1	0	0
	6	0	0	1	1	1	1	1	0	0	0	0	0	0	1	1	1	1	0	0	1	0	1	1	1
	7	0	1	1	1	1	1	1	1	1	0	0	1	1	1	1	1	1	1	1	1	1	1	1	1
	8	1	1	1	1	1	1	1	1	1	1	1	1	1	1	1	1	1	1	1	1	1	1	1	1
		$\eta_d = 1.1$								$\eta_d = 1.1$								$\eta_d = 1.1$							
Parameters (Story Stiffness)	1	1	1	0	0	0	0	0	0	1	1	1	1	1	1	1	1	1	0	0	0	0	0	0	0
	2	0	1	0	0	1	0	0	0	0	1	0	0	0	0	0	0	0	1	0	1	0	0	0	0
	3	0	0	1	0	0	0	0	0	0	0	1	1	0	0	0	0	0	0	0	0	0	0	0	0
	4	0	0	0	1	1	0	0	0	0	0	0	0	0	0	0	0	0	0	1	0	0	0	0	0
	5	0	0	0	0	1	1	0	0	0	0	0	0	1	0	0	1	1	0	0	0	0	0	0	0
	6	0	0	0	1	1	1	1	0	0	0	0	0	0	1	1	1	1	0	0	0	0	1	1	1
	7	0	1	1	1	1	1	1	1	1	0	0	1	1	1	1	1	1	1	1	1	1	1	1	1
	8	1	1	1	1	1	1	1	1	1	1	1	1	1	1	1	1	1	1	1	1	1	1	1	1
		$\eta_d = 1.2$								$\eta_d = 1.2$								$\eta_d = 1.2$							
Parameters (Story Stiffness)	1	1	1	0	0	0	0	0	0	1	1	1	1	1	1	1	1	1	0	0	0	0	0	0	0
	2	0	1	0	0	1	0	0	0	0	1	0	0	0	0	0	0	0	1	0	0	0	0	0	0
	3	0	0	1	0	0	0	0	0	0	0	1	1	0	0	0	0	0	0	0	0	0	0	0	0
	4	0	0	0	1	1	0	0	0	0	0	0	0	0	0	0	0	0	0	1	0	0	0	0	0
	5	0	0	0	0	1	0	0	0	0	0	0	0	0	0	0	1	0	0	0	0	0	0	0	0
	6	0	0	0	0	1	1	1	0	0	0	0	0	0	1	1	1	0	0	0	0	0	1	1	1
	7	0	1	1	1	1	1	1	1	1	0	0	1	1	1	1	1	1	1	1	1	1	1	1	1
	8	1	1	1	1	1	1	1	1	1	1	1	1	1	1	1	1	1	1	1	1	1	1	1	1
		$\eta_d = 1.3$								$\eta_d = 1.3$								$\eta_d = 1.3$							
Parameters (Story Stiffness)	1	1	1	0	0	0	0	0	0	1	1	1	1	1	1	1	1	1	0	0	0	0	0	0	0
	2	0	1	0	0	0	0	0	0	0	1	0	0	0	0	0	0	0	0	0	0	0	0	0	0
	3	0	0	1	0	0	0	0	0	0	0	1	0	0	0	0	0	0	0	0	0	0	0	0	0
	4	0	0	0	1	0	0	0	0	0	0	0	0	0	0	0	0	0	0	1	0	0	0	0	0
	5	0	0	0	0	1	0	0	0	0	0	0	0	0	0	0	0	0	0	0	0	0	0	0	0
	6	0	0	0	0	1	1	1	0	0	0	0	0	0	1	1	0	0	0	0	0	0	1	0	1
	7	0	0	1	1	1	0	1	1	0	0	0	1	1	1	1	1	1	1	1	1	1	1	1	1
	8	1	1	1	1	1	1	1	1	1	1	1	1	1	1	1	1	1	1	1	1	1	1	1	1
		$\eta_d = 1.4$								$\eta_d = 1.4$								$\eta_d = 1.4$							

were chosen at the dominance factor of 1.1. Choosing the preferred sensors at a higher dominance factor will help to eliminate the less important signatures that may show up at a lower dominance factor. A sensor at floor three provides the identifiability for stories one and two, sensor four provides the identifiability for story three, sensor five for story four and sensor six for stories five and six. Identifiability for story seven is provided by three of the sensors while identifiability for story eight is provided by all four.

These sensor suites were chosen for a healthy structure with all stories having a nominal modulus of elasticity of 200 GPa (29000 ksi). This raises the question of will these sensors still be the preferred sensors when the structure becomes damaged and the modulus of elasticity of some members changes. If the physical characteristics of the structure change when damage occurs, then it is possible that the sensor suites, which were chosen using healthy characteristics, could be different for the damaged characteristics. It cannot be known which modulus will be decreased and by how much so it is impossible to determine the preferred sensors for what the exact damaged configuration will be, therefore the preferred sensors for the healthy configuration are used. Alternatively, parameter signature matrices can be created for a large number of random stiffness coefficients and summed together to determine the most valuable sensors for all the possible configurations.

The summed total parameter signature matrix is created by randomizing the initial modulus of elasticity of the members in the structure to values within the acceptable range that damage can occur. For this project the values could be anywhere between 15 percent below or 5 percent above the nominal value of 200 GPa (29000 ksi). From a practical standpoint it does not make sense for damage to cause an increase in the

modulus of elasticity of any of the structural members. The reason that stiffness is allowed to increase is because the method of non-linear least squares can increase the parameters as part of the iterative process before it converges. Parameter signature matrices were created for 100 different cases where the structure consisted of stories with random stiffness coefficients. All of the signature matrices were then summed together. The values in the sum total matrix represent the number of signatures that were picked up out of the 100 damage configurations. It is believed that this is a more accurate signature matrix because it encompasses a broad range of damage. The single parameter signature matrices are only accurate for the undamaged structure, but as a structure gets damaged the signature matrix may change slightly. Furthermore, as the inverse method works it estimates the parameters by increases and decreases them until the response begins to fit the desired curve. The inverse method can change the parameters to any stiffness in a range of values, therefore it is beneficial for the sum total signature matrix to also include a wide range of stiffness values. Shown in Appendix A are a variety or sum total signature matrices for different excitation locations and dominance factors.

Appendix A shows four sum total signature matrices for excitation occurring at each of the floors including the ground. The dominance factors of the four matrices for each excitation location are 1.1, 1.2, 1.3 and 1.5. These matrices were created for all nine excitation location so they could be compared and the best resulting excitation location could be chosen for the damage estimation. These were all created using simulated excitation on a computer model therefore the excitations can be easily changed and moved. It is important to determine the most optimal excitation location using the computer analysis because it is much more difficult to move or change the vibration

generator when it is installed onto the actual structure. Ideally, it is preferred that the optimal excitation locations and sensor positions are determined using the computer analysis so that only one dynamic response from the actual damaged structure is required. Based on the results in Appendix A it appears that the second floor excitation in the eight story structure results in the most populated sum total parameter signature matrices. At a dominance factor of 1.5 the second floor excitations resulted in a total of 2228 flagged signatures while the next highest was the seventh floor with 2144 flagged signatures. A higher number of flagged signatures found in the sum total matrix means that that excitation location created the most unique changes in the sensor responses which is ideal for the estimation procedure.

From the parameter signature matrices resulting from second floor excitations (Table A.2), one choice of a sensor suite would be sensors at floor three, four, six and seven. These four sensors provide a reasonable amount of flagged signatures for each parameter. Floor three provides identifiability to stories one, two and eight. Floor four provides identifiability to stories three and eight. Floor six provides identifiability to stories four and eight, and finally Floor seven provides identifiability to stories six, seven and eight. The only story that lacks much identifiability with unique signatures is story five, however, non-unique signatures may be able to provide identifiability to story 5 even though they do not show up in the signature matrices. Another important excitation location to investigate was the roof (Table A.9). It may not have the most populated signature matrices but, in most cases, will be the preferred location for the vibration generator. At a dominance factor of 1.4 the sum total signature matrix had a total of 1971 flagged signatures. One possible sensor suite for this excitation location

would be at floors two, three, four, six and eight. A sensor at floor four does not really provide better identifiability to any of the parameters but since stories three and four are not represented with any flagged signatures it might be helpful to add the additional sensor.

These suites and a variety of other sensor suites for a range of excitation locations were then used with the inverse method to verify that sensor selection is feasible when using steady state responses. Appendix B displays the results of all of the inverse method parameter estimation procedures for steady state responses. For these cases the damage that was simulated in the damaged structure was represented by a ten percent reduction in the modulus of elasticity in the sixth and seventh stories. Figure B.1 shows the estimated parameters for the case when the structure is excited at the second floor and sensors are used at all eight floors. All eight sensors were used for the first test to verify that the inverse method works properly before sensors are eliminated. The red line shows the actual modulus of elasticity for that story while the blue line shows the estimate of the parameters. After 40 iterations it is apparent that the estimates found using the inverse method correctly converged to the stiffness of each story while using the response of all eight sensors. Figure B.2 shows the estimated parameters for second floor excitation when a reduced suite of sensors is used. Those sensors were three, four, six and seven. As it can be seen, when using what was thought to be the preferred sensors the inverse method did not converge to the correct parameter estimates. The stiffness parameters at the seventh and eighth stories were not estimated correctly. The sensors were moved up in the structure in an attempt to help the inverse method better estimate the stiffness of the higher stories. These sensors were placed on floor three, five, seven

and nine. Even though these would not be considered the preferred sensors based on parameter signatures they did allow the inverse method to converge to the correct parameters. These results can be seen in Figure B.3. This leads to the notion that preferred sensor position is not dependent entirely on the signatures. Other factors could affect the placement of preferred sensors such as how they are grouped in the structure. When the sensors were grouped slightly more toward the bottom of the structure the parameters at the top of the structure were estimated incorrectly as in Figure B.2. But when the sensors were spaced more evenly throughout the structure all of the parameters were estimated correctly. Even though parameter signatures may not be the only factor affecting sensor placement, they are still a very important factor as is shown in Figure B.4. The sensor at floor three is replaced with a sensor at floor two which could be considered a much less influential sensor based on the number of flagged signature it can detect relative to sensor three. In this case, without sensor three, the inverse method is not able to converge which leads us to believe that the number of parameter signatures does play a crucial role in determining the preferred sensors.

Figure B.5 shows the parameter estimates from the inverse method using an excitation at the roof of the eight story building with sensors at all eight floors. Again, the inverse method estimates the parameters with great accuracy when all available sensors are used. Figure B.6 shows that case in which sensors were placed at floors two, three, four, six and eight. Five sensors out of a total of eight available sensors is still a relatively large number. It would be preferred if even less sensors could be used and still accurately estimate the parameters. Figure B.7 shows the results for when the sensor at floor four was removed from the analysis because it was the least significant sensor and it can be

seen that the method does not converge for this case. But again, each of the sensors were moved higher in the structure to promote a more spread out arrangement, sensors at three, five, seven, and nine (Figure B.8) and the method converged properly. Finally, the sensor at floor three was replaced with the much less influential sensor at floor two and the method did not converge because there was not enough information to allow the procedure to estimate the parameters. This provides further evidence of the importance of parameter signatures for preferred sensor placement.

The results from the steady state cases were promising and provided some evidence that sensor selection through parameter signatures is relevant when using the inverse method. However, these results did not provide an exact method of sensor selection that can be relied upon for each and every case. Future research will investigate the causes of this further, but is likely related to interdependence of signatures and richness of the extracted signature which could be better defined as non-binary.

Transient Response

The next step was to determine if using transient responses had any effect on the outcome of the routines. The analyses continued to use a 40 second time history but the responses were all taken from the period of one to nine seconds during the transient stage. Again, the parameter signature matrices were created according to Equation 10 using Guass wavelet transforms and a signature size threshold of d = 5. The perturbation size that was used to determine the parameter sensitivities was $\delta\theta_i = 0.01$. The result was a large set of parameter signature matrices for various excitation locations and dominance factors. A sample of these matrices can be found in Table 10. These matrices were

Table 10 - Parameter Signature Matrices for Ground, Second Floor and Roof Excitations using Transient Responses

		(a) Ground Excitation								(b) 2nd Floor Excitation								(c) Roof Excitation							
		Outputs (Floor Accelerations)								Outputs (Floor Accelerations)								Outputs (Floor Accelerations)							
		2	3	4	5	6	7	8	R	2	3	4	5	6	7	8	R	2	3	4	5	6	7	8	R
Parameters (Story Stiffness)	1	1	1	1	1	0	0	0	0	1	1	1	1	1	1	1	1	1	1	0	0	0	1	1	1
	2	1	1	0	0	0	0	0	0	1	1	1	1	0	0	0	0	0	1	0	0	0	0	0	0
	3	0	0	1	0	0	1	0	0	1	1	1	1	1	1	0	0	0	0	1	0	0	0	1	0
	4	0	0	1	0	1	0	0	0	1	0	1	1	1	0	0	0	0	0	1	1	0	0	1	1
	5	0	0	0	1	1	0	0	0	1	1	1	1	1	0	0	1	1	0	0	1	1	0	0	0
	6	1	1	0	0	1	1	1	1	1	1	1	1	1	1	1	1	1	1	1	1	1	1	1	1
	7	1	1	0	1	1	1	1	1	1	0	1	1	1	1	1	1	1	1	1	1	1	1	1	1
	8	1	1	1	1	1	1	1	1	1	1	1	1	1	1	1	1	1	1	1	1	1	1	1	1
		$\eta_d = 1.1$								$\eta_d = 1.1$								$\eta_d = 1.1$							
Parameters (Story Stiffness)	1	1	0	0	1	0	0	0	0	1	1	1	1	1	1	1	1	1	1	0	0	0	0	0	1
	2	0	1	0	0	0	0	0	0	1	1	1	0	0	0	0	0	0	1	0	0	0	0	0	0
	3	0	0	0	0	0	0	0	0	1	1	1	1	0	0	0	0	0	0	1	0	0	0	0	0
	4	0	0	1	0	0	0	0	0	1	0	1	0	1	0	0	0	0	0	0	1	0	0	1	0
	5	0	0	0	1	1	0	0	0	1	1	0	1	0	0	0	0	0	0	0	1	1	0	0	0
	6	0	0	0	0	1	1	1	1	1	1	1	1	1	1	1	1	1	1	1	1	1	1	0	1
	7	0	0	0	0	1	1	1	1	1	0	0	1	1	1	1	0	0	1	1	1	1	1	1	1
	8	1	1	1	1	1	1	1	1	0	1	1	1	1	1	1	1	1	1	1	1	1	1	1	1
		$\eta_d = 1.2$								$\eta_d = 1.2$								$\eta_d = 1.2$							
Parameters (Story Stiffness)	1	1	0	0	0	0	0	0	0	1	1	1	1	1	1	1	1	1	0	0	0	0	0	0	0
	2	0	0	0	0	0	0	0	0	1	1	1	0	0	0	0	0	0	0	0	0	0	0	0	0
	3	0	0	0	0	0	0	0	0	1	0	1	0	0	0	0	0	0	0	1	0	0	0	0	0
	4	0	0	1	0	0	0	0	0	0	0	1	0	1	0	0	0	0	0	0	0	0	0	0	0
	5	0	0	0	1	1	0	0	0	1	1	0	0	0	0	0	0	0	0	0	0	1	0	0	0
	6	0	0	0	0	1	1	0	1	1	1	1	1	1	1	1	1	1	1	1	1	1	1	0	1
	7	0	0	0	0	0	1	1	1	0	0	0	1	1	1	1	0	0	1	0	1	1	1	1	1
	8	1	1	1	1	1	1	1	1	0	1	1	1	1	1	1	1	1	1	1	1	1	1	1	1
		$\eta_d = 1.3$								$\eta_d = 1.3$								$\eta_d = 1.3$							
Parameters (Story Stiffness)	1	1	0	0	0	0	0	0	0	1	1	1	1	1	1	1	1	1	0	0	0	0	0	0	0
	2	0	0	0	0	0	0	0	0	1	1	0	0	0	0	0	0	0	0	0	0	0	0	0	0
	3	0	0	0	0	0	0	0	0	1	0	0	0	0	0	0	0	0	0	0	0	0	0	0	0
	4	0	0	0	0	0	0	0	0	0	0	0	0	1	0	0	0	0	0	0	0	0	0	0	0
	5	0	0	0	1	0	0	0	0	0	0	0	0	0	0	0	0	0	0	0	0	0	0	0	0
	6	0	0	0	0	0	1	0	1	1	1	1	1	1	1	0	1	1	1	1	1	0	1	0	1
	7	0	0	0	0	0	1	1	1	0	0	0	1	1	1	1	0	0	1	0	1	1	1	1	1
	8	1	1	1	1	1	1	1	1	0	1	1	1	1	1	1	1	1	1	1	1	1	1	1	1
		$\eta_d = 1.4$								$\eta_d = 1.4$								$\eta_d = 1.4$							

created using excitations at the ground, second floor and roof, similar to steady state. For each location the excitation function was a simple sine wave with a period of 0.800 s and amplitude of 44.5 KN (10 kips) that was exposed to the structure over a 40 s time window to create the dynamic response. Four matrices were created for each location, the dominance factors of those four matrices were 1.1, 1.2, 1.3 and 1.4.

Compared to the matrices in Figure 9 it is easy to observe that the matrices created using transient responses are much more populated than those created using steady state and therefore better suited to choose sensors and estimate parameters. In addition to being more populated, the matrices for second floor and roof excitations are able to provide identifiability to every parameter. That was not the case for the same matrices using steady state responses. Because the sensors in the transient matrices can provide a value of 1 for each parameter they meet the requirements to be able to be used in the direct method. This also means that the inverse method should be better suited to correctly estimate the parameter values.

The question arises again if these are appropriate signature matrices for a damaged structure when they were created using undamaged characteristics. To get a better representation of the signature matrices the same procedure was used to create sum total parameter signature matrices for the transient cases. The sum total matrices created using transient responses can be found in Appendix C. Table C.2 replicated below displays the sum total parameter signature matrices for second floor excitations which has a total of 2491 flagged output sensitivities at a dominance factor of 1.5. This was the highest number of flagged output sensitivities for any matrix at that dominance factor. The next highest

matrix was for seventh floor excitation (Table C.7) with a total of 2465 flagged output sensitivities. The roof excitation matrix (Table C.9) had a total of 1940 flagged output sensitivities at a dominance factor of 1.5. For this reason the roof excitation and second floor excitation were examined closely.

Using Table C.2, a sensor suite for second floor excitations can be chosen. One possible sensor suite would be sensors positioned at floors two, three and six. These were chosen from the matrix at the dominance factor of 1.5. Sensors at floors two and three provide identifiability for the lower stories while the sensor at floor six provides identifiability for the upper stories. It can also be observed that sensor at floors four and eight provide the least identifiability. For the roof excitation (Table C.9) a possible sensor suite would be at floors two, three, four and six. Since the matrices are less populated for roof excitation this suite was chosen using the matrix at the dominance factor of 1.3. In this case sensors at the eighth floor and roof provide the least identifiability.

Using these sensor suites the inverse method was tested using transient responses. The results of the parameter estimations using the inverse method are displayed in Appendix D. Figure D.1 displays the results of the parameter estimation using second floor excitation and all eight available sensors. This was done as proof that the procedure works when all available sensors are used. Then the non-essential sensors were removed. The results of the parameter estimation using only sensors two, three, and six for second floor excitation are shown in Figure D.2. Using the sensor suite the inverse method was able to converge to the actual stiffness of each story very accurately. Interestingly, when an additional sensor was removed the procedure still converged to the correct values.

Figure D.3 shows the parameter estimation results using only sensors two and six. The procedure diverged when it was attempted with any less than two sensors. To verify that the procedure was actually dependent on the preferred sensors it was then run using the least influential sensors which were at floors four and eight. The results of this analysis (Figure D.4) show that even with the least important sensor the procedure was still able to converge. This means that for this case even the worst sensors were still affected enough by the damage in the transient phase to allow the inverse method to work. In order to show that sensors with better identifiability are in fact superior to sensors with lower identifiability we needed to switch to a case with a lower overall number of flagged signatures.

Roof excitation was an ideal case because there was less identifiability from all of the sensors and the roof is likely the preferred location for implementation of a vibration generator. Again, the first trial included all available sensors (Figure D.5) and the method converged to the correct parameters. Secondly, the sensors at floors two, three, four and six were tested (Figure D.6) and again the procedure converged. The next step was to remove the sensor at floor four (Figure D.7) and then additionally remove the sensor at floor three (Figure D.8). For both cases the procedure converged. Finally, the inverse method was performed using the least important sensors. When using sensors at floor eight and the roof the procedure did not have enough information to be able to estimate the parameters and did not converge. This also occurred for sensors at floors seven and eight. When the procedure used sensors at floors four, seven and eight it was able to estimate parameters but did not converge to the correct values (Figure D.9).

Figure D.9 is validation that two preferred sensors with high identifiability are better at estimating parameters than three sensors with less identifiability. From this it can be concluded that the inverse method is in fact dependant on some sensors more than others. Therefore if an engineer wishes to choose a sensor suite it is both beneficial and necessary to understand which sensor locations will provide the best identifiability. For the case of second floor excitation every sensor was good enough for the inverse method to accurately converge. That will not happen for every case, which is why picking the preferred sensors will be crucial when choosing a suite.

From the results listed above it is quite clear that using transient response is preferable to using steady state responses. Transient responses were able to reduce the required number of sensors to two while steady state was only able to reduce them to four. Choosing a sensor suite that would work was much more reliable when using transient responses than when using steady state responses. Overall it could be said that steady state could be used if necessary but transient responses is the preferred method when they are available. If steady state is to be used it would be advised to use caution, and choose more sensors as an added measure. It would also be advised to perform multiple studies in order to verify the results.

Additional analyses performed concurrently by Professor Kourosh Danai of the Department of Mechanical and Industrial Engineering at the University of Massachusetts Amherst produced very similar findings as those detailed above while examining more closely the importance and properties of the identifiability of sensor locations. Professor Danai's results are able to verify the validity of the sensor selection method while

detailing the importance of the location and properties of the excitation function that is being utilized. (Danai et al., 2012).

CHAPTER V

PHYSICAL TESTING RESULTS

Due to problems modeling the structural response of the physical test specimens, results that were obtained through analytical testing which showed the validity of the method have not yet been able to be replicated successfully when using the data from physically tested structures. The analytical testing was performed to verify the legitimacy of the preferred sensor selection procedure when being used on structures under perfect conditions. Once verified that the sensor selection method was analytically functional for the purposes specified in this project it was tested again using physical test data to examine its feasibility as an actual procedure. This round of testing has not yet acquired a definitive confirmation that the preferred sensor selection procedure works under real world conditions. This research did, however, provide valuable insight as to what might be required in order for this procedure to work.

Under perfect conditions the mathematical processes used to determine the preferred sensor suite are unaffected by outside factors. Unless the mathematical processes are not affected by the presence of noise, response inconsistencies, modeling discrepancies and other real world factors there is no guarantee that they will work for physical test data. Therefore, the method will need to account for the effects of these real world conditions, through eliminating them or significantly lessening their effects.

Determining the preferred sensors of a system relies heavily on the precise analysis of unique shape attributes of that system's outputs or responses. If the responses

generated by the system are unable to be repeated accurately and consistently or are affected by outside factors then the process of analyzing those responses can become inaccurate leading to an unreliable preferred sensor suite. The more reliable the responses are the greater the likelihood that the process will provide a correct sensor suite. Factors such as noise in the actual structure's response or modeling inconsistencies in the analytical model can lead to discrepancies between the modeled and actual response. Creating a model that can match the response of the actual structure is extremely important in order for this method to work.

Before performing any preferred sensor selection processes the responses of the analytical models detailed in the previous section were compared to the recorded response of the actual structures in order to determine their accuracy. Starting with the simplest model and progressively working toward the most complex, the models were excited and then iteratively modified in an attempt to produce a more accurate response from that model. Simple models were not able to replicate the actual structural response. The simplest two dimensional models were particularly poor at producing a matching response (Figure 15). Modifying and improving the two dimensional structures through adjusting stiffness and damping coefficients did little to improve the quality of the simulated responses. No response generated by the simplified two dimensional structures would have been close enough for the sensor selection process to accurately choose the appropriate sensor suite for the test structures.

As the models become more complicated, they produced marginally better responses, yet no response was ever able to be considered accurate enough for the procedure to work effectively. Therefore the focus of the research was on obtaining a

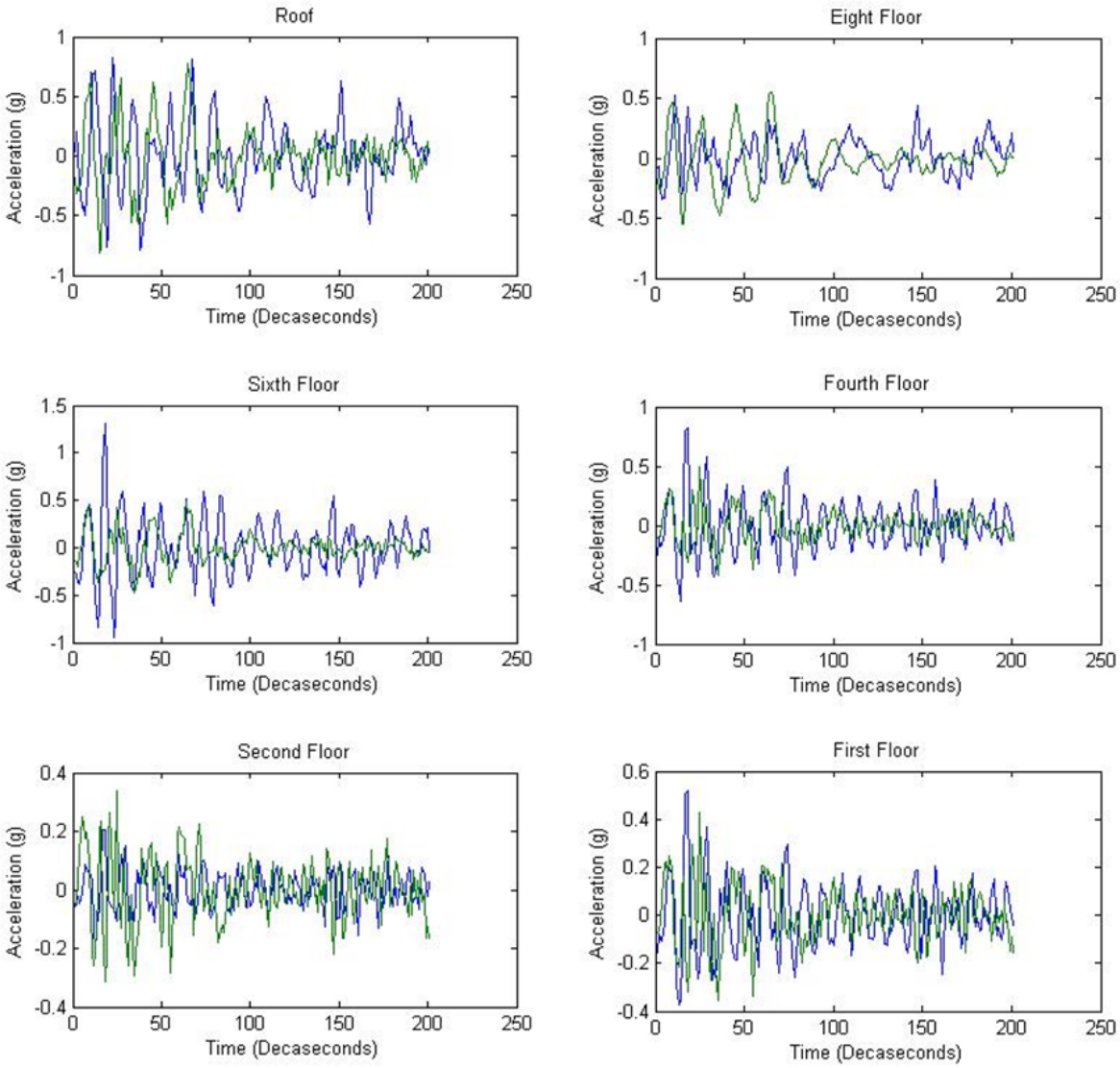

Figure 15 - Two Dimensional, Lightly Reinforced, Completely Elastic Model Response Compared to Response of Actual Test Structure

valid model that could be used in future research. The fully elastic three dimensional model was able to replicate a somewhat similar frequency pattern in some areas of the response however it deviated greatly in others (Figure 16). This was also true for the three dimensional model with plastic hinge elements, though the response was somewhat improved (Figure 17).While the amplitudes of the peak values throughout the response matched reasonably well, there were some major discrepancies between the simulated and actual responses at particular floor levels, especially towards the base of the structure. The three dimensional model with entirely non-linear elements produced very similar result to the model with hinges (Figure 18). Since the fully non-linear model did not improve upon the accuracy of the response yet required a more substantial analysis time the focus of improving the models and bettering the response was put on the hinged element model.

Before improving the overall precision of the responses, it was important to improve the general accuracy of the responses at the bottom floors. It was believed that the problems with the lower floors may have been due to shortcomings with the shake table and/or the attachment between the shake table and specimens. In order to try and improve the accuracy at the lower floors the models were modified to remove any possible discrepancies between how the shake table was assumed to have performed and how did perform. For example, although the structure was presumed to be fully fixed to the shake table it is possible with such large structures that there was some slippage at the structure shake table interface. There is also a very good possibility that with such small time intervals (.002 s) the shake table controller was not able to obtain the feedback and

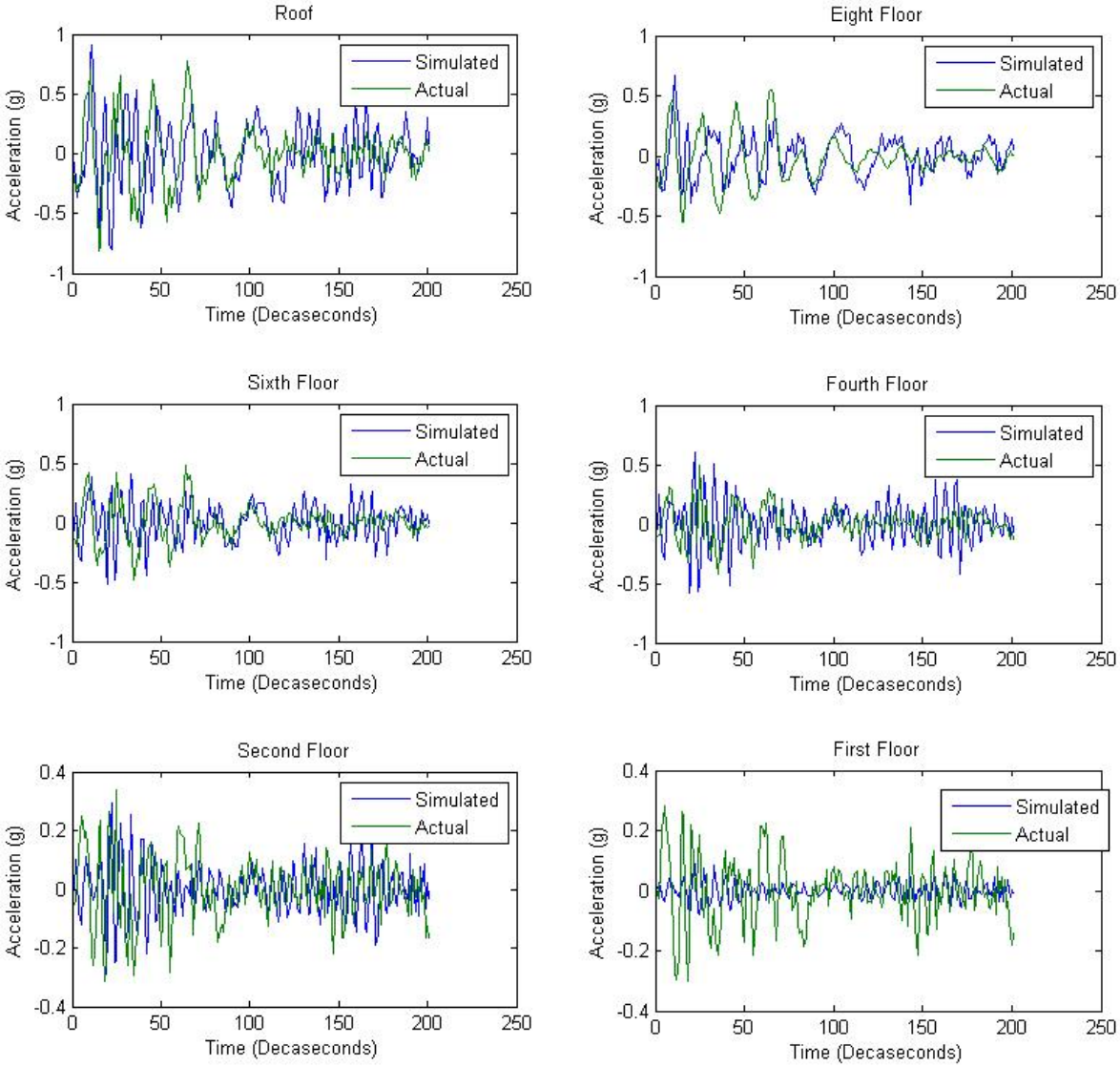

Figure 16 - Three Dimensional, Lightly Reinforced, Completely Elastic Model Response Compared to Response of Actual Test Structure

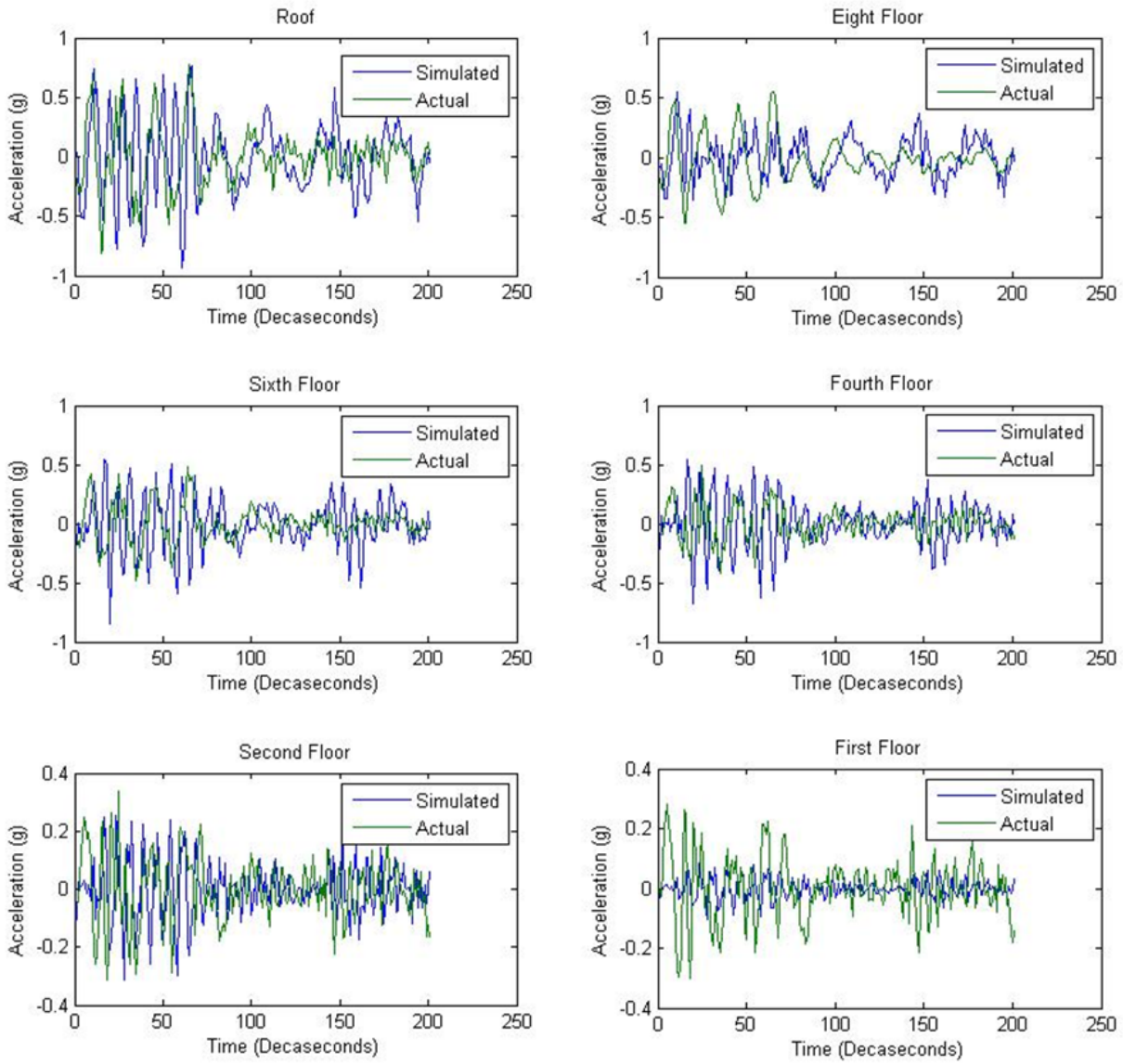

Figure 17 - Three Dimensional, Lightly Reinforced, Hinge Element Model Response Compared to Response of Actual Test Structure

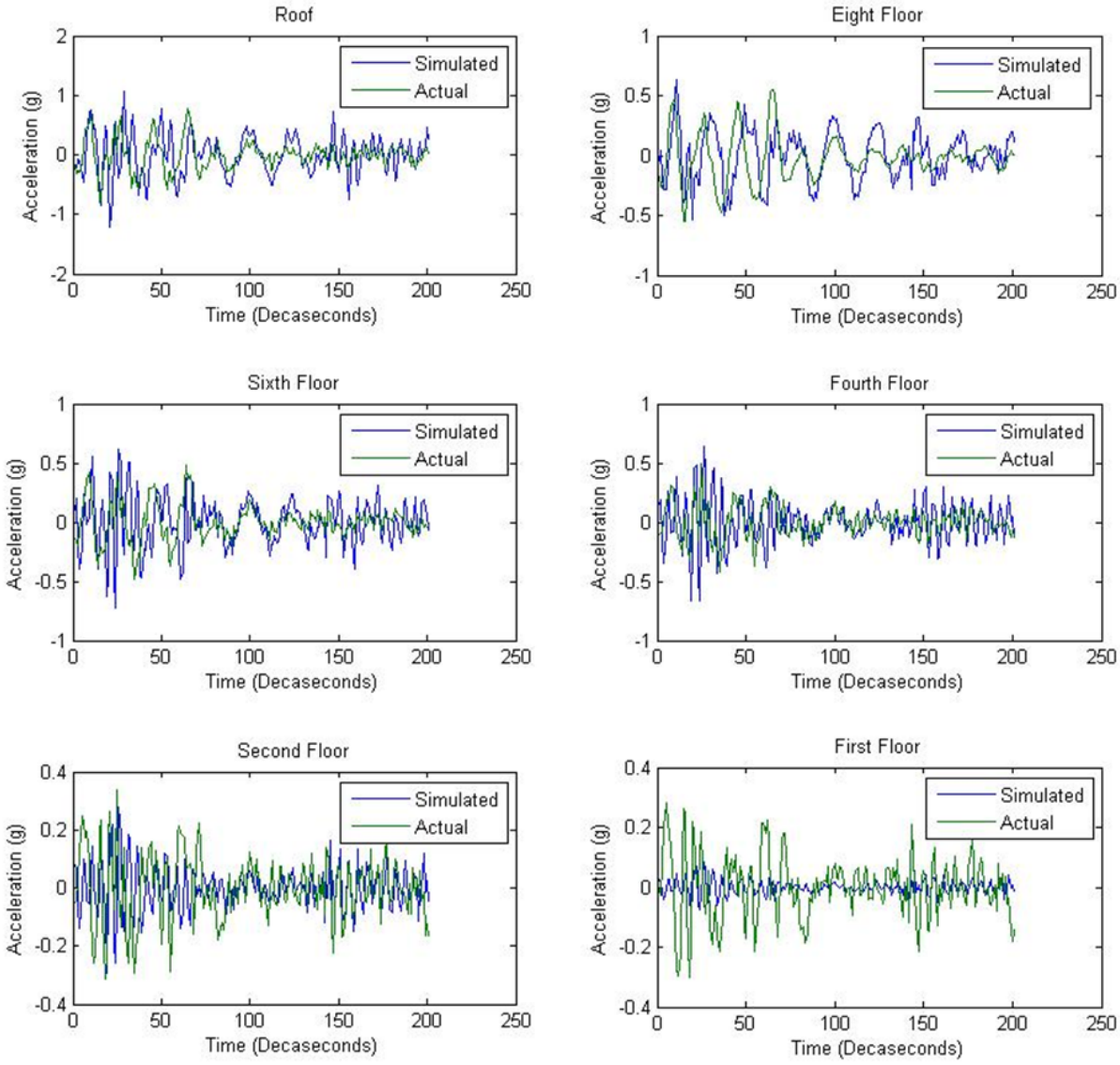

Figure 18 - Three Dimensional, Lightly Reinforced, Completely Plastic Model Response Compared to Response of Actual Test Structure

make corrections to the shake table motions adequately for each time step. This would mean that there were small variations between the input earthquake record and the motion that was output by the shake table. If the motions used to excite the actual structure and simulated structure were different, even slightly, this could cause deviations in the response. To eliminate these potential problems the entire first floor of the model was eliminated. The model was then excited at the second floor (now the bottom most floor in the model) with the recorded response of the second floor from the actual test structure. This would ensure that the model was being excited with exactly the same motion that the actual structure was experiencing. This would eliminate any error that occurred between the input record and the output motion of the shake table, and additionally any error caused by slippage between the shake table and structure. Even with these changes, no significant improvements were seen in the simulated responses; the upper floors synchronized well with the actual response while the response at lower floors still remained significantly different (Figure 19).

Another possible reason for such differences in the responses was thought to be that the stiffness properties that were reported by the original research team differed from what the actual structure contained. The method used to better determine the actual stiffness characteristics of the structure was to iteratively change the values of these characteristics through a process of trial and error to see if a better response could be achieved. The modulus of elasticity of the materials on each floor level were either increased or decreased to increase or decrease the stiffness of that floor respectively. Although this was a time consuming process that required many iterations before significant progress was made, better responses were achieved. After many trials, patterns

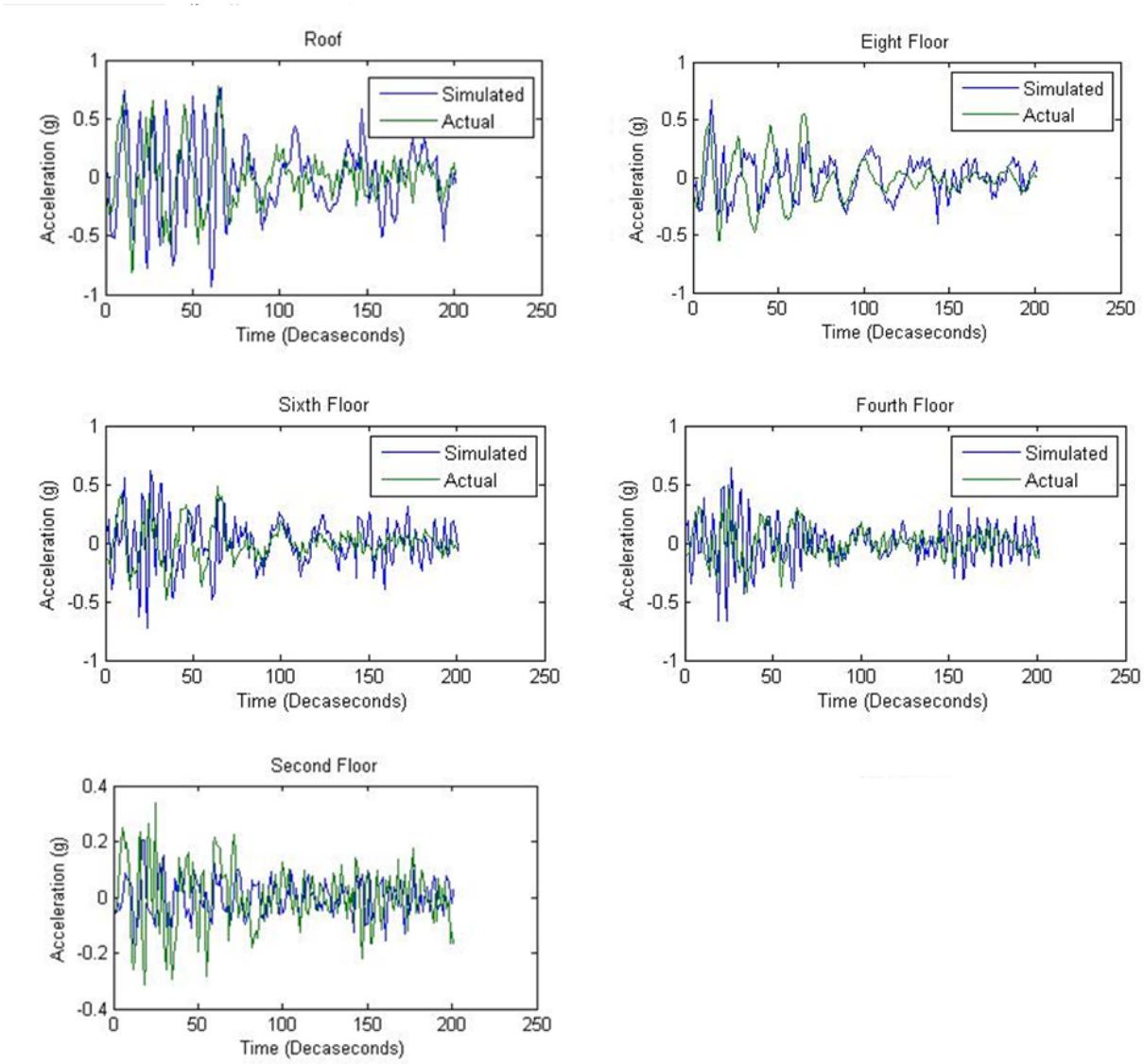

Figure 19 - Three Dimensional Model Response with Bottom Story Removed Compared to Response of Actual Test Structure

began to emerge which began to show how the changing stiffnesses affected the responses. Decreasing the stiffnesses of the lower stories improved the responses at the lower stories, however this negatively affected the responses at the upper stories (Figure 20). To improve the upper stories the stiffnesses at the upper stories were increased and additionally the damping ratio of the structure was increased to a value approaching eight percent. This reduced the accuracy of the lower stories again which was compensated for by lowering the stiffness of these stories even more. This process continued until a reasonably accurate response was able to be achieved consistently for all but the ground story (Figure 21). The model in this configuration had a modulus of elasticity of 172 GPa (25,000 ksi) at the ground floor and increasing linearly at each story up to 276 GPa (40,000 ksi) at the top. The damping ratio in the model was approximately ten percent. While this configuration produced the responses with the most similar shape and amplitudes to the actual responses it was difficult to believe that these were the actual story stiffnesses in the test structures. Since these values produced the best responses so far they were used, and it was this model which was investigated further in an attempt to even better improve the responses.

Once an approximate response was achieved at the majority of the story heights the parameter estimation routine was used in an attempt to further reduce the differences between the actual and simulated responses. This process used the same principles as the damage estimation routine, but instead of trying to estimate the damaged stiffnesses using the original healthy stiffnesses, the actual test structure stiffness values were estimated using the approximate values that were found using trial and error. The simulated

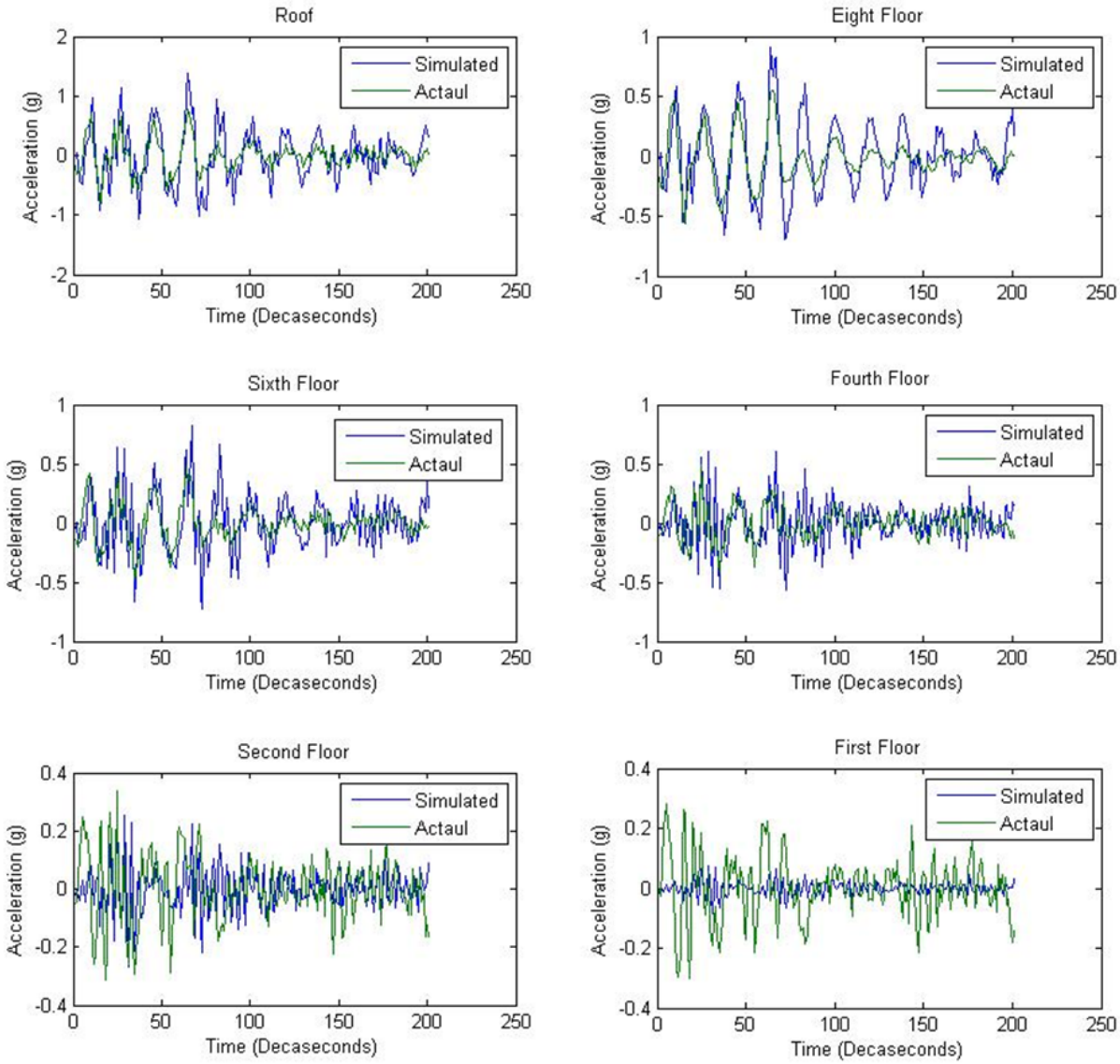

Figure 20 - Three Dimensional, Lightly Reinforced, Hinge Element Model Response with Decreased Stiffness Parameters at Lower Stories Compared to Response of Actual Test Structure

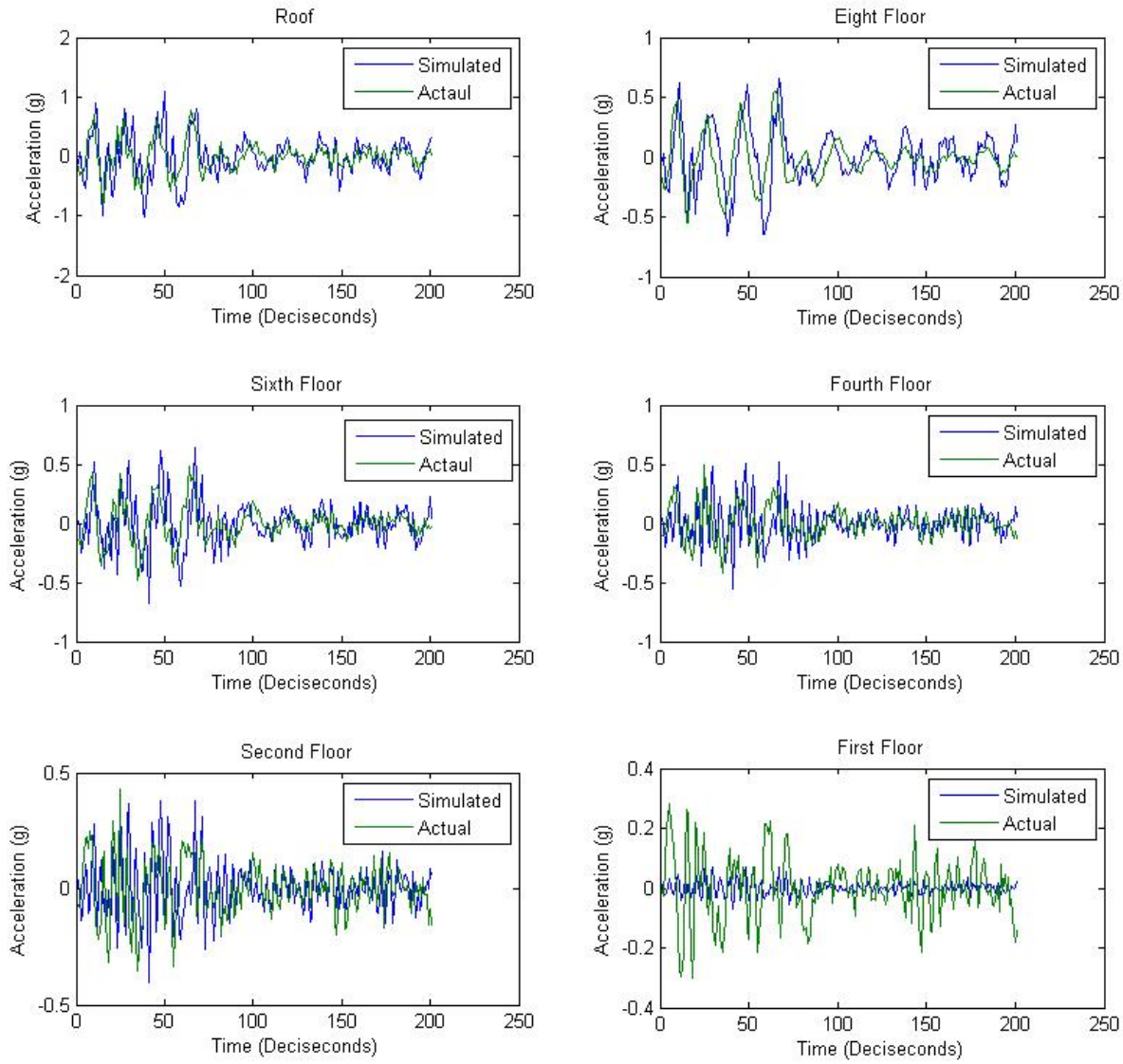

Figure 21 - Three Dimensional, Lightly Reinforced, Hinge Element Model Response with MoE Values Ranging from 172 GPa (25,000 ksi) at the Ground Floor to 276 GPa (40,000 ksi) at the Roof Compared to Response of Actual Test Structure

responses from the model were put into the routine in an attempt to fit them to the actual response by iteratively modifying the stiffness parameters. Initially, responses from all of the stories were input into the parameter estimation routine to provide the best chance for accurate prediction all of the story stiffnesses. The estimation procedure was not able to converge and the estimation failed. To improve the estimation procedure the simulated response of the first floor was removed. This was the response that was still the most different from the actual response, however, even without the first floor response the estimation procedure was not able to converge. Again, the least accurate floor response was removed from the routine but with no effect on the results. More story responses were removed until only the most accurate response remained, but still the routine was not able to converge. By removing inaccurate responses the overall accuracy of the responses improved but since fewer responses were available the procedure had less data to help it achieve the correct parameters. For these reasons the estimation procedure was not able to work with all of the responses because, overall, they were fairly inaccurate, and they were not able to work with only the accurate responses because there were too few to correctly predict that many parameters. Additionally, if the model inaccuracy were due to other parameters (such as modal damping characteristics, time dependent stiffness variations or connection fixity) the estimation would not be expected to converge. Although the responses appeared similar, they were not similar enough to be accurately fitted to the actual responses and therefore the original healthy stiffnesses were not able to be better estimated.

This was a problem for two reasons. The first being that this did not improve the accuracy of the models, and in order for it to improve the accuracy, the models would

need to be improved in some other way first. The second problem was that since the estimation procedure was not able to estimate the healthy stiffness parameters, the estimation procedure would not be able to estimate the damaged stiffness parameters using the models in this state. This was a significant problem because the estimation procedure was not able to work even when using all story responses. The models developed at this time are still too inaccurate for the preferred sensor selection process. Without the damage estimation procedure, a preferred sensor suite is meaningless which points out the importance of having a very precise model when performing this entire procedure. Not only is the accuracy of the model important to provide the most accurate preferred sensor suite but without a very accurate model the damage estimation procedure is unusable.

Furthermore, when damage was introduced into the model (by manually reducing the stiffness parameters at a single floor by 20%) the difference in response that occurred due to the damage was still less significant than the errors between the actual and simulated responses (Figure 22). Since the damage caused less of a change in the response of these models than the inherent error already present in the response, changes in the stiffness parameters could be due to error rather than damage and would not be observable.

In order for this procedure to be validated as a reasonable and reliable method of sensor selection for damage estimation a better method of modeling the structures would need to be used. That was not in the scope of this research. Although the sensor selection procedure was not confirmed for physical test data applications, this does not mean that it is not possible. Additionally, the research was not unsuccessful in providing future

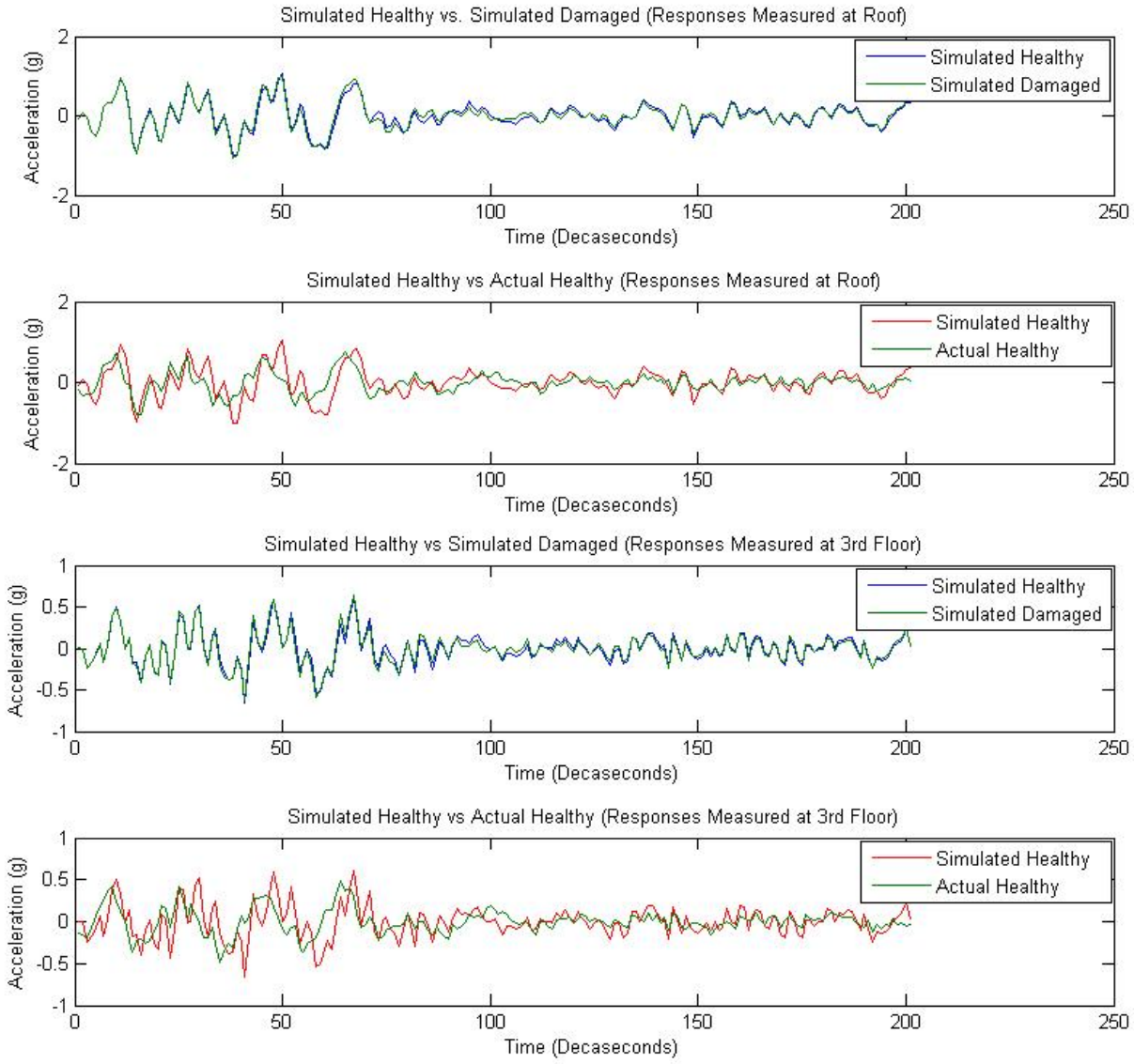

Figure 22 - Three Dimensional, Lightly Reinforced, Hinge Element Model Response With and Without a 20% Stiffness Reduction at the Third Story Compared to Response of Actual Test Structure

insight into what it would take for this procedure to work for real world applications. It was confirmed that analytically the sensor selection process was functional and it was shown that a much more accurate model is required in order for this procedure to work. The simplified two dimensional and idealized three dimensional models were not accurate enough to capture the exact response necessary for the method of sensor selection. The types of models used in this project are currently not shown to be adequate to be used to represent a full size building under real world conditions. However, this procedure should not be ruled out as a viable method to improve damage detection, as it initially requires proper models.

CHAPTER VI

SUGGESTIONS FOR FUTURE WORK

Future work should focus both on better modeling methods as well as ways of improving upon the general method used throughout the research. For example, simple sine wave excitation would mitigate many potential errors related to shake table input and response, and would help simply responses during the modeling process. They would likely make a much better starting excitation during modeling and initial tests before ultimately stepping up to the transient excitations which are better suited for damage estimation. The previous researchers did excite these structures to sine wave ground motions however the responses were not put into the NEES database with the earthquake records, and therefore could not be used for this research. Unfortunately, it was discovered only after the models were created that the sine wave records were never uploaded.

The type of test structure that was used was nearly ideal and should not be changed greatly. They were simple enough that the model geometry was fairly standard with no irregularities to make modeling more difficult than it needs to be. They also were realistic structures for examining and reporting damage. The reinforced concrete material experiences damage almost entirely in the form of cracking and a small amount of reinforcement yielding. Concrete cracking can be readily observed and recorded with ease to verify that the damage estimation is correct. However, concrete has load dependent damage which could result in variations in damage and damping during a single record. Uniform damage, as observed in these tests, may also be more difficult for

the method to observe than isolated damage. Therefore, future research should focus on a localized damage condition prior to advancing to distributed damage conditions.

Improvements to the modeling process may be required. Models are needed that can accurately and precisely simulate the true damage that occurs in the structure. It may therefore be necessary to use fiber section properties in order for the models to capture degrading stiffness accurately. Fiber section properties can capture the exact geometry of the member sections as well as the orientation of the steel reinforcing bars. Additionally, the exact material properties can be assigned to each material rather than calculating an estimated composite material property. Fiber sections are also able to capture yielding and damage variably along the length of the member and throughout the entire cross section, which would likely improve the accuracy of the model. These types of models will take a much more substantial amount of time to create and an even more significant amount of time to analyze.

CHAPTER VII

CONCLUSIONS

This research has focused on a specific method of damage detection and isolation, and sensor selection using parameter signature characteristics of output responses. There are a number of damage estimation and isolation techniques currently in use and begin developed for civil structures. This thesis presented a method that is straight-forward, accurate, versatile and cost-effective; a method that can be performed on moderate height building structures, by any technicians with the required tools and can be done with relative quickness.

Based on the current results it has been determined that a variety of factors can affect the locations of the preferred sensors. The location of the excitation, the frequency of the excitation and the portion of the response that is used can all alter the sensor suite for each analysis. For each structure variations in excitation functions and locations should be investigated and the best could be chosen to use on the actual structure. There are some excitations types that can be eliminated. Ground excitations are impractical for actual use. Excitation frequencies that exceed the frequency of the structures third mode returned an inaccurate dynamic response. A simple sine wave has been shown to yield usable results and is sensible excitation for a vibration generator to create.

Additional factors include steady state versus transient responses as well as the severity and location of damage. The use of the steady state phase of the dynamic response has been shown to work but not as accurately as when using the transient phase. To improve the accuracy using the steady state response more sensors would be required.

The transient response yielded much more accurate and reliable results than the steady state response and should be used whenever possible. The potential problem with using transient responses is the feasibility of correctly controlling the excitation unit.

The location and severity of damage was not observed to affect the outcome of the procedure. The inverse method treats all the parameters as unknowns and is trying to estimate them all, both healthy and damaged, so therefore the value of the parameter is not significant. As long as the sensor outputs provide enough identifiability to the inverse method it should be able to determine the parameters.

Testing the preferred sensor selection method analytically proved that it had the potential to be a significant advancement towards improving the efficiency of structural damage detection. Due to inadequate modeling it was not possible to verify the method against physical test data. It is therefore important to further develop the research to show that this analytically sound procedure could work in the presence of noise and other external factors. The most influential factor that hindered this procedure in real world testing was modeling error. Begin unable to accurately represent the test structures with a simulated model showed the limitations of this procedure without a reasonably accurate analytical simulation of the structure. There is still much research to be done to show that this method of sensor selection can be used effectively in actual structural applications, and while this research was not able to confirm the total validity of this method it did provide valuable insights as to how future research should proceed.

APPENDIX A

SUM TOTAL PARAMETER SIGNATURE MATRICES USING STEADY STATE RESPONSES

Table A.1 - Sum Total Parameter Signature Matrix using Ground Excitation and Steady State Response

		Outputs (Floor Accelerations)								Outputs (Floor Accelerations)							
		2	3	4	5	6	7	8	R	2	3	4	5	6	7	8	R
Parameters (Story Stiffness)	1	100	100	98	84	36	18	5	2	100	90	26	11	9	3	0	0
	2	100	100	71	39	22	17	6	5	7	82	31	11	5	1	1	1
	3	7	9	62	45	24	8	5	3	0	0	25	14	4	2	0	0
	4	4	14	18	68	44	16	8	3	1	1	3	23	12	6	2	0
	5	3	13	32	45	100	53	31	25	2	1	9	9	74	25	11	8
	6	20	41	50	65	88	100	80	90	5	19	18	23	36	100	52	49
	7	55	80	93	97	99	100	100	100	30	58	72	71	81	100	100	100
	8	100	100	100	100	100	100	100	100	100	100	100	100	100	100	100	100
		$\eta_d = 1.1$								$\eta_d = 1.3$							
Parameters (Story Stiffness)	1	100	96	63	25	15	5	0	1	100	71	12	4	4	1	0	0
	2	33	92	47	15	11	5	3	2	1	63	14	4	2	0	1	0
	3	1	1	40	24	14	4	1	0	0	0	8	3	1	0	0	0
	4	3	6	7	38	20	9	2	0	0	0	1	15	4	1	1	0
	5	3	3	13	19	99	37	14	11	0	0	3	3	30	13	3	4
	6	8	30	30	40	63	100	64	70	2	2	9	9	17	100	40	26
	7	39	70	80	84	88	100	100	100	22	40	49	56	71	89	100	100
	8	100	100	100	100	100	100	100	100	100	99	100	100	100	100	100	100
		$\eta_d = 1.2$								$\eta_d = 1.5$							

Table A.2 - Sum Total Parameter Signature Matrix using Floor 2 Excitation and Steady State Response

Parameters (Story Stiffness)	Outputs (Floor Accelerations) 2	3	4	5	6	7	8	R	Outputs (Floor Accelerations) 2	3	4	5	6	7	8	R
1	100	100	100	100	100	100	100	100	100	100	100	100	100	100	100	97
2	62	100	54	50	16	10	5	2	3	100	9	14	3	2	0	1
3	7	22	55	41	19	17	5	6	1	4	8	10	4	3	2	1
4	7	2	0	60	38	15	3	6	0	0	0	24	9	3	1	2
5	6	6	1	8	100	48	20	13	3	0	1	1	41	16	4	2
6	15	15	6	20	19	100	78	73	10	1	2	10	11	100	44	35
7	63	52	37	63	75	66	100	100	35	22	19	39	64	38	100	100
8	100	100	100	100	100	100	100	100	100	98	100	99	100	100	99	100
	$\eta_d = 1.1$								$\eta_d = 1.3$							
1	100	100	100	100	100	100	100	100	100	98	100	100	100	100	98	89
2	7	100	32	22	3	4	0	1	1	100	1	4	0	0	0	0
3	1	5	20	16	9	6	2	1	0	1	2	6	2	0	1	0
4	1	0	0	30	15	4	2	3	0	0	0	9	3	3	0	0
5	5	1	1	1	70	23	7	7	1	0	0	1	23	12	1	1
6	12	1	6	12	14	100	64	52	3	0	0	8	5	75	23	18
7	49	36	29	47	66	51	100	100	25	14	11	27	48	25	100	100
8	100	99	100	100	100	100	99	100	99	95	99	99	99	100	99	99
	$\eta_d = 1.2$								$\eta_d = 1.5$							

Table A.3 - Sum Total Parameter Signature Matrix using Floor 3 Excitation and Steady State Response

		Outputs (Floor Accelerations)								Outputs (Floor Accelerations)							
		2	3	4	5	6	7	8	R	2	3	4	5	6	7	8	R
Parameters (Story Stiffness)	1	100	100	100	100	100	99	87	84	100	80	90	91	82	72	39	45
	2	100	100	100	100	100	99	90	84	100	82	94	90	86	80	47	44
	3	22	22	100	16	11	10	10	2	4	5	12	0	1	0	0	0
	4	2	2	4	19	10	9	5	4	0	0	0	2	2	0	0	0
	5	6	2	6	16	23	16	10	6	0	0	1	1	9	5	1	0
	6	15	7	18	24	48	55	38	44	1	1	3	0	4	24	12	11
	7	52	26	68	72	73	98	100	99	22	4	27	37	25	40	100	96
	8	100	96	100	100	100	100	100	100	98	78	99	100	99	100	99	100
		$\eta_d = 1.1$								$\eta_d = 1.3$							
Parameters (Story Stiffness)	1	100	98	97	98	96	91	59	59	98	54	69	65	65	47	24	24
	2	100	91	99	98	93	94	69	63	100	53	78	70	60	53	21	25
	3	5	10	47	2	2	1	2	1	1	3	1	0	1	0	0	0
	4	0	0	0	5	3	1	1	1	0	0	0	0	1	0	0	0
	5	1	0	2	1	12	8	2	0	0	0	0	0	3	2	0	0
	6	1	1	4	7	13	35	17	14	0	0	0	0	1	16	5	3
	7	36	9	38	50	42	64	100	98	14	4	19	19	13	13	95	86
	8	99	91	100	100	100	100	100	100	95	62	96	99	99	100	95	100
		$\eta_d = 1.2$								$\eta_d = 1.5$							

Table A.4 - Sum Total Parameter Signature Matrix using Floor 4 Excitation and Steady State Response

Parameters (Story Stiffness)	Outputs (Floor Accelerations) 2	3	4	5	6	7	8	R	Outputs (Floor Accelerations) 2	3	4	5	6	7	8	R
1	100	100	60	59	47	40	15	12	100	90	32	26	15	10	2	3
2	54	100	94	72	65	51	18	16	9	94	55	34	26	10	7	1
3	55	100	93	100	100	100	40	32	8	12	56	64	54	48	15	15
4	0	4	10	13	14	20	39	21	0	0	0	4	3	4	2	1
5	1	6	11	40	16	22	11	7	1	1	0	6	5	5	2	3
6	6	18	20	31	84	65	26	34	2	3	4	1	42	46	7	10
7	37	68	80	77	82	100	100	100	19	27	42	38	47	97	100	100
8	100	100	100	100	100	100	100	100	100	99	100	100	100	100	100	100
	$\eta_d = 1.1$								$\eta_d = 1.3$							
1	100	97	37	35	28	25	5	7	100	69	17	13	7	4	0	0
2	32	99	74	54	40	22	9	4	1	78	23	17	14	3	3	0
3	20	47	73	79	80	72	21	22	2	1	36	31	32	15	5	5
4	0	0	3	7	7	8	10	3	0	0	0	2	2	2	0	1
5	1	2	2	12	7	12	5	3	0	0	0	0	2	2	0	2
6	6	4	7	8	56	55	14	16	0	0	1	0	8	29	1	6
7	29	38	61	54	64	100	100	100	11	19	26	21	33	70	100	100
8	100	100	100	100	100	100	100	100	99	96	99	98	100	100	100	100
	$\eta_d = 1.2$								$\eta_d = 1.5$							

Table A.5 - Sum Total Parameter Signature Matrix usingFloor 5 Excitation and Steady State Response

		Outputs (Floor Accelerations)							
		2	3	4	5	6	7	8	R
Parameters (Story Stiffness)	1	100	100	59	32	18	15	6	2
	2	50	100	72	33	26	19	1	5
	3	41	16	100	55	53	32	9	5
	4	60	19	13	100	100	100	41	38
	5	8	16	40	38	23	20	49	33
	6	20	24	31	37	84	74	34	37
	7	63	72	77	80	89	100	100	100
	8	100	100	100	100	100	100	100	100

$\eta_d = 1.1$

		Outputs (Floor Accelerations)							
		2	3	4	5	6	7	8	R
Parameters (Story Stiffness)	1	100	91	26	11	2	3	1	0
	2	14	90	34	12	5	6	0	1
	3	10	0	64	23	20	8	2	0
	4	24	2	4	75	86	98	13	19
	5	1	1	6	3	7	6	5	4
	6	10	0	1	9	45	44	12	10
	7	39	37	38	43	59	99	100	100
	8	99	100	100	100	99	100	100	100

$\eta_d = 1.3$

		Outputs (Floor Accelerations)							
		2	3	4	5	6	7	8	R
Parameters (Story Stiffness)	1	100	98	35	13	9	8	2	0
	2	22	98	54	19	11	12	1	1
	3	16	2	79	36	34	16	3	3
	4	30	5	7	96	100	100	23	21
	5	1	1	12	13	16	10	14	9
	6	12	7	8	18	60	56	21	18
	7	47	50	54	56	70	99	100	100
	8	100	100	100	100	99	100	100	100

$\eta_d = 1.2$

		Outputs (Floor Accelerations)							
		2	3	4	5	6	7	8	R
Parameters (Story Stiffness)	1	100	65	13	6	1	1	0	0
	2	4	70	17	4	1	1	0	0
	3	6	0	31	12	7	3	1	0
	4	9	0	2	43	44	31	3	3
	5	1	0	0	0	4	2	2	0
	6	8	0	0	5	19	29	6	4
	7	27	19	21	26	38	91	100	100
	8	99	99	98	99	98	98	100	100

$\eta_d = 1.5$

Table A.6 - Sum Total Parameter Signature Matrix using Floor 6 Excitation and Steady State Response

		Outputs (Floor Accelerations)							
		2	3	4	5	6	7	8	R
Parameters (Story Stiffness)	1	100	100	47	18	7	10	11	4
	2	16	100	65	26	10	5	1	1
	3	19	11	100	53	25	5	4	3
	4	38	10	14	100	65	42	13	18
	5	100	23	16	23	100	100	62	63
	6	19	48	84	84	83	76	40	39
	7	75	73	82	89	80	100	100	100
	8	100	100	100	100	100	100	100	100

$\eta_d = 1.1$

		Outputs (Floor Accelerations)							
		2	3	4	5	6	7	8	R
Parameters (Story Stiffness)	1	100	82	15	2	1	0	0	1
	2	3	86	26	5	2	0	0	0
	3	4	1	54	20	7	3	0	0
	4	9	2	3	86	19	9	6	1
	5	41	9	5	7	100	100	25	31
	6	11	4	42	45	22	45	14	14
	7	64	25	47	59	43	98	100	100
	8	100	99	100	99	100	100	100	100

$\eta_d = 1.3$

		Outputs (Floor Accelerations)							
		2	3	4	5	6	7	8	R
Parameters (Story Stiffness)	1	100	96	28	9	3	5	0	1
	2	3	93	40	11	3	2	0	0
	3	9	2	80	34	12	4	2	0
	4	15	3	7	100	29	22	8	4
	5	70	12	7	16	100	100	41	43
	6	14	13	56	60	61	55	17	25
	7	66	42	64	70	57	99	100	100
	8	100	100	100	99	100	100	100	100

$\eta_d = 1.2$

		Outputs (Floor Accelerations)							
		2	3	4	5	6	7	8	R
Parameters (Story Stiffness)	1	100	65	7	1	0	0	0	0
	2	0	60	14	1	0	0	0	0
	3	2	1	32	7	4	0	0	0
	4	3	1	2	44	8	3	1	0
	5	23	3	2	4	97	100	14	17
	6	5	1	8	19	9	24	11	4
	7	48	13	33	38	20	80	100	100
	8	99	99	100	98	97	99	100	100

$\eta_d = 1.5$

Table A.7 - Sum Total Parameter Signature Matrix using Floor 7 Excitation and Steady State Response

		Outputs (Floor Accelerations)								Outputs (Floor Accelerations)							
		2	3	4	5	6	7	8	R	2	3	4	5	6	7	8	R
Parameters (Story Stiffness)	1	100	99	40	15	10	5	1	1	100	72	10	3	0	1	0	0
	2	10	99	51	19	5	1	3	2	2	80	10	6	0	0	0	0
	3	17	10	100	32	5	6	4	2	3	0	48	8	3	0	0	0
	4	15	9	20	100	42	19	7	12	3	0	4	98	9	5	1	2
	5	48	16	22	20	100	76	31	36	16	5	5	6	100	45	12	20
	6	100	55	65	74	76	100	98	99	100	24	46	44	45	100	85	78
	7	66	98	100	100	100	100	100	100	38	40	97	99	98	81	100	100
	8	100	100	100	100	100	100	100	100	100	100	100	100	100	99	100	100
		$\eta_d = 1.1$								$\eta_d = 1.3$							
Parameters (Story Stiffness)	1	100	91	25	8	5	1	0	0	100	47	4	1	0	0	0	0
	2	4	94	22	12	2	1	1	0	0	53	3	1	0	0	0	0
	3	6	1	72	16	4	0	1	2	0	0	15	3	0	0	0	0
	4	4	1	8	100	22	12	2	6	3	0	2	31	3	1	0	0
	5	23	8	12	10	100	58	17	24	12	2	2	2	100	26	5	5
	6	100	35	55	56	55	100	94	89	75	16	29	29	24	100	74	65
	7	51	64	100	99	99	93	100	100	25	13	70	91	80	40	100	99
	8	100	100	100	100	100	100	100	100	100	100	100	98	99	97	99	100
		$\eta_d = 1.2$								$\eta_d = 1.5$							

Table A.8 - Sum Total Parameter Signature Matrix using Floor 8 Excitation and Steady State Response

Parameters (Story Stiffness)	Outputs (Floor Accelerations) 2	3	4	5	6	7	8	R
1	100	87	15	6	11	1	1	2
2	5	90	18	1	1	3	0	0
3	5	10	40	9	4	4	0	0
4	3	5	39	41	13	7	3	6
5	20	10	11	49	62	31	25	38
6	78	38	26	34	40	98	99	100
7	100	100	100	100	100	100	100	100
8	100	100	100	100	100	100	100	100

$\eta_d = 1.1$

Parameters (Story Stiffness)	Outputs (Floor Accelerations) 2	3	4	5	6	7	8	R
1	100	39	2	1	0	0	0	0
2	0	47	7	0	0	0	0	0
3	2	0	15	2	0	0	0	0
4	1	0	2	13	6	1	0	1
5	4	1	2	5	25	12	7	6
6	44	12	7	12	14	85	95	92
7	100	100	100	100	100	100	100	100
8	99	99	100	100	100	100	98	100

$\eta_d = 1.3$

Parameters (Story Stiffness)	Outputs (Floor Accelerations) 2	3	4	5	6	7	8	R
1	100	59	5	2	0	0	0	0
2	0	69	9	1	0	1	0	0
3	2	2	21	3	2	1	0	0
4	2	1	10	23	8	2	1	1
5	7	2	5	14	41	17	10	19
6	64	17	14	21	17	94	99	98
7	100	100	100	100	100	100	100	100
8	99	100	100	100	100	100	100	100

$\eta_d = 1.2$

Parameters (Story Stiffness)	Outputs (Floor Accelerations) 2	3	4	5	6	7	8	R
1	98	24	0	0	0	0	0	0
2	0	21	3	0	0	0	0	0
3	1	0	5	1	0	0	0	0
4	0	0	0	3	1	0	0	1
5	1	0	0	2	14	5	2	2
6	23	5	1	6	11	74	80	68
7	100	95	100	100	100	100	100	100
8	99	95	100	100	100	99	83	100

$\eta_d = 1.5$

Table A.9 - Sum Total Parameter Signature Matrix using Roof Excitation and Steady State Response

Parameters (Story Stiffness)	Outputs (Floor Accelerations) 2	3	4	5	6	7	8	R
1	100	84	12	2	4	1	2	1
2	2	84	16	5	1	2	0	0
3	6	2	32	5	3	2	0	1
4	6	4	21	38	18	12	6	0
5	13	6	7	33	63	36	38	11
6	73	44	34	37	39	99	100	100
7	100	99	100	100	100	100	100	100
8	100	100	100	100	100	100	100	100

$\eta_d = 1.1$

Parameters (Story Stiffness)	Outputs (Floor Accelerations) 2	3	4	5	6	7	8	R
1	97	45	3	0	1	0	0	0
2	1	44	1	1	0	0	0	0
3	1	0	15	0	0	0	0	0
4	2	0	1	19	1	2	1	0
5	2	0	3	4	31	20	6	2
6	35	11	10	10	14	78	92	66
7	100	96	100	100	100	100	100	100
8	100	100	100	100	100	100	100	100

$\eta_d = 1.3$

Parameters (Story Stiffness)	2	3	4	5	6	7	8	R
1	100	59	7	0	1	0	0	0
2	1	63	4	1	0	0	0	0
3	1	1	22	3	0	2	0	0
4	3	1	3	21	4	6	1	0
5	7	0	3	9	43	24	19	4
6	52	14	16	18	25	89	98	91
7	100	98	100	100	100	100	100	100
8	100	100	100	100	100	100	100	100

$\eta_d = 1.2$

2	3	4	5	6	7	8	R
89	24	0	0	0	0	0	0
0	25	0	0	0	0	0	0
0	0	5	0	0	0	0	0
0	0	1	3	0	0	1	0
1	0	2	0	17	5	2	2
18	3	6	4	4	65	68	42
100	86	100	100	100	99	100	100
99	100	100	100	100	100	100	100

$\eta_d = 1.5$

APPENDIX B

PARAMETER ESTIMATION CONVERGANCE PLOTS WITH STEADY STATE RESPONCES

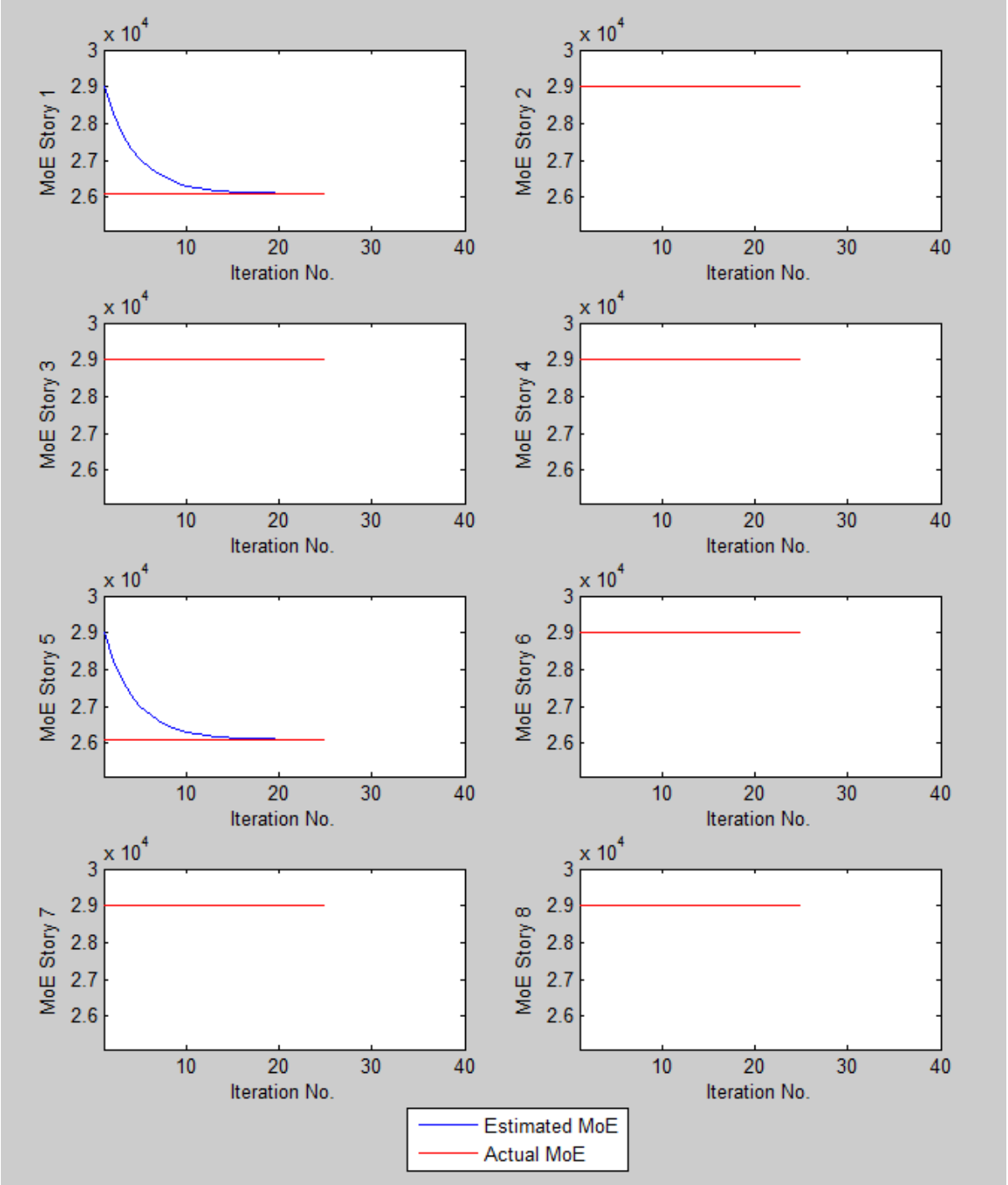

Figure B.1 - Parameter Estimation using all Eight Available Sensors for 2nd Floor Excitation with Steady State Responses

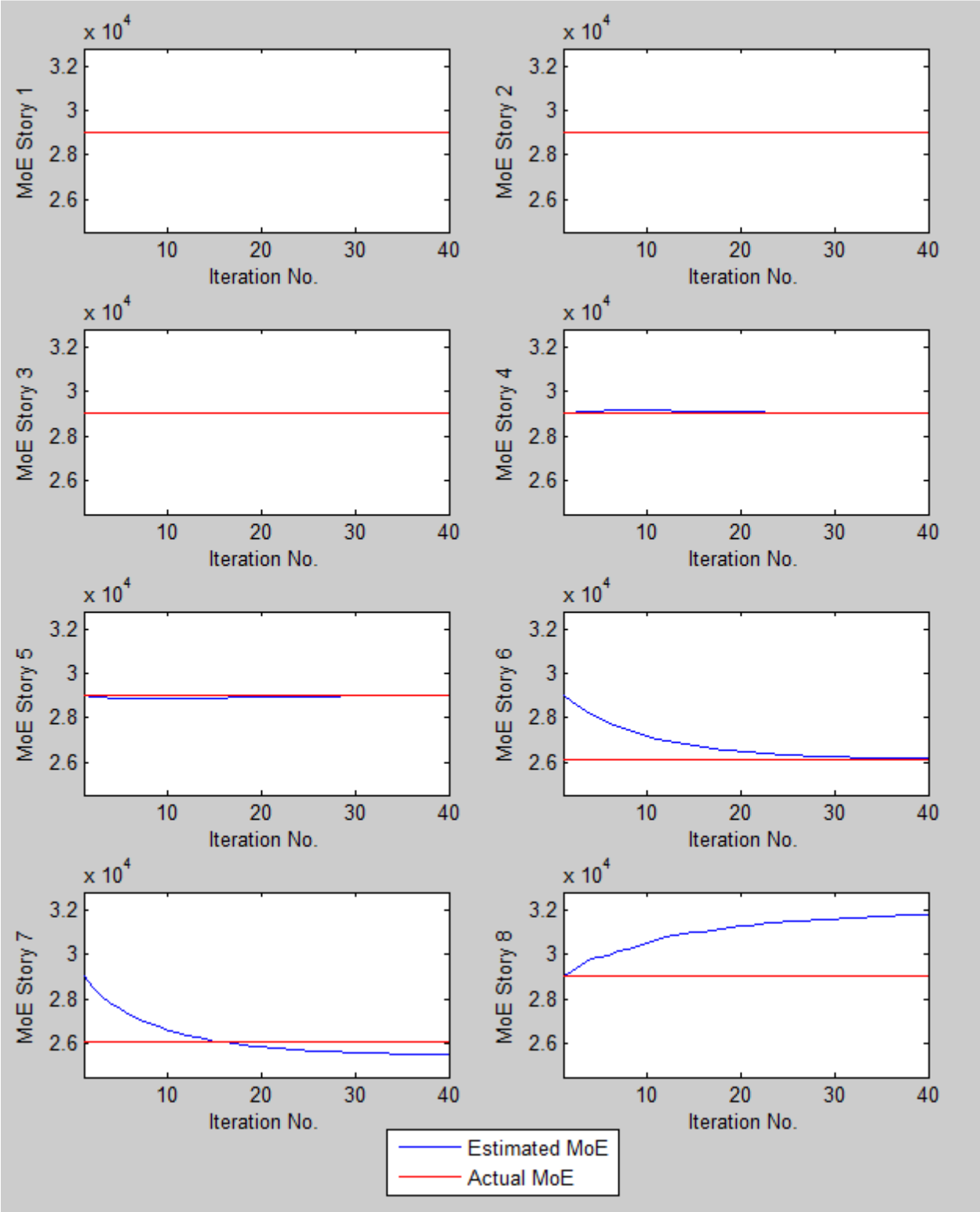

Figure B.2 - Parameter Estimation using Sensors at Floors 3, 4, 6 and 7 for 2nd Floor Excitation with Steady State Responses

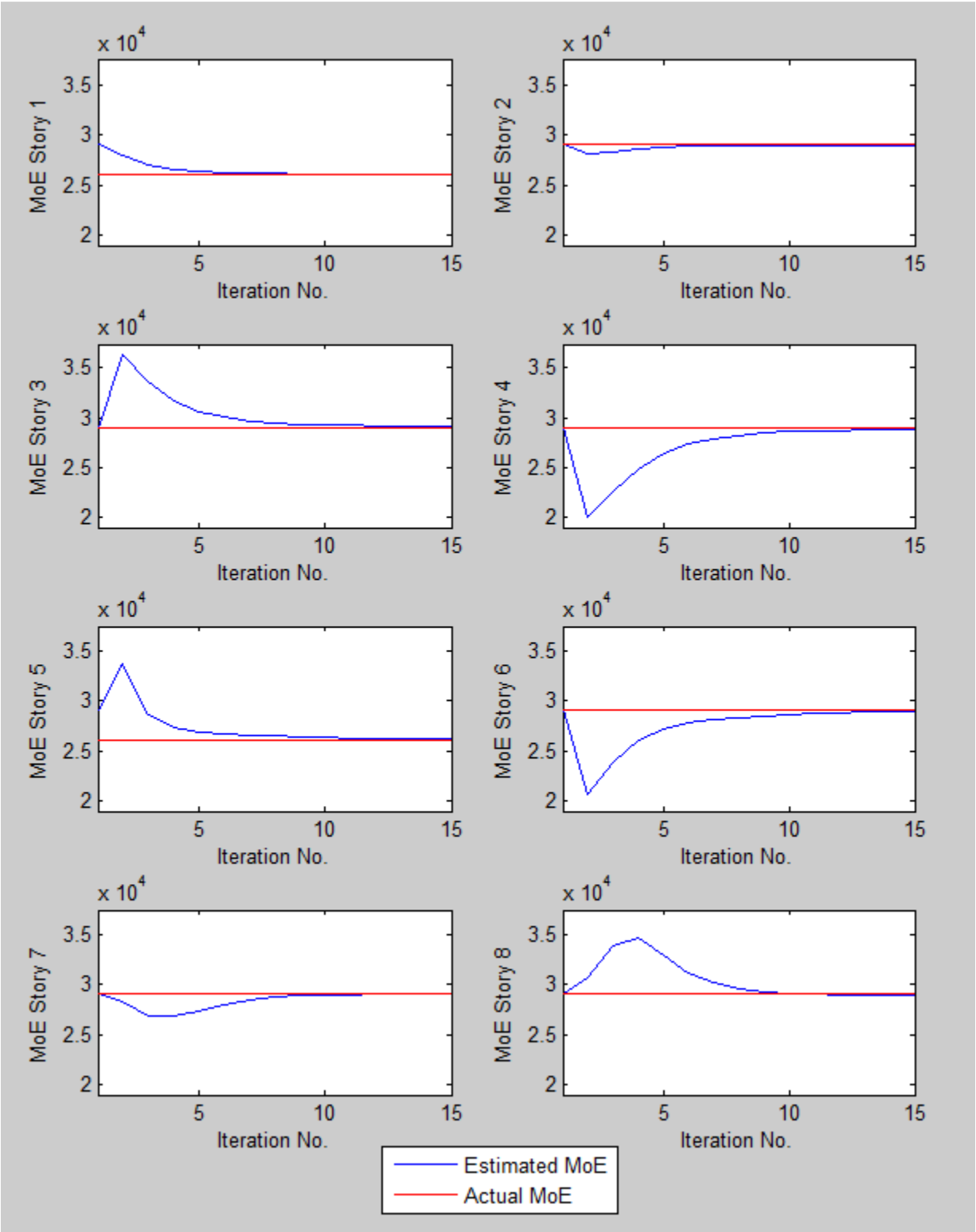

Figure B.3 - Parameter Estimation using Sensors at Floors 3, 5, 7 and Roof for 2nd Floor Excitation with Steady State Responses

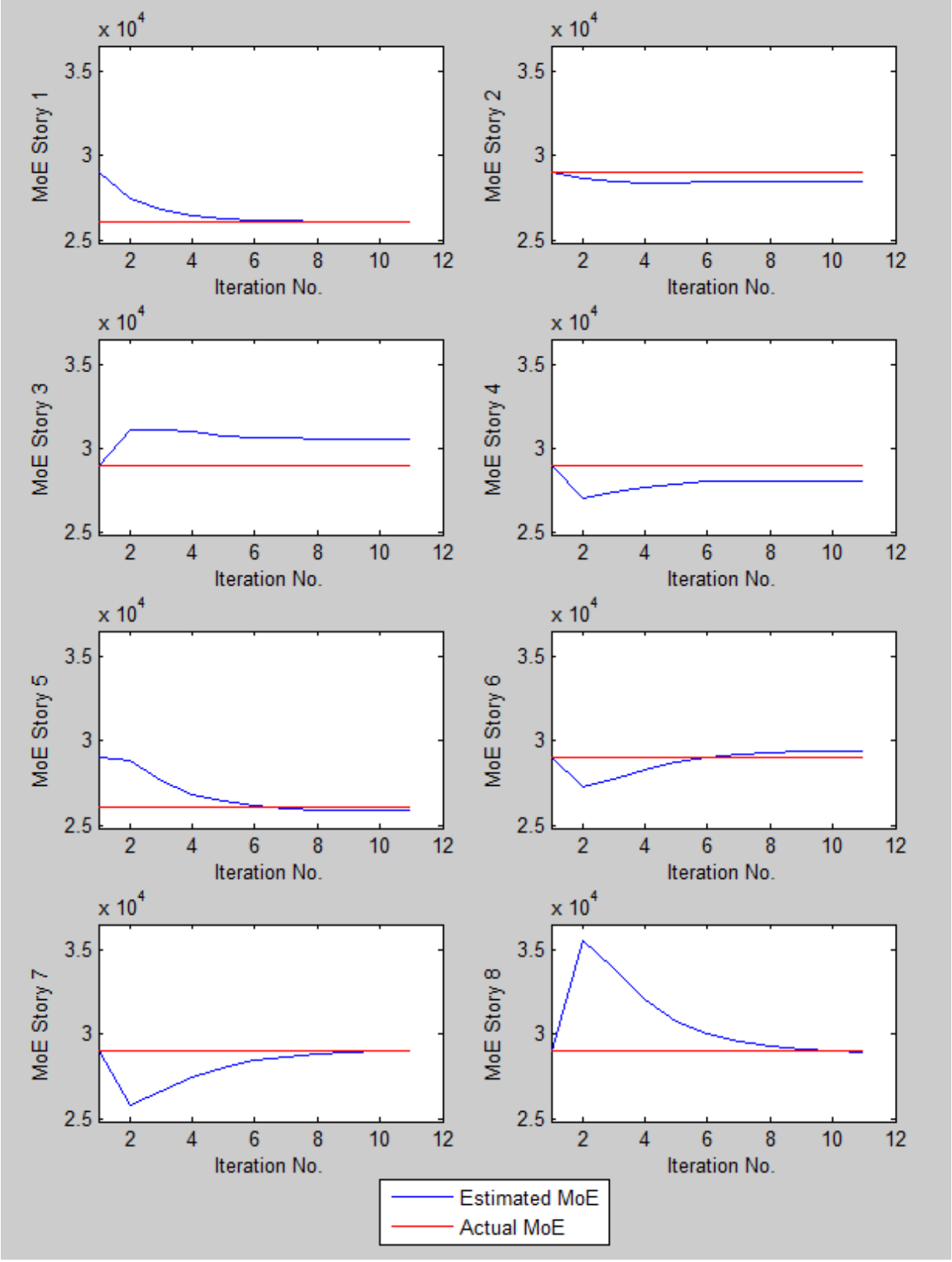

Figure B.4 - Parameter Estimation using Sensors at Floors 2, 5, 7 and Roof for 2nd Floor Excitation with Steady State Responses

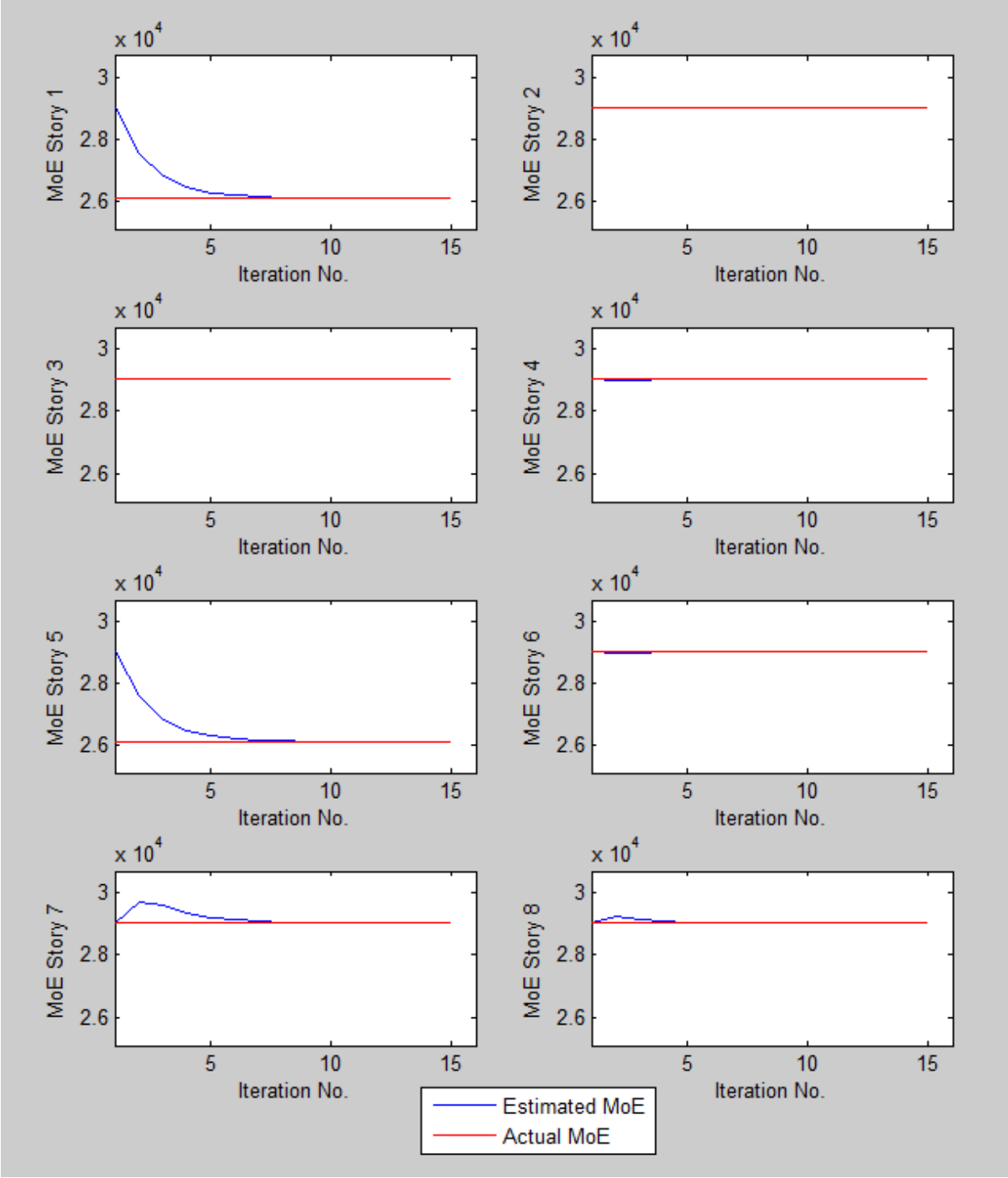

Figure B.5 - Parameter Estimation using All Available Sensors for Roof Excitation with Steady State Responses

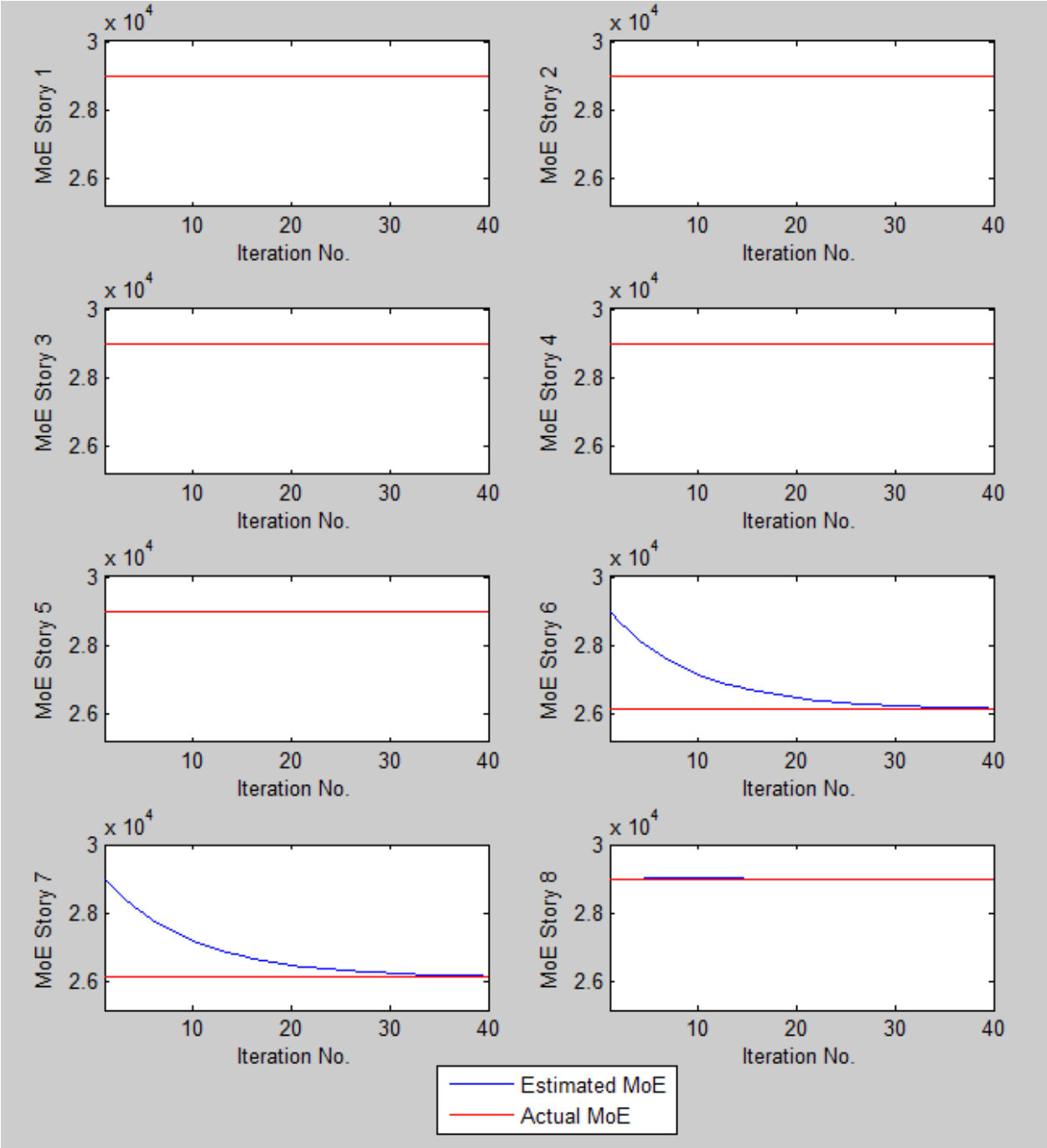

Figure B.6 - Parameter Estimation using Sensors at Floor 2, 3, 4, 6 and 8 for Roof Excitation with Steady State Responses

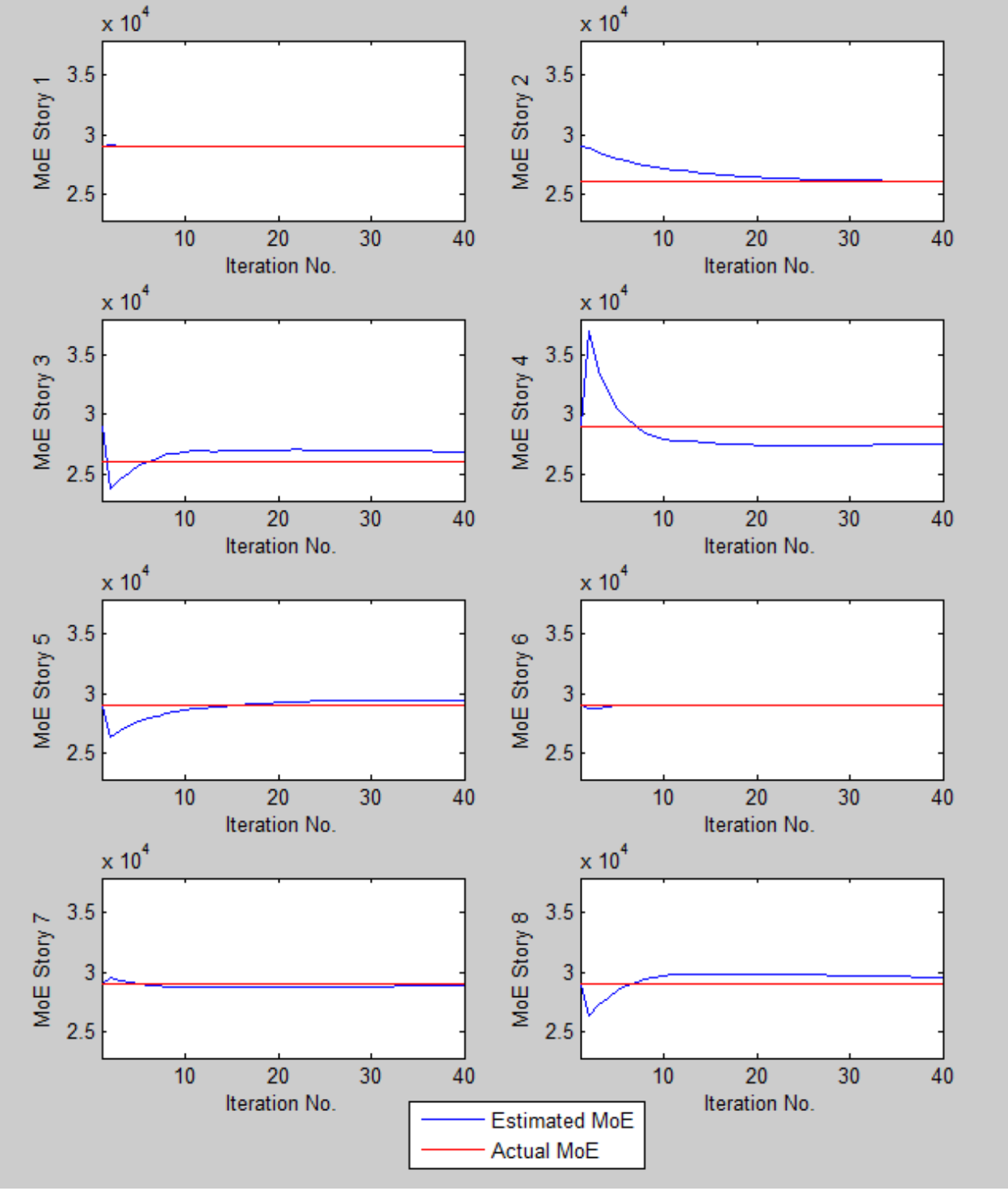

Figure B.7 - Parameter Estimation using Sensors at Floor 2, 3, 6 and 8 for Roof Excitation with Steady State Responses

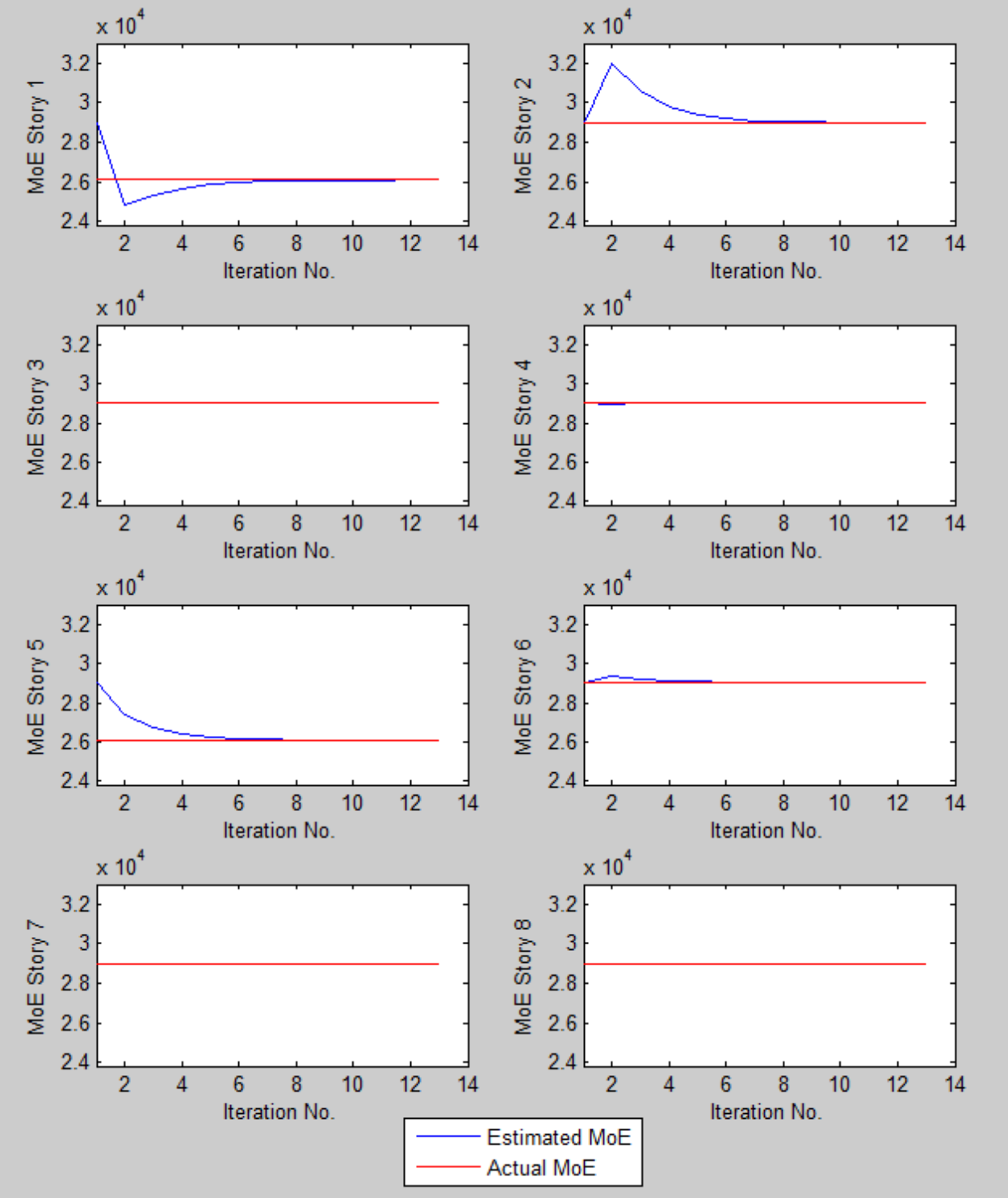

Figure B.8 - Parameter Estimation using Sensors at Floor 3, 5, 7 and Roof for Roof Excitation with Steady State Responses

APPENDIX C

SUM TOTAL PARAMETER SIGNATURE MATRICES USING TRANSIENT RESPONSES

Table C.1 - Sum Total Parameter Signature Matrices for Ground Excitation using Transient Responses

Ground Excitaion

Parameters (Story Stiffness)	Outputs (Floor Accelerations) 2	3	4	5	6	7	8	R
1	100	100	100	100	20	7	1	1
2	47	100	13	7	5	5	2	2
3	14	53	98	29	14	5	5	4
4	9	16	100	39	30	5	6	10
5	3	9	12	100	100	18	16	10
6	59	52	25	35	100	100	54	63
7	97	91	68	90	85	100	100	100
8	100	100	100	100	100	100	100	100

$\eta_d = 1.1$

Parameters (Story Stiffness)	Outputs (Floor Accelerations) 2	3	4	5	6	7	8	R
1	100	2	0	0	0	0	0	0
2	0	2	0	0	0	0	0	0
3	0	0	2	2	0	0	0	0
4	0	0	0	1	0	1	0	0
5	0	0	0	57	6	3	1	0
6	1	2	6	4	36	100	12	9
7	33	36	35	42	36	95	100	95
8	100	100	100	100	100	100	100	100

$\eta_d = 1.5$

Parameters (Story Stiffness)	Outputs (Floor Accelerations) 2	3	4	5	6	7	8	R
1	100	62	67	66	3	0	0	1
2	6	53	6	2	2	0	0	1
3	4	9	13	9	2	2	1	3
4	2	0	100	14	5	2	3	3
5	1	2	5	100	98	11	8	2
6	35	13	16	21	97	100	39	36
7	76	60	52	68	68	100	100	100
8	100	100	100	100	100	100	100	100

$\eta_d = 1.2$

Parameters (Story Stiffness)	Outputs (Floor Accelerations) 2	3	4	5	6	7	8	R
1	100	0	0	0	0	0	0	0
2	0	1	0	0	0	0	0	0
3	0	0	1	0	0	0	0	0
4	0	0	0	1	0	0	0	0
5	0	0	0	13	2	0	0	0
6	0	0	2	2	20	93	5	4
7	19	28	23	33	27	76	100	80
8	99	100	100	100	100	100	100	100

$\eta_d = 1.7$

Parameters (Story Stiffness)	Outputs (Floor Accelerations) 2	3	4	5	6	7	8	R
1	100	11	6	6	0	0	0	0
2	2	17	0	1	1	0	0	0
3	2	3	6	5	0	0	1	1
4	0	0	94	5	2	1	1	1
5	0	0	3	94	51	8	3	0
6	9	5	12	12	78	100	25	21
7	49	51	45	54	60	100	100	100
8	100	100	100	100	100	100	100	100

$\eta_d = 1.3$

Parameters (Story Stiffness)	Outputs (Floor Accelerations) 2	3	4	5	6	7	8	R
1	100	0	0	0	0	0	0	0
2	0	0	0	0	0	0	0	0
3	0	0	0	0	0	0	0	0
4	0	0	0	1	0	0	0	0
5	0	0	0	1	1	0	0	0
6	0	0	1	0	10	38	2	1
7	14	19	18	26	19	56	100	55
8	91	99	100	99	99	99	100	100

$\eta_d = 1.9$

Table C.2 - Sum Total Parameter Signature Matrices for 2nd Floor Excitation using Transient Responses

2nd Floor Excitaion

Parameters (Story Stiffness)	Outputs 2	3	4	5	6	7	8	R
1	100	100	100	100	100	100	100	100
2	100	100	100	57	9	2	1	3
3	100	100	100	88	62	31	3	28
4	99	79	100	97	95	70	6	39
5	100	100	100	100	99	11	14	63
6	100	100	100	100	100	100	100	100
7	89	92	77	100	100	100	100	100
8	93	100	100	100	100	100	100	100

$\eta_d = 1.1$

Parameters (Story Stiffness)	Outputs 2	3	4	5	6	7	8	R
1	100	100	100	100	100	100	100	100
2	61	100	7	3	1	0	0	0
3	6	0	6	2	0	0	0	0
4	27	2	9	8	3	0	2	0
5	16	15	0	0	4	1	0	4
6	97	54	7	35	84	81	28	100
7	6	2	1	39	67	75	94	38
8	15	34	64	95	100	100	100	98

$\eta_d = 1.5$

Parameters (Story Stiffness)	Outputs 2	3	4	5	6	7	8	R
1	100	100	100	100	100	100	100	100
2	100	100	73	30	2	1	1	1
3	99	78	100	10	4	9	0	3
4	90	35	100	41	41	30	4	2
5	98	97	53	91	28	6	5	14
6	100	100	79	99	100	100	94	100
7	57	36	25	98	100	100	100	83
8	69	88	100	100	100	100	100	100

$\eta_d = 1.2$

Parameters (Story Stiffness)	Outputs 2	3	4	5	6	7	8	R
1	100	100	100	100	100	100	100	100
2	10	100	0	0	0	0	0	0
3	0	0	1	0	0	0	0	0
4	10	0	4	0	0	0	0	0
5	3	8	0	0	1	1	0	2
6	62	17	2	5	61	39	15	100
7	1	1	0	22	36	52	66	16
8	7	15	40	78	100	100	100	91

$\eta_d = 1.7$

Parameters (Story Stiffness)	Outputs 2	3	4	5	6	7	8	R
1	100	100	100	100	100	100	100	100
2	98	100	34	13	1	0	0	0
3	70	15	89	3	3	1	0	1
4	73	11	61	21	15	5	3	0
5	67	47	13	32	12	3	1	5
6	100	94	41	91	99	100	62	100
7	28	8	13	89	99	100	100	58
8	47	73	99	100	100	100	100	100

$\eta_d = 1.3$

Parameters (Story Stiffness)	Outputs 2	3	4	5	6	7	8	R
1	100	100	100	100	100	100	100	100
2	10	100	0	0	0	0	0	0
3	0	0	1	0	0	0	0	0
4	2	0	0	0	0	0	0	0
5	2	1	0	0	1	0	0	1
6	19	2	2	1	30	26	5	78
7	0	1	0	9	32	35	33	13
8	6	9	24	61	100	100	98	78

$\eta_d = 1.9$

Table C.3 - Sum Total Parameter Signature Matrices for 3rd Floor Excitation using Transient Responses

3rd Floor Excitaion

Parameters (Story Stiffness)	Outputs 2	3	4	5	6	7	8	R
1	100	100	100	100	100	100	45	81
2	100	100	100	100	100	100	100	100
3	100	100	100	76	92	52	14	13
4	79	53	100	53	75	18	4	13
5	100	100	100	100	35	1	4	31
6	100	100	100	100	100	100	99	100
7	92	89	75	96	100	100	100	100
8	100	100	100	100	100	100	100	100

$\eta_d = 1.1$

Parameters (Story Stiffness)	Outputs 2	3	4	5	6	7	8	R
1	100	25	15	8	1	1	0	5
2	100	100	22	3	0	2	3	0
3	0	45	89	0	1	0	0	0
4	2	0	34	1	0	0	0	0
5	15	8	1	19	0	0	0	0
6	54	72	5	4	77	49	15	99
7	2	0	5	32	25	55	100	26
8	34	55	78	93	100	100	100	100

$\eta_d = 1.5$

Parameters (Story Stiffness)	Outputs 2	3	4	5	6	7	8	R
1	100	99	100	100	70	43	4	17
2	100	100	100	98	64	51	71	100
3	78	95	100	13	3	5	4	3
4	35	15	100	20	21	2	0	3
5	97	91	27	100	8	1	1	3
6	100	100	83	57	100	100	86	100
7	36	23	31	74	91	96	100	89
8	88	97	100	100	100	100	100	100

$\eta_d = 1.2$

Parameters (Story Stiffness)	Outputs 2	3	4	5	6	7	8	R
1	100	6	2	3	0	1	0	0
2	100	87	3	1	0	0	2	0
3	0	27	77	0	1	0	0	0
4	0	0	6	1	0	0	0	0
5	8	3	0	2	0	0	0	0
6	17	28	1	2	31	27	8	67
7	1	0	2	20	16	34	100	14
8	15	32	62	86	100	100	100	100

$\eta_d = 1.7$

Parameters (Story Stiffness)	Outputs 2	3	4	5	6	7	8	R
1	100	89	87	76	10	9	0	5
2	100	100	88	23	15	11	6	44
3	15	79	100	3	1	1	0	2
4	11	3	100	6	6	2	0	2
5	47	33	8	99	2	1	0	0
6	94	99	41	27	99	100	36	100
7	8	2	21	50	57	83	100	55
8	73	91	97	98	100	100	100	100

$\eta_d = 1.3$

Parameters (Story Stiffness)	Outputs 2	3	4	5	6	7	8	R
1	100	3	2	3	0	0	0	0
2	100	46	0	0	0	0	0	0
3	0	10	49	0	0	0	0	0
4	0	0	2	0	0	0	0	0
5	1	1	0	1	0	0	0	0
6	2	8	0	1	7	15	5	34
7	1	0	1	11	12	24	93	8
8	9	14	44	74	100	100	99	94

$\eta_d = 1.9$

Table C.4 - Sum Total Parameter Signature Matrices for 4th Floor Excitation using Transient Responses

4th Floor Excitaion

Parameters (Story Stiffness)	Outputs (Floor Accelerations) 2	3	4	5	6	7	8	R
1	100	100	100	100	100	12	8	13
2	100	100	19	12	25	20	5	6
3	100	100	100	100	100	100	100	100
4	100	100	100	100	100	100	100	100
5	100	100	55	100	40	5	2	11
6	100	100	98	64	100	100	85	100
7	77	75	98	99	98	100	100	100
8	100	100	100	100	100	100	100	100

$\eta_d = 1.1$

Parameters (Story Stiffness)	Outputs (Floor Accelerations) 2	3	4	5	6	7	8	R
1	100	15	4	2	1	0	0	0
2	7	22	0	0	0	0	0	0
3	6	89	17	1	2	0	1	2
4	9	34	99	88	88	46	0	1
5	0	1	0	90	2	0	0	0
6	7	5	3	2	27	89	7	27
7	1	5	15	37	36	63	100	39
8	64	78	75	100	100	100	100	100

$\eta_d = 1.5$

Parameters (Story Stiffness)	Outputs (Floor Accelerations) 2	3	4	5	6	7	8	R
1	100	100	100	77	31	1	3	4
2	73	100	4	2	2	3	0	1
3	100	100	100	100	89	95	94	100
4	100	100	100	100	100	100	100	38
5	53	27	11	100	9	0	0	5
6	79	83	44	9	95	100	35	100
7	25	31	58	81	85	96	100	100
8	100	100	100	100	100	100	100	100

$\eta_d = 1.2$

Parameters (Story Stiffness)	Outputs (Floor Accelerations) 2	3	4	5	6	7	8	R
1	100	2	1	0	0	0	0	0
2	1	3	0	0	0	0	0	0
3	3	77	3	1	0	0	1	0
4	4	6	17	44	51	7	0	0
5	0	0	0	40	2	0	0	0
6	2	1	2	1	3	61	4	8
7	0	2	5	21	18	46	100	18
8	40	62	64	92	100	100	100	100

$\eta_d = 1.7$

Parameters (Story Stiffness)	Outputs (Floor Accelerations) 2	3	4	5	6	7	8	R
1	100	87	64	7	7	0	1	1
2	34	88	0	1	1	1	0	0
3	89	100	97	22	20	23	6	98
4	61	100	100	100	100	96	66	9
5	13	8	4	100	2	0	0	1
6	41	41	6	5	81	100	14	96
7	13	21	30	65	64	88	100	82
8	99	97	99	100	100	100	100	100

$\eta_d = 1.3$

Parameters (Story Stiffness)	Outputs (Floor Accelerations) 2	3	4	5	6	7	8	R
1	100	2	1	0	0	0	0	0
2	0	0	0	0	0	0	0	0
3	1	49	2	1	0	0	0	0
4	0	2	4	10	16	2	0	0
5	0	0	0	3	2	0	0	0
6	2	0	2	1	0	35	2	5
7	0	1	1	11	14	31	100	11
8	24	44	49	83	100	100	100	100

$\eta_d = 1.9$

Table C.5 - Sum Total Parameter Signature Matrices for 5th Floor Excitation using Transient Responses

5th Floor Excitaion

		Outputs (Floor Accelerations)							
		2	3	4	5	6	7	8	R
Parameters (Story Stiffness)	1	100	100	100	55	11	3	0	4
	2	57	100	12	7	3	3	0	0
	3	88	76	100	100	52	23	22	19
	4	97	53	100	100	100	100	100	100
	5	100	100	100	100	100	28	83	100
	6	100	100	64	59	100	100	19	96
	7	100	96	99	100	80	100	100	100
	8	100	100	100	100	100	100	100	100

$\eta_d = 1.1$

		Outputs (Floor Accelerations)							
		2	3	4	5	6	7	8	R
Parameters (Story Stiffness)	1	100	8	2	0	0	0	0	0
	2	3	3	0	0	0	0	0	0
	3	2	0	1	1	0	0	0	0
	4	8	1	88	4	10	32	2	0
	5	0	19	90	100	29	0	7	13
	6	35	4	2	1	90	87	4	7
	7	39	32	37	56	18	100	100	100
	8	95	93	100	100	100	100	100	100

$\eta_d = 1.5$

		Outputs (Floor Accelerations)							
		2	3	4	5	6	7	8	R
Parameters (Story Stiffness)	1	100	100	77	8	3	2	0	1
	2	30	98	2	2	0	0	0	0
	3	10	13	100	62	17	2	0	2
	4	41	20	100	100	100	100	84	84
	5	91	100	100	100	98	3	32	69
	6	99	57	9	20	100	100	12	56
	7	98	74	81	99	51	100	100	100
	8	100	100	100	100	100	100	100	100

$\eta_d = 1.2$

		Outputs (Floor Accelerations)							
		2	3	4	5	6	7	8	R
Parameters (Story Stiffness)	1	100	3	0	0	0	0	0	0
	2	0	1	0	0	0	0	0	0
	3	0	0	1	0	0	0	0	0
	4	0	1	44	0	0	12	1	0
	5	0	2	40	85	11	0	1	8
	6	5	2	1	0	62	55	1	2
	7	22	20	21	33	11	91	100	83
	8	78	86	92	99	100	100	100	100

$\eta_d = 1.7$

		Outputs (Floor Accelerations)							
		2	3	4	5	6	7	8	R
Parameters (Story Stiffness)	1	100	76	7	4	1	1	0	0
	2	13	23	1	1	0	0	0	0
	3	3	3	22	13	5	1	0	0
	4	21	6	100	91	99	91	12	16
	5	32	99	100	100	71	2	21	32
	6	91	27	5	5	100	100	8	19
	7	89	50	65	95	32	100	100	100
	8	100	98	100	100	100	100	100	100

$\eta_d = 1.3$

		Outputs (Floor Accelerations)							
		2	3	4	5	6	7	8	R
Parameters (Story Stiffness)	1	100	3	0	0	0	0	0	0
	2	0	0	0	0	0	0	0	0
	3	0	0	1	0	0	0	0	0
	4	0	0	10	0	0	1	0	0
	5	0	1	3	46	4	0	1	3
	6	1	1	1	0	39	40	0	2
	7	9	11	11	21	7	79	100	49
	8	61	74	83	91	100	100	100	100

$\eta_d = 1.9$

Table C.6 - Sum Total Parameter Signature Matrices for 6th Floor Excitation using Transient Responses

6th Floor Excitaion

Parameters (Story Stiffness)	Outputs (Floor Accelerations) 2	3	4	5	6	7	8	R
1	100	100	100	11	3	2	11	31
2	9	100	25	3	5	7	4	2
3	62	92	100	52	8	3	4	3
4	95	75	100	100	26	23	35	36
5	99	35	40	100	100	100	100	100
6	100	100	100	100	100	100	44	100
7	100	100	98	80	54	100	100	100
8	100	100	100	100	100	100	100	100

$\eta_d = 1.1$

Parameters (Story Stiffness)	Outputs (Floor Accelerations) 2	3	4	5	6	7	8	R
1	100	1	1	0	0	0	0	0
2	1	0	0	0	0	0	0	0
3	0	1	2	0	0	0	0	0
4	3	0	88	10	0	0	0	0
5	4	0	2	29	89	90	43	28
6	84	77	27	90	100	99	4	18
7	67	25	36	18	11	97	100	97
8	100	100	100	100	100	100	100	100

$\eta_d = 1.5$

Parameters (Story Stiffness)	2	3	4	5	6	7	8	R
1	100	70	31	3	2	1	1	4
2	2	64	2	0	0	0	1	1
3	4	3	89	17	0	1	1	1
4	41	21	100	100	5	5	2	2
5	28	8	9	98	100	100	100	100
6	100	100	95	100	100	100	25	100
7	100	91	85	51	32	100	100	100
8	100	100	100	100	100	100	100	100

$\eta_d = 1.2$

Parameters (Story Stiffness)	2	3	4	5	6	7	8	R
1	100	0	0	0	0	0	0	0
2	0	0	0	0	0	0	0	0
3	0	1	0	0	0	0	0	0
4	0	0	51	0	0	0	0	0
5	1	0	2	11	42	20	24	7
6	61	31	3	62	81	84	1	3
7	36	16	18	11	4	83	100	82
8	100	100	100	100	100	100	100	100

$\eta_d = 1.7$

Parameters (Story Stiffness)	2	3	4	5	6	7	8	R
1	100	10	7	1	1	0	0	2
2	1	15	1	0	0	0	1	0
3	3	1	20	5	0	0	0	1
4	15	6	100	99	3	1	1	0
5	12	2	2	71	100	100	98	92
6	99	99	81	100	100	100	14	86
7	99	57	64	32	19	100	100	100
8	100	100	100	100	100	100	100	100

$\eta_d = 1.3$

Parameters (Story Stiffness)	2	3	4	5	6	7	8	R
1	100	0	0	0	0	0	0	0
2	0	0	0	0	0	0	0	0
3	0	0	0	0	0	0	0	0
4	0	0	16	0	0	0	0	0
5	1	0	2	4	15	9	16	3
6	30	7	0	39	22	42	1	1
7	32	12	14	7	3	59	100	57
8	100	100	100	100	100	100	100	100

$\eta_d = 1.9$

Table C.7 - Sum Total Parameter Signature Matrices for 7th Floor Excitation using Transient Responses

7th Floor Excitaion

Parameters (Story Stiffness)	Outputs (Floor Accelerations) 2	3	4	5	6	7	8	R
1	100	100	12	3	2	0	7	82
2	2	100	20	3	7	1	3	3
3	31	52	100	23	3	14	2	2
4	70	18	100	100	23	5	8	9
5	11	1	5	28	100	49	7	23
6	100	100	100	100	100	100	100	100
7	100	100	100	100	100	100	100	100
8	100	100	100	100	100	100	100	100

$\eta_d = 1.1$

Parameters (Story Stiffness)	Outputs (Floor Accelerations) 2	3	4	5	6	7	8	R
1	100	1	0	0	0	0	0	0
2	0	2	0	0	0	0	0	0
3	0	0	0	0	0	0	0	0
4	0	0	46	32	0	0	0	1
5	1	0	0	0	90	1	1	0
6	81	49	89	87	99	100	100	100
7	75	55	63	100	97	95	100	100
8	100	100	100	100	100	100	100	100

$\eta_d = 1.5$

Parameters (Story Stiffness)	Outputs (Floor Accelerations) 2	3	4	5	6	7	8	R
1	100	43	1	2	1	0	2	4
2	1	51	3	0	0	1	0	2
3	9	5	95	2	1	1	1	0
4	30	2	100	100	5	1	3	6
5	6	1	0	3	100	7	4	8
6	100	100	100	100	100	100	100	100
7	100	96	96	100	100	100	100	100
8	100	100	100	100	100	100	100	100

$\eta_d = 1.2$

Parameters (Story Stiffness)	Outputs (Floor Accelerations) 2	3	4	5	6	7	8	R
1	100	1	0	0	0	0	0	0
2	0	0	0	0	0	0	0	0
3	0	0	0	0	0	0	0	0
4	0	0	7	12	0	0	0	1
5	1	0	0	0	20	0	0	0
6	39	27	61	55	84	100	100	99
7	52	34	46	91	83	75	100	88
8	100	100	100	100	100	100	100	100

$\eta_d = 1.7$

Parameters (Story Stiffness)	Outputs (Floor Accelerations) 2	3	4	5	6	7	8	R
1	100	9	0	1	0	0	0	0
2	0	11	1	0	0	0	0	1
3	1	1	23	1	0	0	1	0
4	5	2	96	91	1	0	1	2
5	3	1	0	2	100	3	3	2
6	100	100	100	100	100	100	100	100
7	100	83	88	100	100	100	100	100
8	100	100	100	100	100	100	100	100

$\eta_d = 1.3$

Parameters (Story Stiffness)	Outputs (Floor Accelerations) 2	3	4	5	6	7	8	R
1	100	0	0	0	0	0	0	0
2	0	0	0	0	0	0	0	0
3	0	0	0	0	0	0	0	0
4	0	0	2	1	0	0	0	1
5	0	0	0	0	9	0	0	0
6	26	15	35	40	42	86	89	85
7	35	24	31	79	59	47	100	73
8	100	100	100	100	100	100	100	100

$\eta_d = 1.9$

Table C.8 - Sum Total Parameter Signature Matrices for 8th Floor Excitation using Transient Responses

8th Floor Excitaion

Parameters (Story Stiffness)	Outputs (Floor Accelerations) 2	3	4	5	6	7	8	R
1	100	45	8	0	11	7	6	89
2	1	100	5	0	4	3	0	4
3	3	14	100	22	4	2	5	2
4	6	4	100	100	35	8	20	83
5	14	4	2	83	100	7	27	17
6	100	99	85	19	44	100	100	83
7	100	100	100	100	100	100	100	100
8	100	100	100	100	100	100	100	100

$\eta_d = 1.1$

Parameters (Story Stiffness)	Outputs (Floor Accelerations) 2	3	4	5	6	7	8	R
1	100	0	0	0	0	0	0	0
2	0	3	0	0	0	0	0	0
3	0	0	1	0	0	0	0	1
4	2	0	0	2	0	0	0	1
5	0	0	0	7	43	1	1	0
6	28	15	7	4	4	100	9	12
7	94	100	100	100	100	100	100	100
8	100	100	100	100	100	100	100	100

$\eta_d = 1.5$

Parameters (Story Stiffness)	Outputs (Floor Accelerations) 2	3	4	5	6	7	8	R
1	100	4	3	0	1	2	2	17
2	1	71	0	0	1	0	0	0
3	0	4	94	0	1	1	1	1
4	4	0	100	84	2	3	2	15
5	5	1	0	32	100	4	9	8
6	94	86	35	12	25	100	69	39
7	100	100	100	100	100	100	100	100
8	100	100	100	100	100	100	100	100

$\eta_d = 1.2$

Parameters (Story Stiffness)	Outputs (Floor Accelerations) 2	3	4	5	6	7	8	R
1	100	0	0	0	0	0	0	0
2	0	2	0	0	0	0	0	0
3	0	0	1	0	0	0	0	0
4	0	0	0	1	0	0	0	0
5	0	0	0	1	24	0	1	0
6	15	8	4	1	1	100	5	7
7	66	100	100	100	100	100	100	100
8	100	100	100	100	100	100	100	100

$\eta_d = 1.7$

Parameters (Story Stiffness)	Outputs (Floor Accelerations) 2	3	4	5	6	7	8	R
1	100	0	1	0	0	0	0	1
2	0	6	0	0	1	0	0	0
3	0	0	6	0	0	1	1	1
4	3	0	66	12	1	1	1	3
5	1	0	0	21	98	3	4	4
6	62	36	14	8	14	100	28	27
7	100	100	100	100	100	100	100	100
8	100	100	100	100	100	100	100	100

$\eta_d = 1.3$

Parameters (Story Stiffness)	Outputs (Floor Accelerations) 2	3	4	5	6	7	8	R
1	100	0	0	0	0	0	0	0
2	0	0	0	0	0	0	0	0
3	0	0	0	0	0	0	0	0
4	0	0	0	0	0	0	0	0
5	0	0	0	1	16	0	0	0
6	5	5	2	0	1	89	3	4
7	33	93	100	100	100	100	100	100
8	98	99	100	100	100	100	100	100

$\eta_d = 1.9$

Table C.9 - Sum Total Parameter Signature Matrices for Roof Excitation using Transient Responses

Roof Excitaion

Parameters (Story Stiffness)	Outputs (Floor Accelerations) 2	3	4	5	6	7	8	R
1	100	81	13	4	31	82	89	91
2	3	100	6	0	2	3	4	4
3	28	13	100	19	3	2	2	6
4	39	13	100	100	36	9	83	58
5	63	31	11	100	100	23	17	29
6	100	100	100	96	100	100	83	100
7	100	100	100	100	100	100	100	100
8	100	100	100	100	100	100	100	100

$\eta_d = 1.1$

Parameters (Story Stiffness)	Outputs (Floor Accelerations) 2	3	4	5	6	7	8	R
1	100	5	0	0	0	0	0	2
2	0	0	0	0	0	0	0	0
3	0	0	2	0	0	0	1	0
4	0	0	1	0	0	1	1	0
5	4	0	0	13	28	0	0	2
6	100	99	27	7	18	100	12	19
7	38	26	39	100	97	100	100	100
8	98	100	100	100	100	100	100	100

$\eta_d = 1.5$

Parameters (Story Stiffness)	2	3	4	5	6	7	8	R
1	100	17	4	1	4	4	17	46
2	1	100	1	0	1	2	0	0
3	3	3	100	2	1	0	1	2
4	2	3	38	84	2	6	15	11
5	14	3	5	69	100	8	8	12
6	100	100	100	56	100	100	39	91
7	83	89	100	100	100	100	100	100
8	100	100	100	100	100	100	100	100

$\eta_d = 1.2$

2	3	4	5	6	7	8	R
100	0	0	0	0	0	0	0
0	0	0	0	0	0	0	0
0	0	0	0	0	0	0	0
0	0	0	0	0	1	0	0
2	0	0	8	7	0	0	1
100	67	8	2	3	99	7	8
16	14	18	83	82	88	100	100
91	100	100	100	100	100	100	100

$\eta_d = 1.7$

Parameters (Story Stiffness)	2	3	4	5	6	7	8	R
1	100	5	1	0	2	0	1	13
2	0	44	0	0	0	1	0	0
3	1	2	98	0	1	0	1	0
4	0	2	9	16	0	2	3	2
5	5	0	1	32	92	2	4	5
6	100	100	96	19	86	100	27	62
7	58	55	82	100	100	100	100	100
8	100	100	100	100	100	100	100	100

$\eta_d = 1.3$

2	3	4	5	6	7	8	R
100	0	0	0	0	0	0	0
0	0	0	0	0	0	0	0
0	0	0	0	0	0	0	0
0	0	0	0	0	1	0	0
1	0	0	3	3	0	0	1
78	34	5	2	1	85	4	3
13	8	11	49	57	73	100	86
78	94	100	100	100	100	100	100

$\eta_d = 1.9$

APPENDIX D

PARAMETER ESTIMATION CONVERGANCE PLOTS WITH STEADY STATE RESPONCES

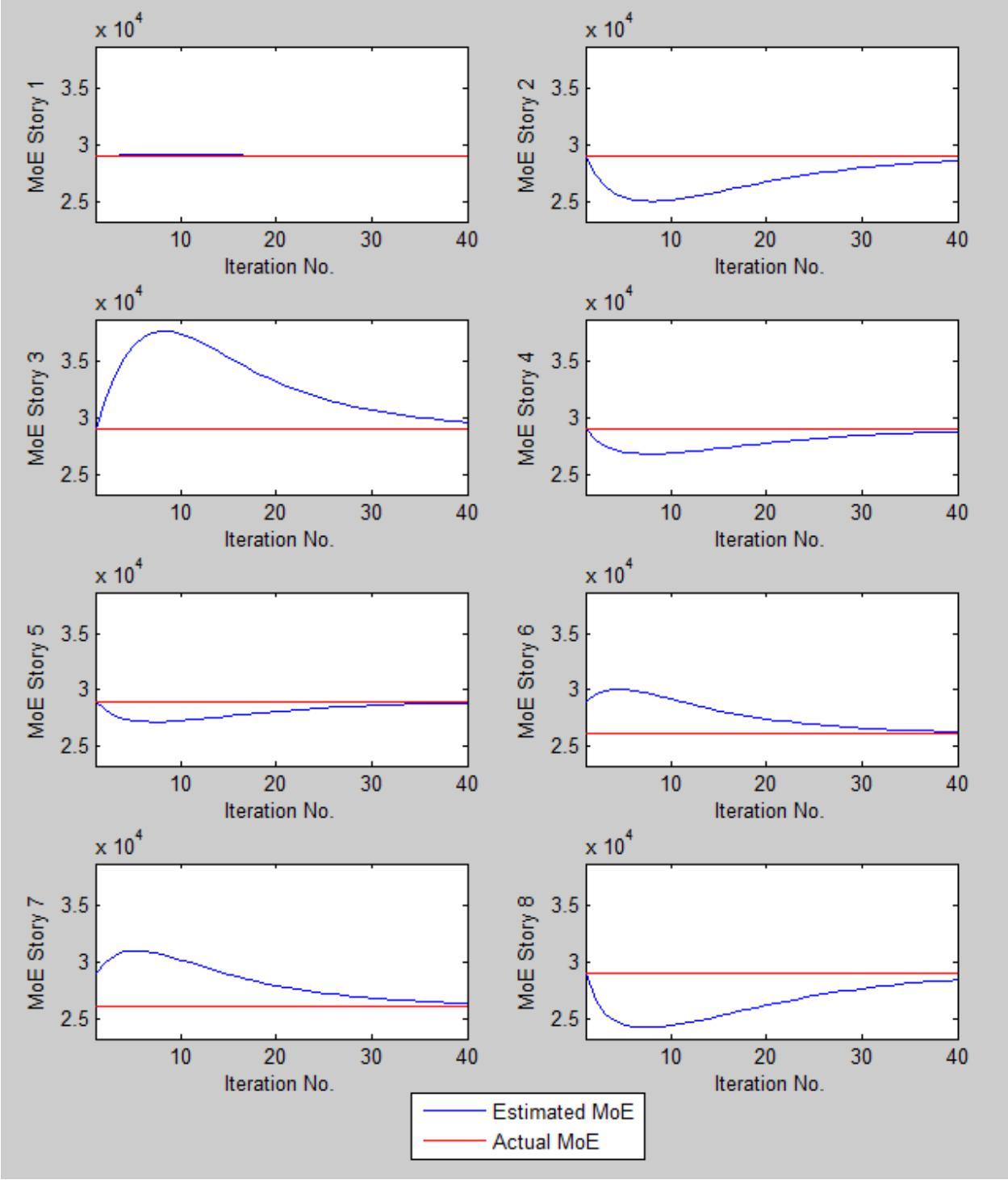

Figure D.1 - Parameter Estimation using All Available Sensors for 2nd Floor Excitation with Transient Responses

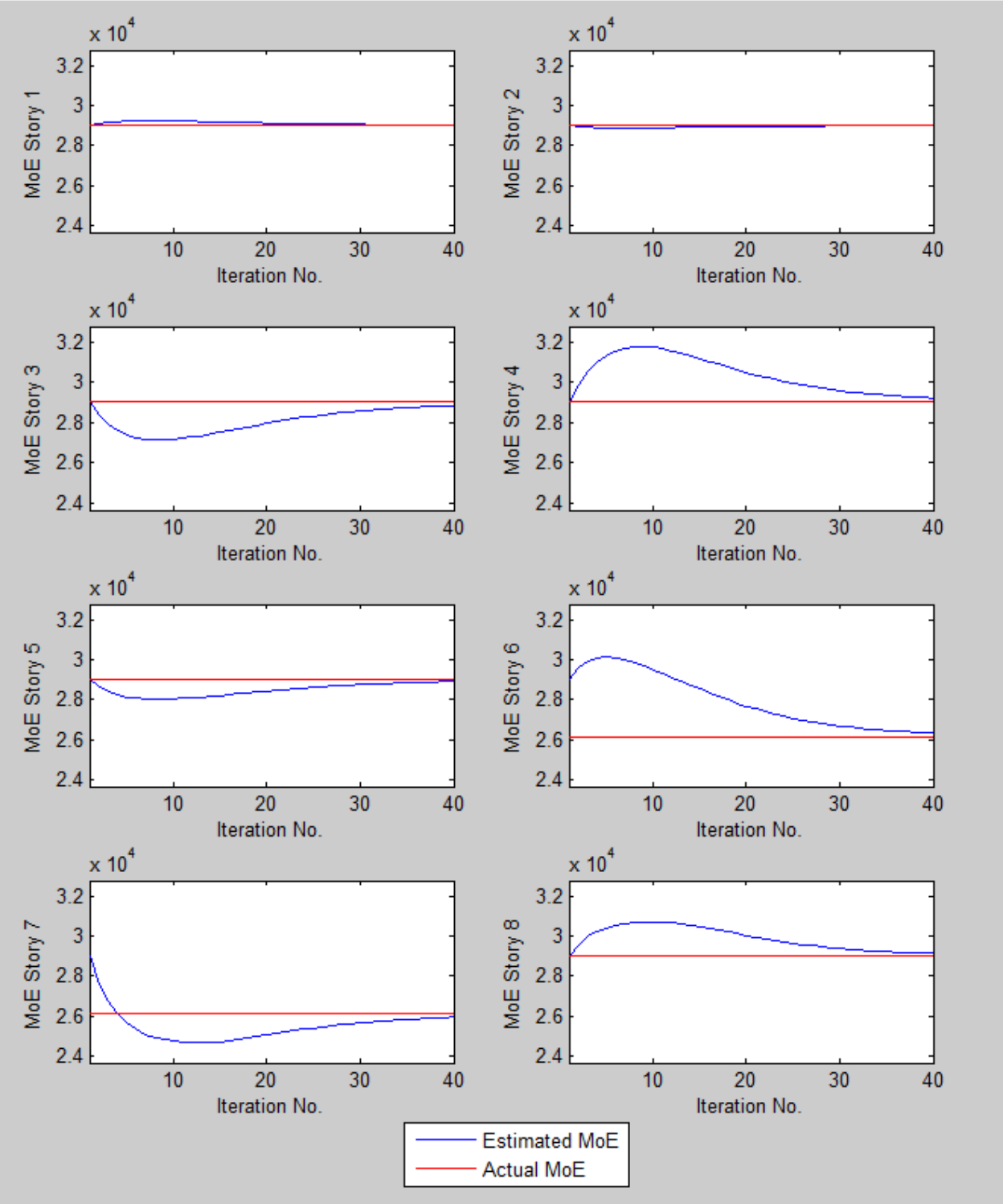

Figure D.2 - Parameter Estimation using Sensors at Floors 2, 3 and 6 for 2nd Floor Excitation with Transient Responses

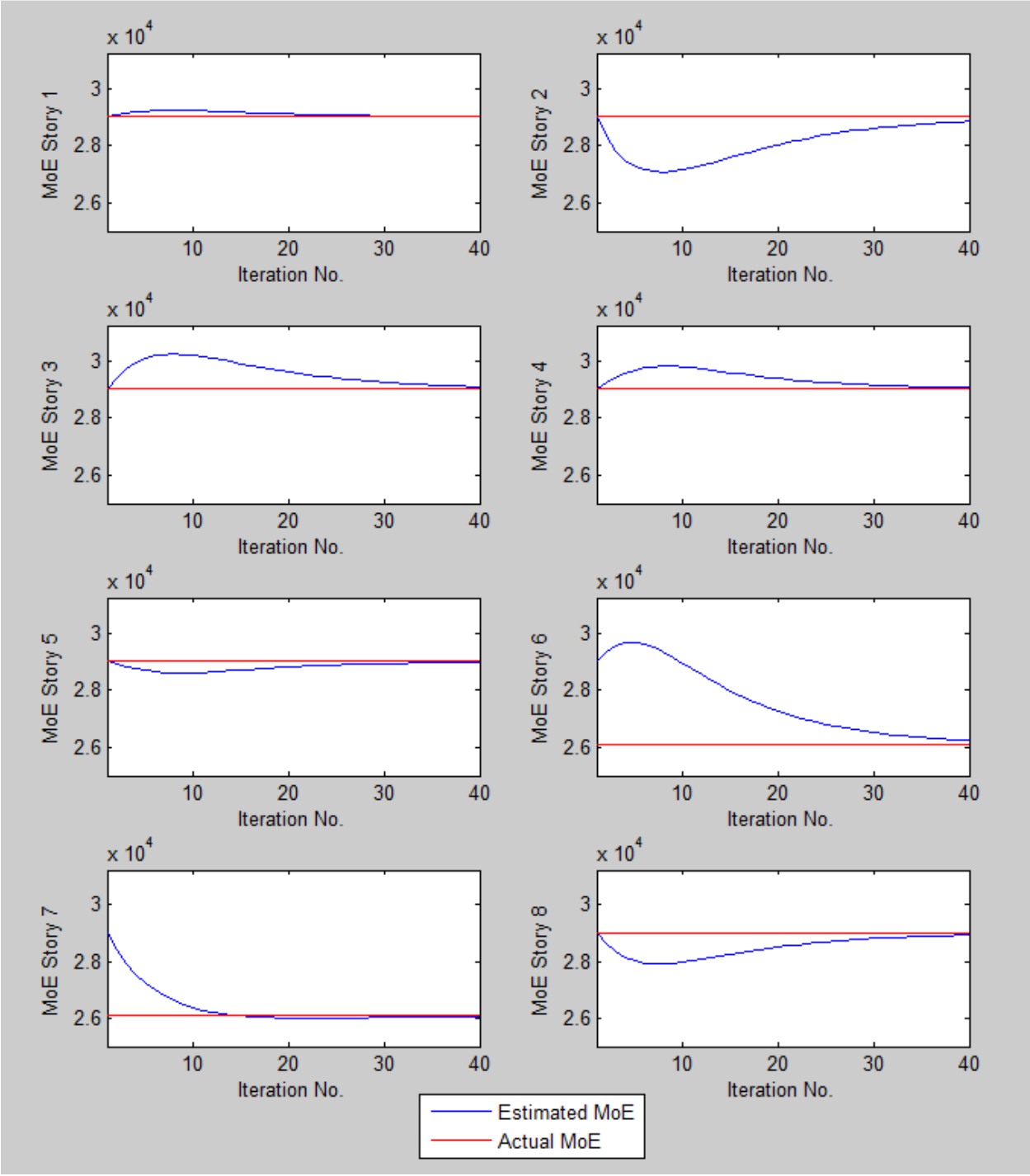

Figure D.3 - Parameter Estimation using Sensors at Floors 2 and 6 for 2nd Floor Excitation with Transient Responses

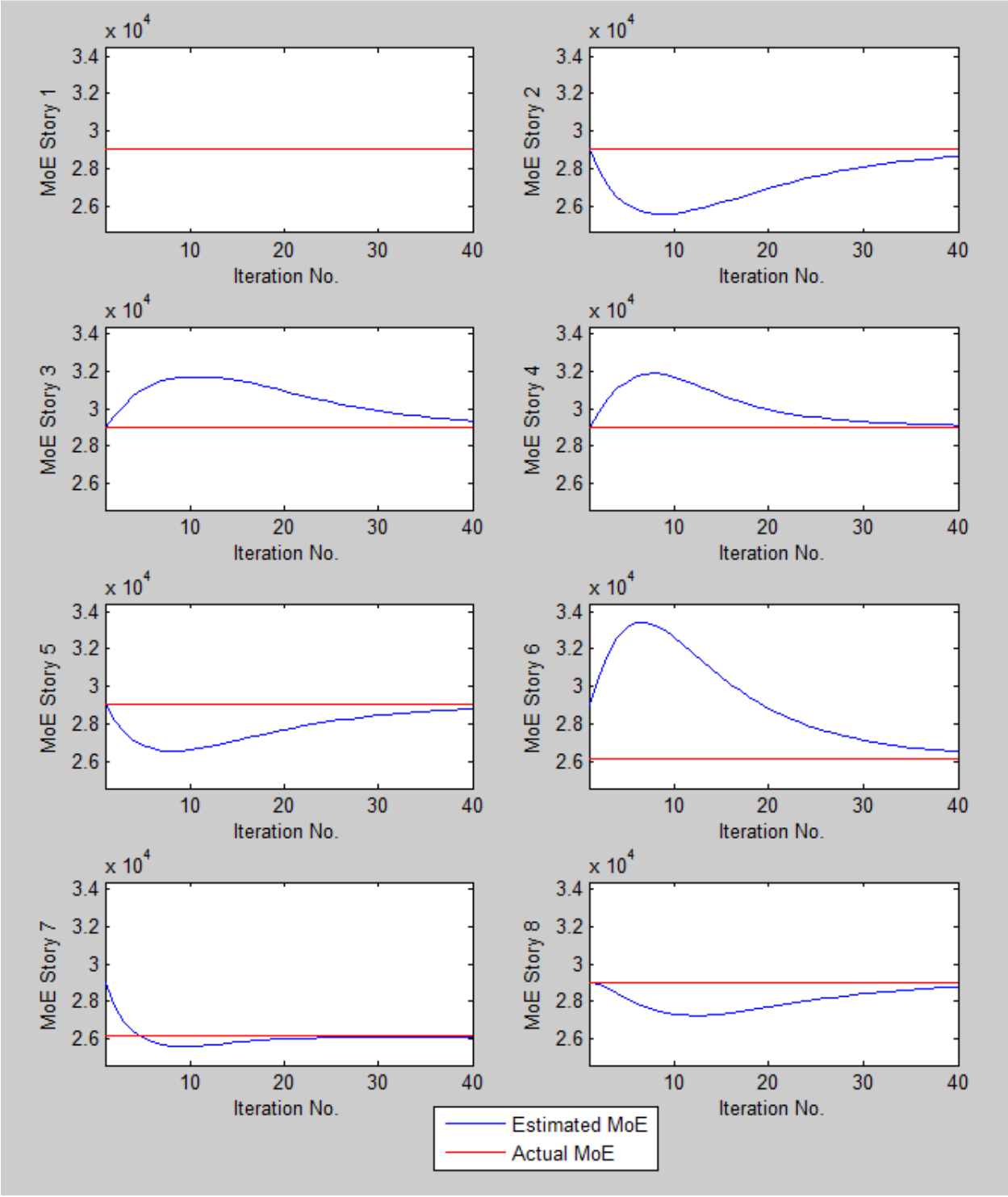

Figure D.4 - Parameter Estimation using Sensors at Floors 4 and 8 for 2nd Floor Excitation with Transient Responses

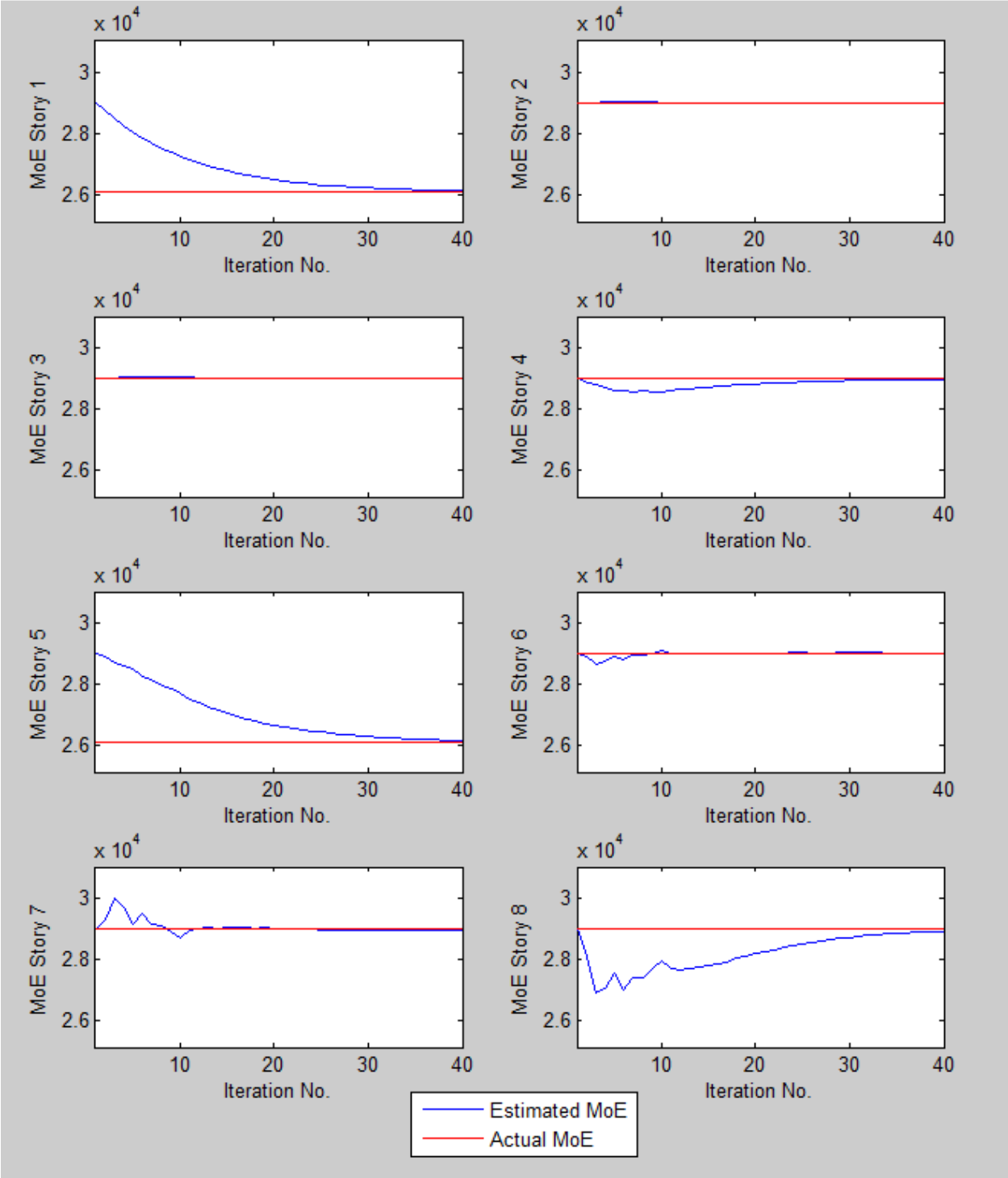

Figure D.5 - Parameter Estimation using All Available Sensors for Roof Excitation with Transient Responses

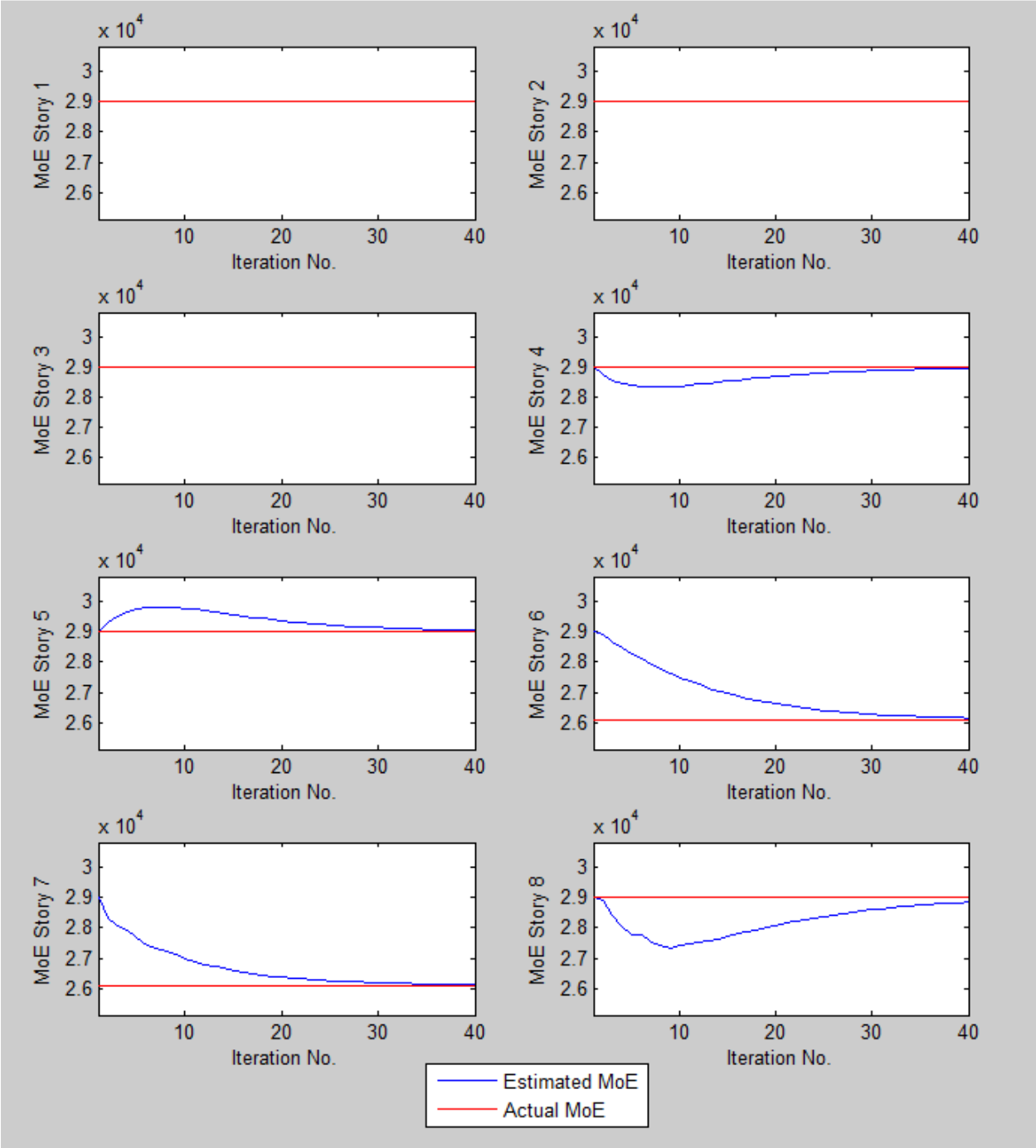

Figure D.6 - Parameter Estimation using Sensors at Floors 2, 3, 4 and 6 for Roof Excitation with Transient Responses

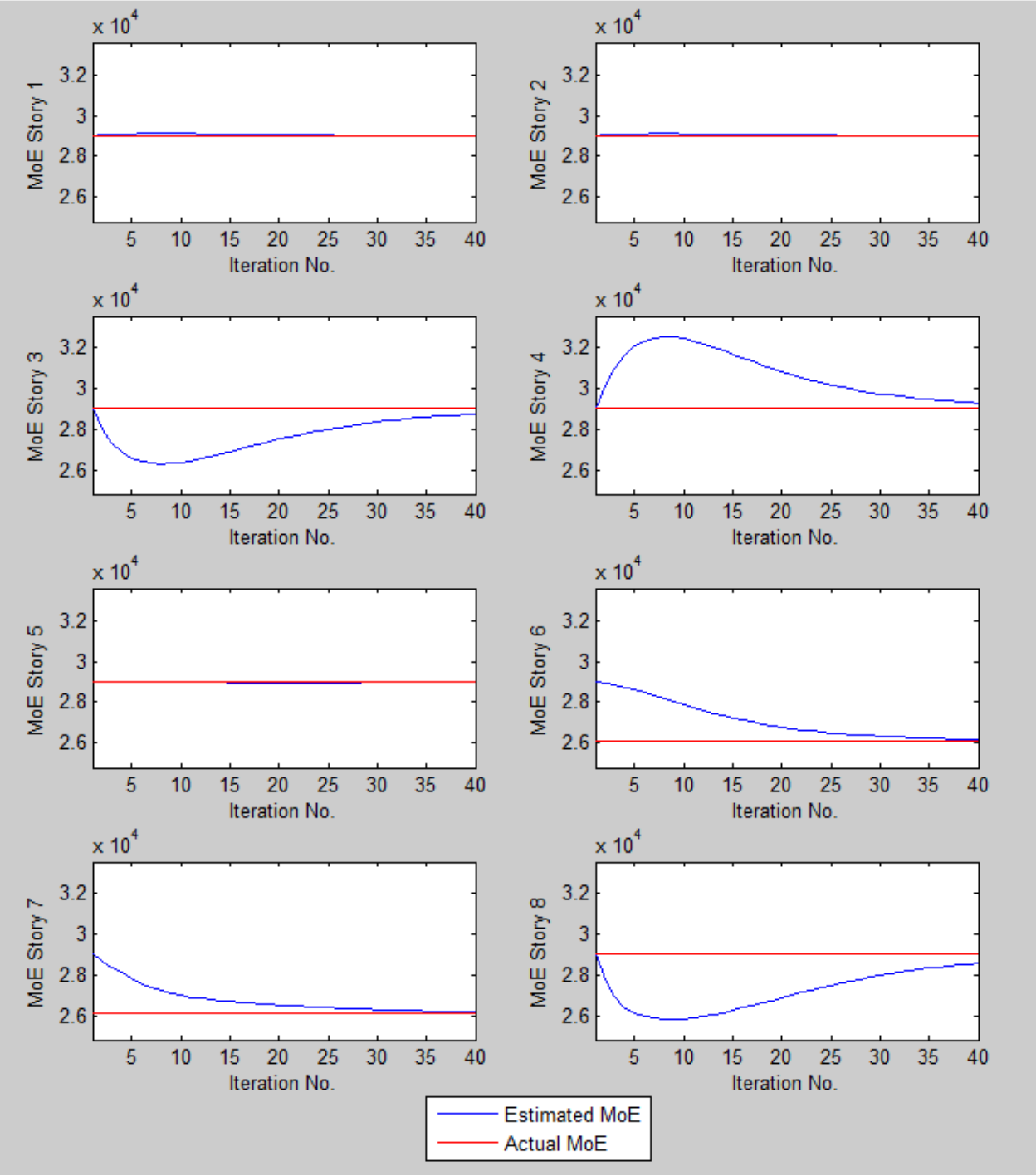

Figure D.7 - Parameter Estimation using Sensors at Floors 2, 3 and 6 for Roof Excitation with Transient Responses

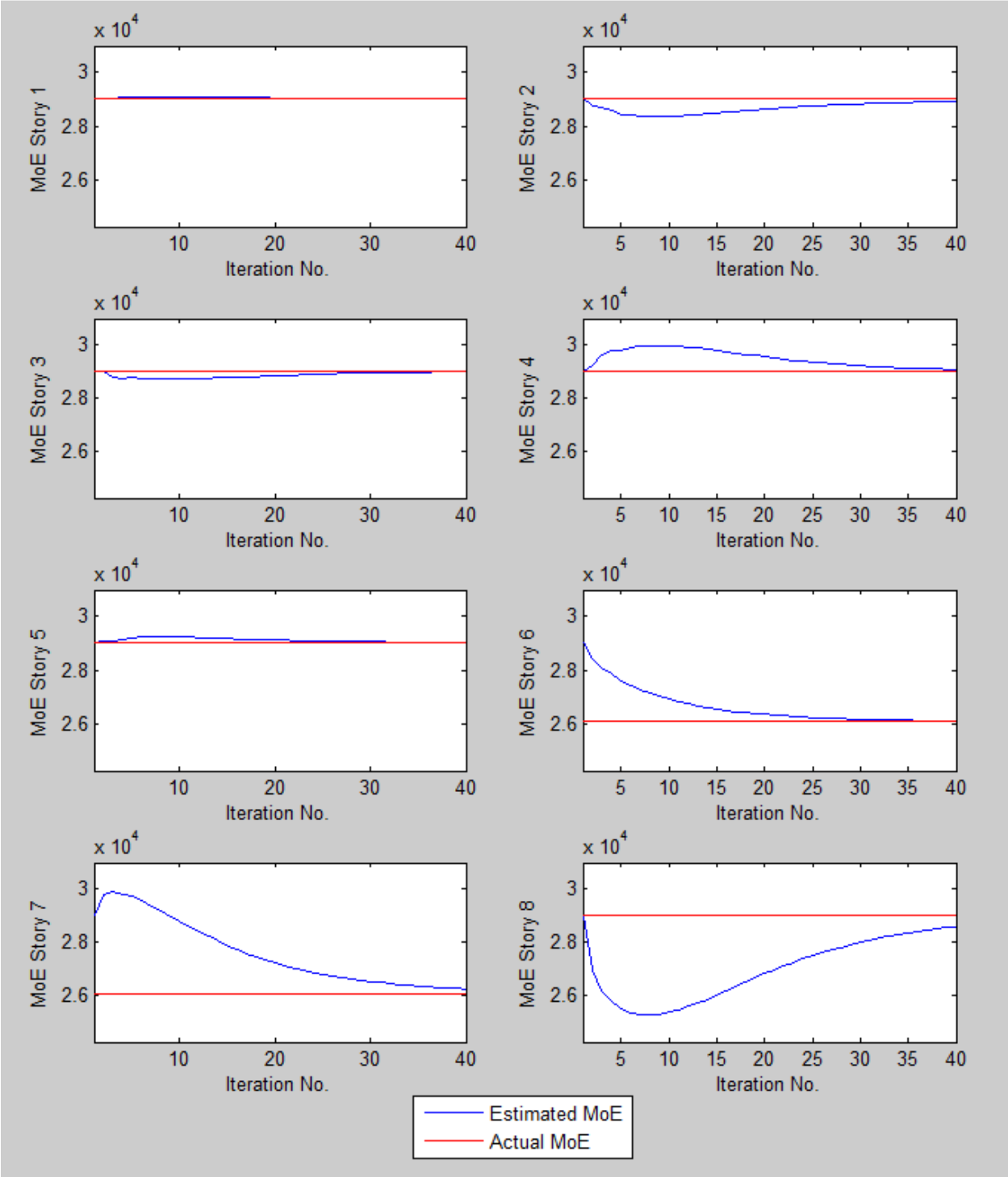

Figure D.8 - Parameter Estimation using Sensors at Floors 2 and 6 for Roof Excitation with Transient Responses

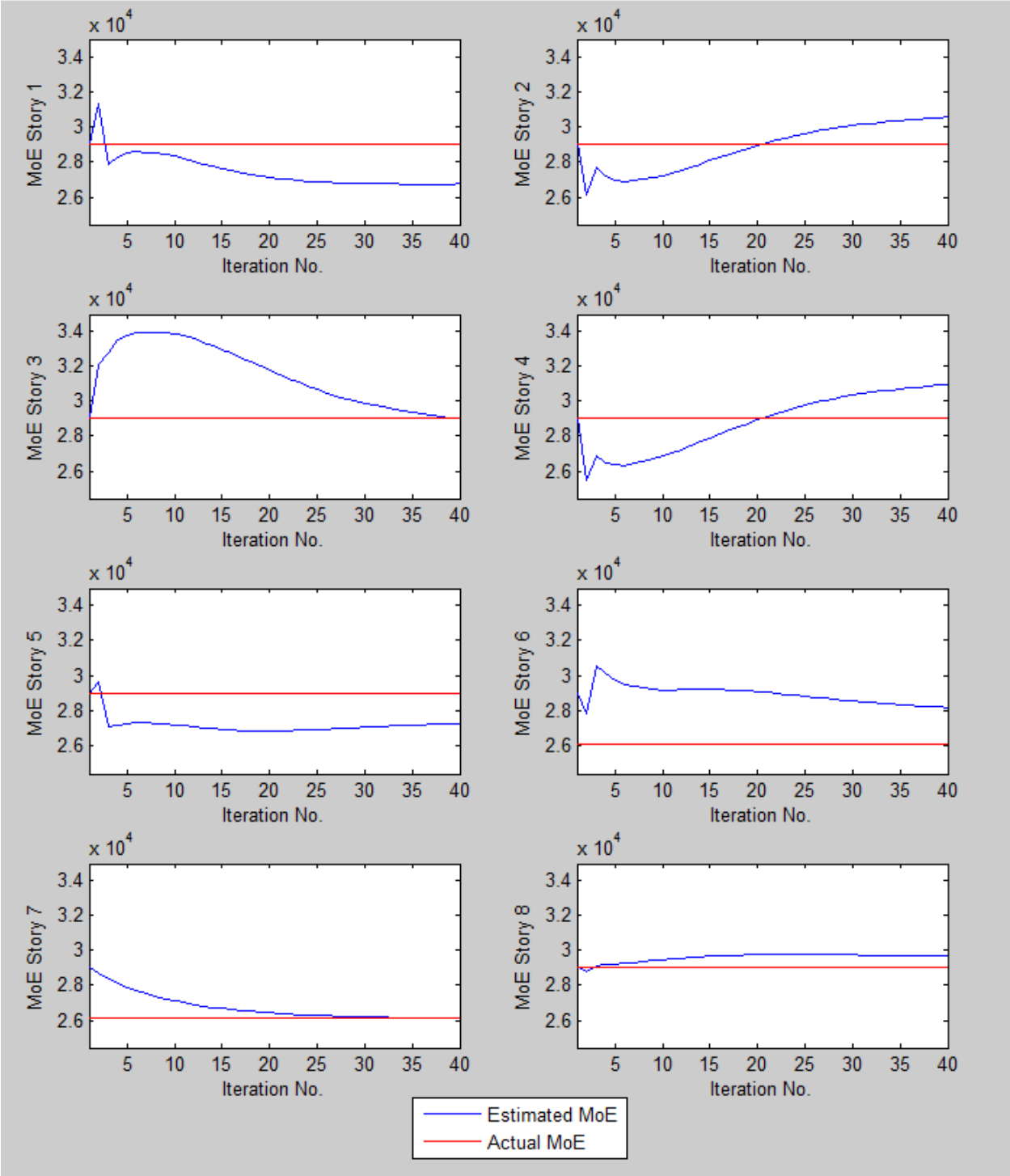

Figure D.9 - Parameter Estimation using Sensors at Floors 4, 7 and 8 for Roof Excitation with Transient Responses

REFERENCES

Abrams; Sozen. "Experimental Study of Frame-Wall Interaction in Reinforced Concrete Structures Subjected to Strong Earthquake Motions" 1979. University of Illinois at Urbana-Champaign.

Danai, K., and McCusker, J. R., 2009, "Parameter Estimation by Parameter Signature Isolation in the Time-Scale Domain," *ASME Journal of Dynamic Systems, Measurement, and Control,* Vol. 131, No. 4, 041008.

Danai, K., Styckiewicz, M., and Civjan, S., 2011,"Direct Method of Damage Isolation for Civil Structures via Shape Comparison of Dynamic Response Measurements," *Computer and Structures.*

Danai, K., Civjan, S., and Styckiewicz, M., 2012, "Sensor Location Selection for Structures via Identiability Analysis in the Time-Scale Domain," *Sound and Vibrations.*

Farrar, C. R., and Jaurequi, D. A., 1998, "Comparative Study of Damage Identification Algorithms Applied to a Bridge: 1. Experiment," *Smart Mate. Struct 7.,* Vol. 704, pp. 704-719.

Friswell, M. I., 2007, "Damage Identification using Inverse Methods," *Philosophical Transactions of the Royal Society A,* Vol. 365, pp. 393-410.

Hartley, H. O., 1961, "Gauss-Newton Method for the Fitting of Non-Linear Regression Functions by Least Squares," *American Statistical Association,* Vol. 3, No. 2, May 1961, pp 269-280.

Mallet, S., and Hwang, W. L., 1992, "Singularity Detection and Processing with Wavelets," *IEEE Transactions on Information Theory,* Vol. 38, No. 2, pp. 617-643.

McCusker, J. R., and Danai, K., 2010, "Measurement Selection for Engine Transients by Parameter Signatures," *ASME Trans. on Eng. for Gas Turbines and Power,* Vol. 132, Issue 12, 121601.

McCusker, J. R., Danai, K., and Kazmer, D. O., 2010, "Validation of Dynamic Models in the Time-Scale Domain," *ASME Journal of Dynamic Systems, Measurement, and Control,* Vol. 132, No. 6, 061402.

Ohtori, Y., Christenson, R. E., Spencer Jr., B. F., and Dyke, S. J., "Benchmark Control Problems Seismically Excited Nonlinear Buildings," http://sstl.cee.illinois.edu/benchmarks/bench3def/nlbench_jpub.pdf.

Yang, J. N., Lei, Y., Lin, S., and Huang, N., "Hilbert-Huang Based Approach for Structural Damage Detection," *Journal of Engineering Mechanics,* Vol. 130, No. 1, Jan. 1, 2004, pp. 85-95.

Yuen, K., Katafygiotis L. S., Papadimitriou C., and Mickleborough N. C., 2001, "Optimal Sensor Placement Methodology for Identification with Unmeasured Excitations," *ASME Journal of Dynamic Systems, Measurement, and Control,* Vol. 123, Dec. 2001, pp 677-686.